FINITE DEFLECTION DYNAMIC ANALYSIS OF RIGID-PLASTIC BEAMS

by

REZA VAZIRI

B.Sc (ENG), University of London, U.K., 1982

A THESIS SUBMITTED IN PARTIAL FULFILMENT OF

THE REQUIREMENTS FOR THE DEGREE OF

MASTER OF APPLIED SCIENCE

in

THE FACULTY OF GRADUATE STUDIES

Department of Civil Engineering

We accept this thesis as conforming

to the required standard

THE UNIVERSITY OF BRITISH COLUMBIA

April 1985

In presenting this thesis in partial fulfilment of the requirements for an advanced degree at the University of British Columbia, I agree that the Library shall make it freely available for reference and study. I further agree that permission for extensive copying of this thesis for scholarly purposes may be granted by the head of my department or by his or her representatives. It is understood that copying or publication of this thesis for financial gain shall not be allowed without my written permission.

Department of Civil Engineering

The University of British Columbia
1956 Main Mall
Vancouver, Canada
V6T 1Y3

Date May 1, 1985

ABSTRACT

An analytical procedure, which retains the influence of finite deflections, is developed herein for the dynamic behaviour of rectangular shaped rigid-plastic beams. In the general formulation of the problem deformation is assumed to proceed under two distinct mechanisms depending on the extent to which the value of the peak pressure exceeds the static collapse pressure of the beam. These mechanisms are described by kinematically admissible velocity fields that satisfy the appropriate continuity conditions. The governing equations of motion are derived from a variational statement consisting of the principle of virtual work and D'Alembert's principle. The conventional parabolic yield surface (which describes the coupling action between axial forces and bending moments at yield) and its associated flow rule are adopted to describe the plastic behaviour of the beam material. The kinematic small but finite deflection analysis, in which the membrane forces and bending moments interact, generally leads to basic equations which are of nonlinear character. These resulting equations are solved analytically and closed form expressions are developed for the prediction of maximum permanent deformation of the beam. A dynamic membrane analysis is carried out in those cases when the input energy is sufficiently high that the beam undergoes moderately large deformation (i.e. deflections of the order of beam thickness). Finally the dependence of the permanent deflection on the applied pressure and impulse is obtained for a family of rectangular pulses. This relationship is represented by an isoresponse curve in a form convenient for direct engineering use.

TABLE OF CONTENTS

LIST OF TABLES

LIST OF FIGURES

LIST OF FIGURES - Continued

LIST OF FIGURES - Continued

LIST OF SYMBOLS

All symbols are specifically defined where they are first introduced in the text. The principal symbols are listed here for convenience. When more than one meaning has been assigned to a symbol, the correct use will be obvious from the context in which they are being used.

A	total cross-sectional area of the beam
A_1, A_2	areas of fully plastic compressive and tensile regions on either side of the zero-stress axis
A_e	are of the cross-section bounded by the zero stress axis and the equal area axis
A_n, C_n	coefficients of the n^{th} sine term in the Fourier series given by Equations (3.66) and (3.74)
B_n, D_n	coefficients of the n^{th} cosine term in the Fourier series given by the Equations (3.65) and (3.74)
E	modulus of elasticity
$F(1/\sqrt{2}, \phi)$	incomplete elliptic integral of the first kind with modulus $1/\sqrt{2}$ and amplitude ϕ.
I	total impulse (area under the pressure-time curve)
I_o	ideal impulse corresponding to an initial condition on velocity
I_s	second moment of area of the beam cross-section
K	complete elliptic integral of the first kind with modulus $1/\sqrt{2}$
K.E.	kinetic energy
L	half-beam length
M	critical bending moment

$M(x)$	bending moment at any section distance x from the midspan
M_o	limit moment in pure bending
M_y	bending moment at incipient yield
N	critical axial load
N_o	limit axial force in pure tension
P	static load per unit length
P^*	static load carrying capacity at finite deflections
$P(t)$	dynamic pressure-time loading function
P_m	dynamic load intensity
P_o	static collapse pressure according to the linear bending-only-theory defined by Equation (2.15)
$\bar{P}$	P_m/P_o; nondimensional pressure parameter
$\bar{P}_c$	nondimensional pressure parameter corresponding to a step load which causes the same central deflection as the equivalent rectangular pressure pulse
Q	defined by Equation (4.8b)
R	ratio of the input kinetic energy to the maximum strain energy that can be absorbed by the beam
S	area swept by the deforming beam mechanism
T	time at which the travelling hinges arrive at the midspan
T_e	fundamental period of elastic vibration of the beam
V_o	amplitude of the equivalent sinusoidal velocity profile at the initiation of string phase
δW_{ext}	external virtual work done by the loads
δW_{int}	internal virtual work dissipated in plastic deformation
Zp	plastic section modulus
a	defined by Equation (3.45)

b	beam width
b_1	defined by Equation (4.14a)
c	constant defined in Equation (3.59)
c_1	defined by Equation (4.14b)
e	distance between the zero stress axis and the equal area axis
f	yield function
$g(t)$	given by Equation (3.125b)
h	beam depth
i	number of statical redundancies of the beam
k	$1/\sqrt{2}$; modulus of the elliptic integrals
m	mass per unit length of beam
$\bar{m}$	M/M_o; dimensionless moment
$\bar{n}$	N/N_o; dimensionless membrane force
q	defined by Equation (4.15b)
$r(t)$	distance between the plastic hinge and the support point at time t
$\bar{r}_p$	lever arm of the plastic moment defined by Equation (2.4)
s	defined by Equation (4.15a)
t	time
t_f	time at which beam reaches its permanent position
t_s	the instant at which the string phase is initiated
t^*	$t-t_s$
t^{**}	$t - \tau$
u	$F(1/\sqrt{2}, \phi)$; argument of the Jacobian elliptic functions
w	transverse deflection of the beam defined in Figure 3.2
w_o	centrepoint deflection

x	coordinate along beam axis (measured from beam centre)
x_o	coordinate along beam axis (measured from the left-hand support)
y, z	orthogonal coordinate axes defined in Figure 2.4
$\bar{y}$, $\bar{y}_2$	centroidal distances of the areas A_1 and A_2 on either side of the equal area axis (measured from the latter axis as shown in Figure 2.4)
α	defined by Equation (3.42)
β	I^2/mhP_o; nondimensional impulse parameter
β_o	$I^2{}_o/mhP_o$; location of the vertical asymptote in the $\bar{P}$ - β plane
β_c	the value of the impulse parameter beyond which the dynamic pulse can be characterized by a step load
β_m	the value of β which marks the transition from Phase II (b) to Phase I (b) in the medium pressure range and is given by Equation (3.84)
γ	defined by Equations (3.95) and (4.9a)
δ	first variation or virtual change of a quantity
δ_f	$w_o(t_f)$; final plastic displacement of mid-point
Δ	increment of a quantity
ε	axial extension of the equal area axis
ζ	defined by Equation (3.86)
η, η_c	defined by Equations (3.132) and (3.131c)
θ	beam rotation at the supports
κ	curvature
λ	defined by Equation (3.36)

Λ	defined by Equation (3.102)
μ	dimensionless time scale defined by Equation (3.75) and given in terms of $\bar{P}$, β by Equation (3.81)
μ_c	value of μ when β is replaced by β_c in Equation (3.81)
ν	defined by Equation (3.38)
ξ	dummy integration variable
$\rho(t)$	plastic hinge position (measured from the midspan) at time t
ρ_o	initial hinge location given by Equation (3.127)
σ	stress
σ_o	yield stress in pure tension
τ	pulse duration
ϕ	$\cos^{-1}\sqrt{(w_o/\alpha)}$; amplitude of the elliptic integral F
ϕ_s	value of ϕ at initiation of string phase given by Equation (3.53b)
$\Phi(x_o)$	shape function at initiation of string phase
χ	$a\tau$; defined by Equation (3.91)
ψ	rotation at the hinge section
$\Psi_n(t^*)$	n^{th} time-dependent coefficient in the Fourier series representation of the string phase solution given by Equation (3.61)
ω	dimensionless time scale defined by Equation (3.68)
Ω	strain energy
$\dot{(\ )}$	$\frac{\partial}{\partial t}(\ )$
$(\ )'$	$\frac{\partial}{\partial x}(\ )$
$[\ ]$	difference between the values of the considered quantity on either side of a travelling hinge

$( )_f$ final state of ( )

$\tilde{( )}$ approximate value of ( )

ACKNOWLEDGEMENTS

The author wishes to take this opportunity to express his appreciation to his supervisors, Dr. M.D. Olson and Dr. D.L. Anderson, for their patient guidance and advice throughout the execution of this work. I am also deeply grateful to Dr. D.S. Mofflin for numerous helpful discussions.

I wish to continue to acknowledge the financial support of the Canadian Department of National Defence (through a contract from the Defence Research Establishment Suffield).

I would like to thank my parents and my brother Hans Vaziri, for their support and encouragement throughout my graduate work.

CHAPTER I

INTRODUCTION

1.1 BACKGROUND STUDY

The behaviour of structures under transient dynamic loads sufficiently strong to cause large permanent deformation is a subject of considerable interest, but is also one of great complexity from both a theoretical and experimental standpoint. Severe dynamic pressure pulses can arise in a wide variety of practical situations. Examples are in the slamming of a ship's hull in heavy seas, in buildings subjected to internal gaseous explosions, in containment pressure vessels for nuclear reactors, in water wave impact on a barrier or offshore platform, in various military applications where pulses of this type are generated by the detonation of high explosives, and in collisions of aircrafts, automobiles, trains and hydrovehicles involving hypervelocity impact. In many of these circumstances the intensity of the dynamic loads are so large as to cause significant plastic deformation of the structure. This behaviour cannot be described by the equations of the elastic domain (as may be found in standard texts on classical vibration theory of elastic structures), but must be interpreted by relations capable of including large "plastic strains" and permanent deformations encountered in these processes. It is of general engineering interest to have techniques at hand which enable reasonable predictions of these permanent structural damages and from viewpoint of engineering design to improve energy absorbing capabilities of structures to withstand the destructive action of high-intensity transient loads. Some of the most damaging effects are produced by explosive detonations in the close proximity of structures, usually the

result of air-blast loading. Therefore, the general dymamic "response" of structures to blast loading situations is an all inclusive example and subject of current interest. A principal feature of the response to transient loading is the permanent deformation that occurs in structural elements, and it is clear that these deformations must not spread beyond tolerable limits. Situations often arise where limited deformations play an important role in serviceability of a structure undergoing a large deformation. Therefore, in situations where the severity of loading is such that permanent structural damage occurs, the design engineer is often concerned with the magnitude of the resulting deformations. The major part of this thesis is devoted to estimation of permanent displacements of structures subjected to violent dynamic overloads of transient nature. The discussion shall be restricted to large plastic deformations of basic structural elements with particular emphasis on beams and will not be concerned with complicated structures comprising many of the basic elements. It should be noted that we are not concerned with localized plastic flow which lead to failure of the structure by shearing or tearing caused by sufficiently high levels of dynamic load. However, failure from a structural standpoint such as tearing and shear failures in explosively loaded clamped beams were studied and discussed by Menkes and Opat (Reference 1). In what follows we shall assume that conditions of load intensity and distribution, geometry of the structure, and material behaviour are such that general structural deformation occurs, even though the latter might be a rather restricted aspect of structural behaviour.

1.2 LITERATURE REVIEW

The general field of dynamic plastic analysis of structures is broad and

the pertaining published literature is far too extensive to be adequately covered by this report. A number of survey articles on dynamic plastic structural analysis have appeared during the last few years (Reference 2-5) including a recent compilation and analysis of published research results on air-blast response of beams and plates by Ari-Gur et al (Reference 6). Among the numerous articles in the field of dynamic plasticity only a few topics of interest will be discussed, with consideration largely given to the theoretical methods of analysis of beams. However, those wishing to know more of other aspects of this field are referred to the thorough review articles mentioned (Reference 2-6). In what appears to be one of the earliest works in this field, Lee and Symonds (Reference 7) treated with a comparatively simple method of analysis the problem of a transverse impact force (assumed to be a symmetrical triangular pulse shape) applied at the midpoint of a uniform beam with free ends. The analysis was based on a rigid-plastic idealization of the beam material. This assumption led to the use of a localized plastic deformation called a "plastic hinge" as a means of describing the deflection process. the plastic hinge mechanism is not restricted to dynamic analyses and has widely been used in static problems. The concept has evolved from the most valuable early studies of plastic theory by Lord Baker (Reference 8) and others at the University of Cambridge. The rigid-plastic assumption has gained wide favour in dynamic plasticity in view of its relative mathematical simplicity. However, it is restricted to materials that exhibit a certain amount of ductility (e.g. mild steel). Non-ductile or brittle materials tend to act completely elastic and an analysis using rigid-plastic model is not applicable. The rigid-plastic analysis is in error for materials that exhibit appreciable strain-hardening. Lee and Symonds analysis

(Reference 7) had an additional limitation in that the deformations were assumed to be sufficiently small for the usual small deflection beam theory to be applicable. They introduced the concept of "moving plastic hinge" in order to satisfy certain kinematic requirements during the motion of the beam.

Symonds (Reference 9) extended the analysis of (Reference 7) to include the response of the free-free beam to other types of pulse loads. In his treatment of a free-free rigid-plastic beam acted on by a concentrated dynamic load he concluded that the final plastic deformation for any load shape was dependent primarily on the impulse of the load (namely the time integral of the applied pressure) and not on the precise details of its time history. However, his conclusions were based on loadings which were essentially "impulsive"†. Evidently the shape of the load was not important for the range of maximum load levels that were considered.

In a subsequent paper (Reference 10) Symonds obtained simple solutions for clamped and simply supported beams subjeted to uniformly distributed loading of time histories that satisfied the restricted definition of the so-called "blast type" loading (i.e. loads that instantaneously rise to a peak magnitude and then monotonically decrease in a short interval of time. Rectangular pulses are a special class of blast-type loads).

Symonds and Mentel (Reference 11) studied the influence of axial

---

† By impulsive loading it is implied that the load time history can be described by a Dirac delta function which instantaneously imparts some velocity profile to the structure. This impulse that coresponds to an initial condition on velocity is termed "ideal impulse" or "pure impulse" and must be distinguished from the impulse which is defined as the area under the dynamic load-time curve.

restraints on the behaviour of rigid-plastic beams loaded with a transverse pressure impulse. In this study the beam was assumed to have a rectangular cross-section and the central portion of the beam was given an initial velocity which led to a greatly simplified analysis. The theoretical work of (Reference 11) predicted permanent deformations which were considerably smaller than those obtained from the corresponding simple first order bending-only-theory even when maximum deflections only of the order of the beam depth were permitted. Symonds and Mentel also described the gradual transition of clamped and simply supported beams from an initial behaviour, governed by the interaction between axial forces and bending moments, to a final stage where deformations were governed primarily by in-plane membrane (i.e. axial) forces.

Humphreys (Reference 12) conducted a series of experimental tests on flat steel beams using sheet explosives to provide sufficiently high uniform impulsive loading in order to produce large plastic deformations. The resulting final deformations were compared with the rigid-plastic theory of Symonds and Mentel (Reference 11) and it was found that the theoretical predictions were generally higher by about 20-30 percent than the observed deformations. The experimental results also revealed that the superimposed elastic vibrations were small, amounting (in peak amplitude) to about 5 percent of the plastic motion. It was then concluded that for engineering purposes the rigid-plastic solution including axial constraints gave a fairly good approximation to the level of plastic damage encountered under impulsive loading. Dynamic analysis of rigid-plastic curved beams with axial constraints under impulsive loading has been presented by Chen et al (Reference 13). The results were compared with the rigid-plastic straight beams treated by Symonds and Mentel (Reference 11) and

favourable agreement was achieved.

In his three part presentation, Nonaka (References 14 - 16) made a theoretical and experimental investigation into the response of clamped beams, with constraints against axial displacements at the ends. The beam carried a concentrated mass at its centre and was subjected to large transverse impact loading at the mass. In Part 1 (Reference 14) Nonaka aimed at solving the plastic interaction problem of bending, extension and shear based on a fixed yield surface (parabolic cylinder) and the assumption of a rigid, perfectly plastic beam subjected to impulsive-type loading. It was found that the shear effect played a dominant role in beams with noncompact cross-sections (i.e. I-sections) and also if the attached mass was small in comparison with the beam mass. It was also surmized that, for a large mass ratio the major portion of deformation occured during the last phase of motion in which the two halves of the beam rotated about the clamped ends (i.e. deformation occurred under a one-degree-of-freedom mode). In Part 2, the author attempted to make a more realistic calculation for the duration of load pulse, strain rates (in an approximate manner) and elastic effects. The analysis was based upon a simplified one degree of freedom mode assumption and shear deformations were neglected. From the results of the foregoing analysis it appeared that consideration of load duration improved the predictions of the simple rigid-plastic theory. It was also noted that the results of the assumption of impulsive loading (i.e. load with infinitely large magnitude applied for an infinitesimally short duration) became better when elastic effects were considered. Experimental results of Part 3 agreed quite well with the theoretical predictions of permanent deformations in Part 2 which incorporated the strain-rate and elastic effects. Agreement was more pronounced for aluminum specimens

tested. It seemed that the assumption of concentrated plastic regions or the one degree of freedom mode was less appropriate for mild-steel.

Jones (Reference 15) suggested a simple method for estimating the combined influence of strain-hardening and strain-rate sensitivity on the permanent deformation of rigid-plastic beams loaded impulsively. The results of this work indicated that considering either strain-hardening or strain-rate sensitivity alone gave permanent deformations which were similar to those predicted by an analysis retaining both effects simultaneously. Moreover, the results suggested that it was not necessary to include either of the forementioned effects for beams having large span-depth ratios. It was proposed that the theoretical procedures could be simplified by using square yield surfaces which circumscribed or inscribed the exact parabolic yield surface. This simplification lent itself to simple bounds on permanent displacements which were quite accurate. The behaviour of rigid-plastic rectangular beams subjected to uniform "dynamic" step loads of finite durations were investigated by Jones (Reference 16) using an approximate theoretical procedure. The influence of finite deflections or geometry changes wre retained in the analysis but effects of strain-rate sensitivity and strain-hardening were disregarded. This theoretical procedure utilized time-independent deformation profiles which had a shape identical to the corresponding static collapse fields. However, past a certain range of magnitude of the pressure pulse, the deformed shapes of beams loaded dynamically are expected to be time-dependent and consequently different from the associated static collapse mechanism. Further theorems which accounted for time-dependent response profiles had to be derived to examine the accuracy of the theoretical procedures of (Reference 16).

Krajcinovic (Reference 17) derived a closed-form solution for the dynamic infinitesimal response of a simply supported rigid-plastic beam subjected to a uniformly distributed dynamic load of arbitrary pressure-time history. As opposed to the restrictions on the type of loading in the earlier literature, the method outlined in Reference 17 proved to be capable of dealing with cases in which the load had a finite rise time. Solutions for specific pulse shapes known from the previous literature could be obtained directly as special cases from the general formulas derived in Reference 17. In addition to the usual rigid-plastic restrictions, it was asumed that the beam deformations were small and that the plastic interaction of bending moments with axial and shear forces were negligible. Major difficulties were encountered, steming from the non-stationary nature of plastic hinges and the resulting time-dependent mechanisms of deformation.

In all the preceding discussions, apart from the work by Nonaka (Reference 14, Part II), the theoretical analyses were based on the rigid-plastic hypothesis and consequently elastic vibrations were ignored. However, the solutions so obtained are expected to be close to reality only if the external dynamic energy imparted to the beam exceeds the maximum amount of energy that could be stored in the beam in the form of elastic strain energy (Reference 7). The influence of material elasticity has to be retained in the theoretical analysis when the forementioned condition ceases to apply. In an excellent survey of beam studies carried out by Symonds (Reference 18), it was pointed out that material elasticity could have a significant effect on the beam response when external dynamic pressure pulses have durations which are comparable with the natural period of elastic vibrations of the beam. In an attempt to assess the range

of validity of rigid-plastic type of analysis Seiler, Cotter and Symonds (Reference 19) reconsidered the problem of simply supported beam subjected to impulsive loading, by treating the material of the beam as behaving in an approximate elastic-plastic manner. It was found that a complete solution of the beam problem in which both the elastic vibrations and plasticity condition were taken into account was extremely difficult to obtain. Witmer et al (Reference 20) formulated a general numerical method using finite-difference approach to predict large dynamic elastic and post-elastic responses of simple structures including beams. The proposed wholly numerical method took into account the effect of elastic-plastic behaviour, strain hardening, strain-rate and large deflections. The analysis, though simple and straight-forward, required considerable amount of computing time.

A number of references on numerical dynamic analysis of elastoplastic structures can be cited in the review articles (References 2-6). These methods are of course required for full details of the structural response but remain expensive and rather time consuming.

1.3 PURPOSE AND SCOPE OF THE PRESENT WORK

It is clear from a survey of the pertinent literature that there are very few "exact" rigid-plastic solutions which retain the influence of finite deflections and moreover account for the time distribution of the dynamic loading. Most attention has been directed towards the dynamic deformation of beams in which bending moments alone are believed to be preponderant and thereby membrane forces are disregarded in the analysis. Most authors also replace the external dynamic pressure by an impulse which imparts to the unloaded structure an initial velocity field. In practice,

however, the blast load which acts on a beam or structure often persists for a considerable period of time rather than behaving like a pure impulse as assumed in numerrous articles. It is the purpose of this thesis, therefore, to study the behaviour of a rigid, perfectly plastic rectangular beam subjected to a rectangular pressure pulse of finite duration. We will determine the permanent deformation of a symmetrically supported beam whose ends are constrained against in-plane axial motions. The eventual goal is to construct isoresponse plots† (or critical load curves) which are of particular interest to the designer or analyst in interpreting the results. Attempt will be made to solve the problem analytically without recourse to extensive numerical methods or computer programmes.

Chapter 2 is intended to familiarize the reader with the theoretical concepts involved in the analytical treatment of the problem. The assumptions that impose important limitations on the validity of the theory are also introduced.

Chapter 3 outlines an in-depth analysis of the problem, supplemented by a tabulated summary of the results. A discussion of the results is incorporated at the end of this Chapter.

Chapter 4 describes the construction of isoresponse curves according to the complete theory of this thesis.

Chapter 5 outlines the conclusions that can be drawn from the results of the present analysis. The applicability of the analytical treatment is discussed upon and also areas of future research are suggested.

---

† These are curves that represent the combinations of scaled pressure and scaled impulse which cause the same scaled maximum displacement. For further information see (Reference 21).

CHAPTER II

THEORETICAL BACKGROUND

2.1 INTRODUCTION

The object of the present chapter is to outline the underlying assumptions that are made in the mathematical formulation of the general problem and to familiarize the reader with the fundamentals of plasticity (both static and dynamic concepts) pertinent to the problem at hand.

2.2 ASSUMPTIONS

In the present theoretical study of the dynamic behaviour of beams, the following assumptions have been made or implied.

i) The material of the beam is assumed to be ductile obeying a rigid-perfectly plastic type of stress-strain relation. This assumption is made because of interest that lies in moderately large plastic deformations and in order to simplify the mathematical analysis to a certain extent. Owing to its importance, a general discussion on the concepts of rigid-plastic idealizaion will be given in the next section. In structural dynamics, this assumption is known (Reference 18) to be appropriate if

   a) The kinetic energy associated with the external dynamic pressure pulse significantly exceeds the elastic strain energy that can be absorbed by the structure before yielding occurs. The ratio R of these two energies for beams must be at least greater than 3 so that it could be considered as adequately large for this purpose (Reference 22).

   and if

b) the load duration is short compared to the fundamental period of elastic vibrations of the beam. Under the rigid-plastic assumption the elastic deformations are ignored and the beam remains rigid until the first plastic hinge is generated. All the internal plastic deformations take place at the plastic hinge section only when the state of stress at that section lies on a fixed yield surface. These concepts are discussed in detail in Section 2.3.

ii) The influence of strain rates and strain-hardening on the material properties are ignored. The effect of high rates of strain is to raise the yield stress of ductile materials and is of considerable importance in dynamic problems. Rate sensitivity can be accounted for with a simplified approach first developed by Perrone (Reference 23). With this approach the rate-sensitive structure is replaced by one which is rate-insensitive but with variable yield stress. This can be done by making use of the results of the rate-insensitive analysis to be presented herein. However, since the inclusion of rate sensitivity increases the complexity of the problem, it has been ignored in the following analysis.

iii) The beam material is homogenous and isotropic. It therefore provides the same magnitude of yield moment for both positive and negative curvature changes.

iv) We restrict ourselves to blast-type pulses shown in Figure 2.1 with each pulse consisting of an instantaneous rise to the peak pressure P_m (force per unit length of the beam) followed by a continuous monotonic decay to zero pressure. That is, we admit pulse shapes of the type

$$P(t) = \begin{cases} P_m(1-t/\tau)^{1/n-1} & \text{for } 0 < t < \tau \\ 0 & \text{for } t > \tau \end{cases}$$

with

$$\dot{P}(t) < 0 \qquad \text{for } t > 0$$

The parameter n determines the rate of the pressure decay and is limited to take on values which satisfy the following inequality

$$0 < n < 1$$

The rectangular pulse (n = 1) is thus a limiting case in this family of pulse shapes.

vii) The effects of the transverse shear deformations and rotary inertia are negligible.

viii) Although finite deflections are considered their magnitude is assumed small compared to L (the half-span length of the beam). This requires the square of the slope of the deflection curve to be small compared with unity.

ix) Stretching is assumed to result only from transverse displacements. Therefore horizontal displacement and accelerations are disregarded. The axial load can therefore be taken as constant over the length

x) The yield condition and all the relations of static plasticity are assumed to remain valid.

xi) The analysis to follow does not include the possibility of buckling but only the effect of in-plane axial forces on the stable behaviour of the beam.

xii) Longitudinal stress wave propagations through the beam are ignored.

xiii) Conventional Bernoulli-Euler beam theory assumptions are made. These are:

a) Originally plane cross-sections remain plane after deformation occurs.

b) Stresses other than longitudinal stresses are negligible.

c) Longitudinal yield stress is the same in flexure as in direct tension or compression.

2.3 BASIC CONCEPTS OF STATIC PLASTICITY

The main concepts of static plasticity used in this thesis along with theoretical preliminaries of the analysis are discussed in the following section.

2.3.1 RIGID-PLASTIC IDEALIZATION

This material idealization results in a stress-strain relation of the type shown diagrammatically in Figure 2.2. According to this diagram a rigid-plastic beam has an infinite rigidity until the induced longitudinal stress σ in every fibre of the beam at a particular section reaches a constant value $\pm\sigma_o$, the static yield stress. At this point indefinite yielding can occur.

If the influence of the shear and axial force is neglected, as is customary, the behaviour of a rigid-plastic beam can be described in terms of the bending moment M at any cross-section of the beam, and the corresponding angle of rotation ψ. The rigid-plastic mathematical model for the moment-curvature relationship is shown in Figure 2.3 and is the same for beams of all cross-sectional shapes. According to this model, no

deformation occurs until the bending moment at a particular section reaches the limit moment M_o in absolute value. Any attempt to increase this moment will cause unrestricted rotation of the beam in the corresponding sense and the beam acts as if hinged at the section with the only resistance being the moment M_o. A "plastic hinge" is said to occur at such a section where all the fibres on either side of the zero-stress axis are stressed to the yield stress σ_o thus rendering the entire section "fully plastic". Figure 2.4 shows the fully plastic stress distribution on a typical section with one axis of symmetry. The section is being bent about an axis at right angles to the axis of symmetry. The portion of the cross-section of area A_1 lying above the zero stress axis is yielding in compression while the plastic zone of area A_2 below the zero stress axis is yielding in tension. In the absence of axial thrust, the resultant normal force on the cross-section must be zero. Therefore the longitudinal force equilibrium yields:

$$0 = \sigma_o A_2 - \sigma_o A_1$$

or

$$A_1 = A_2 \qquad (2.1)$$

where $\sigma_o A_1$ = the total longitudinal compressive force on the fibres above the zero stress axis z-z, acting through the centroid of A_1 i.e. point C_1 in Figure 2.4.

and $\sigma_o A_2$ = the total longitudinal tensile force on the fibres below the zero stress axis z-z, acting through the centroid of A_2, i.e. point C_2 in Figure 2.4.

It follows from Equation (2.1) that under pure plastic bending the zero- stress axis divides the beam cross-section into two equal areas. The zero- stress axis is, in fact an "equal area" axis. In general this axis will

not pass through the centroid of the whole cross-section, as does the elastic neutral axis. However, for a doubly symmetrical section the equal area axis and the elastic neutral axis coincide. If the toal area of the cross-section is A, then

$$A_1 = A_2 = \frac{1}{2} A \qquad (2.2)$$

Considering the moment equilibrium about the equal area axis, we have

$$M_o = \frac{1}{2} A (\bar{y}_1 + \bar{y}_2) \sigma_o \qquad (2.3)$$

in which $\bar{y}_1$, $\bar{y}_2$ are the distances of the centroids C_1, C_2 respectively, measured from the equal area axis. The limit moment M_o (also termed the plastic moment) is the moment required to produce a plastic hinge in the section. Under pure plastic bending this is the greatest moment that the section can sustain at full plasticity. It will be shown in the next section that in the presence of axial force the moment producing the hinge is less than M_o. The moment M_o usually can be taken equal to $\sigma_o Z_p$, where Z_p is the plastic section modulus defined by the relation;

$$Z_p = \frac{M_o}{\sigma_o} = \frac{1}{2} A\bar{r}_p \qquad (2.4)$$

Hence, $\bar{r}_p = \bar{y}_1 + \bar{y}_2$ is the lever arm of the plastic moment (Figure 2.4).

2.3.2 PLASTIC INTERACTION OF BENDING MOMENT AND AXIAL LOAD: YIELD SURFACE

The bending moment may act alone, as considered above, or in combination with direct axial load. In what follows the behaviour of beams subjected to bending moment combined with direct axial load will be described. We attempt to find a critical combination of axial force N and bending moment M that will cause a section to reach a fully plastic state of stress and thereby lead to the formation of a plastic hinge at that section of the beam. Consider the general case of cross-section having at least one axis of symmetry (Figure 2.5b), which coincides with the plane of bending. The normal axial load N acts through the weighted centre of area O (i.e. point where the axis of symmetry and equal area axis intersect) and is thought of as being tensile corresponding to positive state of stress. If a situation arises whereby the normal force N does not act at the equal area axis of the cross-section, account must be taken of any eccentricities of the applied load N relative to this axis, when calculating the bending moments. The effect of the tensile axial load N is to displace the zero stress axis from its original position (i.e. the equal area axis) by an amount e, so that an area A_e (shaded in the cross-section diagram) is transferred from compression to tension.

From the stress distribution diagram of Figure (2.5c) the longitudinal force equilibrium equation can be written as:

$$N = \sigma_o A/2 + \sigma_o A_e - \sigma_o (A/2 - A_e)$$

Thus

$$N = 2\sigma_o A_e \qquad (2.5)$$

The axial force may therefore be considered as being supported, at yield stress, by an inner area $2A_e$ of the section equally divided above and below the equal area axis. The remaining outer area of the section is available for bending moment. The axial force given by Equation (2.5) can also be thought of as the net resultant of a fictitious stress distribution of mangitude $2\sigma_o$ acting over the area A_e of the cross-section. The fully plastic stress distribution (Figure 2.6a) can therefore be resolved into two parts; one part representing the original fully plastic distribution of stress in the absence of axial load (Figure 2.6b) and one part representing the fictitiously formed stress distribution carrying the axial load (Figure 2.6c). Superimposing these stress distributions and considering the moment equilibrium about the equal area axis, yields,

$$M = M_o - N\bar{y}_e \tag{2.6}$$

in which $\bar{y}_e$ denotes the distance of the centroid of the transferred area A_e from the equal area axis and is given by;

$$\bar{y}_e = \frac{\int_0^e b(y)\, y\, dy}{\int_0^e b(y)\, dy} \tag{2.7}$$

where b(y) is the width of the section at a distance y from the equal area axis (Figure 2.7). Equation (2.6) can be recast into the following dimensionless form;

$$\frac{M}{M_o} = 1 - \left(\frac{N}{N_o}\right) \frac{N_o}{M_o} \bar{y}_e \qquad (2.6a)$$

where N_o denotes the limiting value of the axial force in simple tension without bending and is defined by,

$$N_o = \sigma_o A \qquad (2.8)$$

It should be noted that the quantity $\bar{y}_e$ depends upon the geometry of the section and magnitude of the axial load, so that the right hand side of Equation (2.6a) is generally a non-linear function of N. It is convenient to define dimensionless stress variables by

$$\bar{n} = \frac{N}{N_o} , \quad \bar{m} = \frac{M}{M_o} \qquad (2.9)$$

by making use of Equations (2.4), (2.8) and (2.9) we can rewrite Equation (2.6a) as

$$\bar{m} = 1 - 2\bar{n} \frac{\bar{y}_e}{\bar{r}_p} \qquad (2.6b)$$

The presence of axial load therefore reduces the moment carrying capacity of the section which would otherwise be M_o. Equation (2.6b) can be given a simple geometrical interpretation in a plane with rectangular coordinates $\bar{n} = \frac{N}{N_o}$ and $\bar{m} = \frac{M}{M_o}$. The resulting curve is referred to as the interaction curve for combined bending and tension. Any combination of

axial force and bending moment that represents a point on the interaction curve corresponds to a fully plastic section of the beam. Points inside the curve represent stress distributions which are less than fully plastic and states of stress corresponding to points outside the curve are not admissible. Therefore the interaction curve may also be called the "yield curve" or "yield surface" of the beam cross-section.

By considering bending to occur in the opposite sense and keeping the direction of the axial force unchanged, the yield curve can be completed to cover cases where hogging bending moment and tensile axial force are co-existent at a beam section. Figure 2.8 illustrates yield curves for some typical cross-sections, each bent about the equal area axis and acted on by a normal tensile force through the centre of area O. In all cases the yield surface is found to be convex and bounded by the rectangle with the vertices $(0, \pm 1)$, $(+1, \pm 1)$ in the $\bar{n}, \bar{m}$ coordinate system. If the section is doubly symmetric, then the yield curve will also be symmetrical with respect to the $\bar{n}$ axis; in the most general case, it need not be (Figure 2.8iii, iv). It should be noted that for compact cross-sections (in which the shear area and the cross-sectional area can be assumed equal) the yield curve is dominated by Equation (2.6b), no matter where the zero stress axis may lie on the beam section. However, for non-compact cross-sections such as I-sections, the yield surface is based on two different relations between $\bar{m}$, $\bar{n}$ depending on whether the zero stress axis lies on the web or on the flange. We shall hereafter restrict ourselves to compact cross-sections for which the plastic interaction of bending moment and axial load is controlled by a single equation.

2.3.3 YIELD CONDITION AND THE ASSOCIATED FLOW LAW

There exists a function of the non-dimensional stress components $(\bar{n}, \bar{m})$, the so-called "yield function" given by;

$$f(\bar{n}, \bar{m}) \equiv \bar{m} + 2\bar{n}\frac{\bar{y}_e}{\bar{r}_p} - 1 \qquad (2.10)$$

where the beam reaches its limit state of stress under a critical combination of axial load and bending moment when $f = 0$. The material cannot tolerate stress distributions for which $f > 0$. Therefore the yield condition is satisfied everywhere in the beam if $f < 0$ is maintained.

In accordance with the rigid, perfectly plastic assumption no deformation occurs at a section when the state of stress at that section is such that $f < 0$. Plastic flow can only occur when the stress point $(\bar{n}, \bar{m})$ at a section lies on the yield surface, i.e. when $f = 0$. This corresponds to the formation of a plastic hinge at the section. The plastic deformation that takes place at the hinge section consists of both axial extension ε and rotation ψ as indicated by the strained geometry of the section in Figure (2.5d).

The general solution is usually found using incremental theory thus we shall speak of increments of deformations or deformation rates $\delta\varepsilon$, $\delta\psi$ rather than total deformation quantities, ε, ψ.

Because of the indefinite nature of perfectly-plastic flow the magnitudes of $\delta\varepsilon$, $\delta\psi$ cannot be determined uniquely without consideration of other constraints. However, it is possible to obtain the ratio $\delta\varepsilon/\delta\psi$ from the "flow rule" of plasticity theory. The flow rule establishes a relationship between the state of stress and plastic strain rate, and can be

described in the same geometrical terms as the yield curve if associated plastic flow is assumed.

Consider a set of plastic deformation axes $N_o\delta\varepsilon$, $M_o\delta\psi$ coincident with the stress axes $\bar{n}$, $\bar{m}$ respectively (Figure 2.9). The flow rule states that the plastic deformation vector with components $(N_o\delta\varepsilon, M_o\delta\psi)$ is perpendicular to the yield curve at the corresponding stress point $(\bar{n}, \bar{m})$ causing these deformations (Figure 2.9).

We may therefore express the plastic flow rule mathematically as follows:

$$\frac{M_o\delta\psi}{N_o\delta\varepsilon} \cdot \frac{d\bar{m}}{d\bar{n}} = -1 \qquad (2.11)$$

Since the yield curve is a level curve of the yield function $f(\bar{n}, \bar{m})$ on which $f = 0$, we can obtain an expression for its gradient $d\bar{m}/d\bar{n}$ in terms of partial derivatives of f. We therefore have;

$$0 = df = \frac{\partial f}{\partial \bar{n}} d\bar{n} + \frac{\partial f}{\partial \bar{m}} d\bar{m}$$

or
$$\frac{d\bar{m}}{d\bar{n}} = -\frac{\partial f}{\partial \bar{n}} \Big/ \frac{\partial f}{\partial \bar{m}} \qquad (2.12)$$

From Equations (2.11) and (2.12) it follows that

$$\frac{N_o\delta\varepsilon}{M_o\delta\psi} = \frac{\partial f}{\partial \bar{n}} \Big/ \frac{\partial f}{\partial \bar{m}} \qquad (2.13)$$

2.3.4 COLLAPSE REQUIREMENTS

A beam at collapse has to satisfy three conditions. First, equilibrium must be satisfied, that is, the internal stress variables (i.e. bending moments and axial loads) must be in equilibrium with the applied loads. Secondly, the beam at collapse must be capable of deforming as a mechanism, due to the formation of a sufficient number of plastic hinges. Each plastic hinge reduces the degree of indeterminancy of the beam by one. If the original number of statical redundancies of the beam is i, the formation of i plastic hinges will make the beam statically determinate. One further hinge will turn the statically determinate beam into a collapse mechanism. The beam with i redundancies will therefore require (i + 1) plastic hinges at collapse state. Thirdly, the distribution of bending moment and axial load must be such that the yield condition ($f \leq 0$) is not violated at any section of the beam.

Therefore, the three essential conditions that have to be satisfied by a beam at collapse are those of;

a) Mechanism

b) Equilibrium (2.14)

c) Yield ($f \leq 0$)

If these three conditions are satisfied simultaneously, then the correct solution to the problem will be obtained and the corresponding applied load will be the exact collapse load (or limit load) of the beam.

2.3.5 FUNDAMENTAL THEOREMS OF LIMIT ANALYSIS

The general methods of limit analysis are based upon three fundamental theorems which are:

i) The equilibrium or lower bound theorem

ii) The kinematic or upper bound theorem

iii) The uniqueness theorem

The above fundamental theorems are concerned with the value of the load intensity at collapse of a structure. Formal proofs of these theorems will not be given here but instead they will be stated and described briefly.

i) Equilibrium or Lower Bound Theorem

According to this theorem, the applied loads cannot be critical if a system of stress resultants (N, M) can be found that are in equilibrium with the external loads and that nowhere violate the yield condition ($f \leq 0$).

Therefore any solution that satisfies the equilibrium condition and the yield condition of (2.14) simultaneously, gives rise to a lower bound estimation of the critical collapse load. The beam need not collapse under these circumstances since there may not be sufficient plastic hinges formed to produce a mechanism. Since the yield condition is not always reached at sufficient points to form a mechanism, this theorem is often referred to as the "safe theorem".

ii) The Kinematic or Upper Bound Theorem

This theorem states that, any solution derived from a kinematically admissible deformation mechanism, and which satisfies the yield criteria at the hinge or slip lines, gives an upper bound to the collapse load or the correct collapse load, if the chosen mechanism happens to be the correct one. It may be shown that in deriving a solution from an assumed mechanism, the yield condition

is not necessarily satisfied everywhere. Such a solution is an upper bound, i.e., collapse will occur at a lower value of the load, therefore the theorem is accordingly termed the "unsafe theorem".

iii) The Uniqueness Theorem

This theorem results from a combination of the static and kinematic theorems. According to this theorem, if a spatial stress distribution (consisting of both bending and axial stresses) is found which satisfies equilibrium and does not exceed the yield criterion at any point along the beam, and in which sufficient plastic hinges form to constitute a valid mechanism, then the upper and lower bounds coincide and this solution gives the correct collapse load. It can be proved that in this case the collapse mechanism and the bending moment distribution are unique. In general, an exact solution cannot be found for complicated structures and one has to resort to approximate solutions provided by the first two theorems in order to obtain close bounds for the critical collapse loads.

It can be seen from the foregoing discussion that bounds on the collapse load can be determined by satisfying the three conditions of (2.14) in pairs as follows:

Exact

- Mechanism Condition
- Equilibrium Condition

} Upper bound (unsafe)

- Equilibrium Condition
- Yield Condition

} Lower bound (safe)

2.4 BASIC CONCEPTS OF DYNAMIC PLASTICITY

In this section typical deformation profiles of symmetrically supported beams subjected to uniform blast-type pressure loadings are described and illustrated. The notion of travelling plastic hinges is discussed and relations between various kinematic quantities on either side of the moving plastic hinges are also given in this section.

2.4.1 MECHANISMS OF DEFORMATION

The dynamic behaviour of rigid-plastic beams under uniformly distributed pressure loading can be characterized by various mechanisms of deformation. It is found in the available literature on dynamic plasticity (Reference 17), that these deformation profiles are dependent on the intensity of the external pressure pulses. The following is intended as a review of the earlier theoretical procedures used to describe the dynamic response of symmetrically supported beams. For simplicity it is assumed that the end supports are free to move axially, so that the beam deformations are purely flexural.

Let us consider a symmetrically supported rigid-plastic beam of constant mass per unit length m, constant plastic moment M_o and length 2L (Figure 2.10a,b). The beam is acted upon by a blast pulse P(t) (force per unit length) Figure 2.10c, uniformly distributed over the entire span. The load is applied instantaneously at time t = 0 and held on the beam for a time duration τ. There are generally three distinct modes of deformation depending on the magnitude of the peak pressure P_m in relation to the static collapse pressure P_o. This latter quantity is easily determined from a static collapse analysis as outlined in the previous section. The results are given by:

$$P_o = \begin{cases} 2\ M_o/L^2 & \text{for the simply supported beam} \\ 4\ M_o/L^2 & \text{for the fixed end beam} \end{cases} \qquad (2.15)$$

The above values are the exact static collapse pressures which satisfy all three requirements of collapse as given by Equation (2.14).

If a simply supported beam (for which i = 0) is subjected to its static collapse pressure, a plastic hinge will form at the midspan and rotation then occurs at the plastic hinge of the midpoint and the natural hinges at the ends as shown in Figure (2.11a). For a beam fixed at both ends, (i.e. i = 2), plastic hinges form at the fixed ends as well as the midpoint giving rise to displacement configuration which is similar to that of the simply supported beam at the collapse state.

It is therefore expected that for pressure intensities slightly beyond the static collapse pressure (i.e. $P_m > P_o$) both beams deform in the same manner. Thus any deformation mechanism that is assumed for a simply supported beam stays valid for a built-in beam except that collapse in each case occurs under different pressures P_o as given by Equation (2.15).

Using the appropriate definitions of P_o given by Equation (2.15), we can distinguish three different stages of deformation according to whether the load intensity is "low" ($P_m < P_o$), "medium" ($P_o < P_m < 3\ P_o$) or "high" ($P_m > 3\ P_o$). Experimental studies of these specific phases of loading have indicated that the deformation process is as follows:

i) Low pressure range: as long as $P_m < P_o$ the bending moment throughout the beam is less than the fully plastic moment M_o and no deformation occurs (Figure 2.12a) in the rigid-plastic sense.

ii) Medium pressure range: if the load intensity falls in the range, $P_o < P_m < 3 P_o$, the static collapse mechanism is assumed to hold, that is, deformation proceeds with a central plastic hinge and each half of the beam rotates as a rigid body. The beam continues to deform in the single hinge mode until the kinetic energy acquired under the action of pressure is wholly absorbed into plastic work at the central hinge section. Thus, plastic deformation continues until the transverse velocity of the beam is reduced to zero. At this instant the entire beam comes to rest.

iii) High pressure range: if $P_m > 3 P_o$ the single hinge mode of deformation results in a moment distribution $M(x)$ greater than the plastic moment M_o for some $0 < x < L$, where x is measured from the midspan. Consequently to satisfy the yield condition two symmetrically located plastic hinges immediately form (with the onset of loading) at a distance $\sqrt{(3P_o/P_m)}L$ from each end† (Figure 2.12c). As P_m increases indefinitely the hinges move towards the supports. In the special case of impulsive loading when $P_m \to \infty$, the hinges are momentarily formed at the support points (Reference 11). Between the hinges a flat central plastic zone exists where the bending moment $M(x) = M_o$. This region of constant moment must have zero shear, and this would only be possible if the accelerations at all points in the region vanish. Unless the pressure is held constant on the beam (i.e. rectangular pulse), the hinge points on either side of the midspan start moving

---

† For a proof of this see for example Krajcinovic (Reference 17).

toward the centre while the beam continues to deform in the transverse direction. As soon as the hinge has moved to its new position, the moment at the original section drops to a value below M_o and no further rotation occurs there. This is equivalent to a reversal of bending moment as illustrated by the dashed line on the moment - curvature diagram of Figure 2.3. According to this diagram unloading will occur rigidly when the moment M_o is removed. A permanent distortion will therefore occur at the section where the plastic hinge passes through. The segment of the beam along which the hinge has passed attains a permanent deformation that is curved in shape. The precise shape of the deflection curve is dependent on the pressure-time history P(t). In fact the curvature generated is equal to the relative angular velocity divided by the velocity of motion of the hinge along the beam (see Section 2.4.2). The beam segments on either side of the travelling hinge rotate as rigid bodies. As the pressure decreases toward the end of the loading pulse, the hinges move closer to the centre and finally coalesce to form a central plastic hinge. Thereafter the beam deforms according to the single hinge mode until the motion ceases. It is worthy of note that in the special case of a rectangular pulse the two hinges remain stationary while the load is applied and then converge toward the midspan when unloading occurs (i.e. for $t > \tau$). (It is tacitly assumed that the pressure is of sufficient intensity so that the motion continues up to or beyond $t = \tau$).

In Figure 2.13 the final deflection shape of the beam is depicted for some representative values of $3P_o/P_m$ when the loading is assumed to be a rectangular pulse. It can be seen from this figure that as $3P_o/P_m$

decreases (i.e. as the load becomes impulsive) the central curved part of the permanently distorted beam increases in size.

2.4.2. KINEMATIC CONDITIONS ACROSS THE MOVING HINGE

The various quantities on either side of the travelling plastic hinge are required to obey certain kinematic restraints which are described in the following. We restrict the following discussion to the travelling hinge mechanism of Figure 2.12c. Owing to its symmetrical shape we refer to the left-hand half of this mechanism.

Let $\rho(t)$ denote the distance of the hinge point from the beam centre and $w_\rho(t)$ be the transverse displacement at the hinge, both quantities varying with time t. In order to satisfy the requirements of geometrical compatibility when shear deformations are ignored, the displacement w_ρ and velocity $\dot{w}_\rho$ must be continuous across the moving hinge section for all time t. Thus,

$$[w_\rho] = w(x=\rho^+,t) - w(x=\rho^-,t) = 0$$

$$[\dot{w}_\rho] = \dot{w}(x=\rho^+,t) - \dot{w}(x=\rho^-,t) = 0 \qquad (2.16)$$

where [ ] denotes the discontinuity of the enclosed quantity across the hinge and ρ^-, ρ^+ designate sections just to the right and just to the left, respectively, of the hinge section.

Also we employ the following derivative notation:

$$(\dot{}) = \frac{\partial}{\partial t}(\,) \qquad ; \qquad (\,)' = \frac{\partial}{\partial x}(\,)$$

Consider a particular instant of time t when the hinge is at a typical distance $\rho(t)$ from the centre. In an infinitesimal increment of time Δt the hinge moves an incremental distance $\Delta\rho$ towards the centre. During this interval of time the two segments of the beam separated by the plastic hinge rotate by an amount $\Delta\theta$ with respect to each other (Figure 2.14). The permanent curvature acquired by the differential element of length $\Delta\rho$ is

$$\kappa = \frac{\Delta\theta}{\Delta\rho} = \frac{\Delta\theta}{\Delta t} \Big/ \frac{\Delta\rho}{\Delta t}$$

or in the limit as $\Delta t \to 0$

$$\kappa = \dot{\theta} \Big/ \dot{\rho} \qquad (2.17)$$

where $\dot{\rho}$ is the velocity of the moving hinge. Since $\dot{\theta}$ is the relative angular velocity of the two segments of the beam on either side of the hinge section, we can write

$$\dot{\theta} = - \left[\dot{w}' \right]_{\rho} \qquad (2.18)$$

where the minus sign arises from the sign conventions of the problem.

Observing that the segment $0 < x < \rho(t)$ remains flat (corresponding to zero curvature) throughout the motion, we can interpret the quantity κ as the difference in curvature across the hinge point. Thus, for small deflections (i.e. $\theta^2 << 1$), we may write

$$\kappa = \left[w'' \right]_{\rho} \qquad (2.19)$$

Using Equations (2.18) and (2.19) in Equation (2.17), yields the following jump condition:

$$[\dot{w}'_\rho] + \dot{\rho}\,[w''_\rho] = 0 \tag{2.20}$$

Thus taking account of the discontinuity in curvature, the angular velocity $\dot{\theta}$ is discontinuous across a non-stationary hinge point (for which $\dot{\rho} \neq 0$). It can also be shown that

$$[\dot{w}_\rho] + \dot{\rho}\,[w'_\rho] = 0 \tag{2.21}$$

which implies that across a moving hinge (i.e $\dot{\rho} \neq 0$), owing to the continuity of velocity (Equation (2.16)), the slope angle θ must be continuous. From the differentiation of Equation (2.21) with respect to time t it follows that

$$[\ddot{w}_\rho] + \dot{\rho}\,[\dot{w}_\rho] + \ddot{\rho}\,[w'_\rho] = 0 \tag{2.22}$$

Now, since the slope is continuous across a travelling hinge, the last term on the left hand side vanishes and we have

$$[\ddot{w}_\rho] + \dot{\rho}\,[\dot{w}_\rho] = 0 \tag{2.23}$$

As an implication of the above jump condition, the transverse acceleration must be discontinuous across a moving hinge.

The significance of the above kinematic relations become apparent when we consider time-dependent, kinematically admissible displacement and velocity profiles.

We are now in a position to formulate our mathematical model of the motion of an axially constrained rigid-plastic beam under uniformly distributed, time-dependent loading P(t).

CHAPTER III

FORMULATION AND ANALYSIS OF THE PROBLEM

3.1 STATEMENT OF THE PROBLEM

This chapter presents a theoretical study of the behaviour of a rigid-perfectly plastic beam, symmetrically supported with constraints against in-plane displacements at the ends. The beam is subjected to a suddenly applied blast-type pressure pulse uniformly distributed over the width and the whole length of the beam. Although the governing equations are derived for a general section geometry and pressure-time relationship, they are solved only for the simplest case, that of a beam with rectangular section acted upon by a rectangular pulse such as the one shown in Figure 3.1. In formulating the problem the assumptions of Section 2.2 are employed. Both the fixed end beam, allowing no rotation except by plastic hinge, and the simply supported beam, allowing rotation by natural hinges will be discussed. An in-depth analysis that retains the influence of finite deflections or geometry changes is presented only for the case of a simply supported beam. It is believed that the treatment of a fixed-end beam closely resembles that of a simply supported beam when appropriate modifications are made in the final results of the latter analysis. It will be shown in Section 3.4 how the results for these two cases may be expressed in a common form. The theoretical analysis outlined herein is intended to cover all ranges of load intensities beyond the static collapse load.

3.2 STATIC ANALYSIS

In the following section the basic concepts of limit analysis are

extended to axially constrained simply supported beams loaded statically in which axial forces as well as bending moments must be taken into account. The role of the change of geometry on the load carrying capacity of the beam will be investigated. In this study, the load carrying capacity is estimated by assuming an approximate mechanism of deformation. Initially it is presumed that the zero-stress axis remains within the beam cross-section so that membrane forces and bending moments are coexistent. A purely membrane analysis is also presented to account for the case when the zero stress axis falls outside the beam surface.

It will be observed that when finite deflections or geometry changes are permitted, the beam can support external loads considerably greater than those predicted by the infinitesimal bending-only-theory. This increased load carrying capacity is shown to be a result of the favourable influence of membrane forces that accompany finite transverse deflections.

3.2.1 APPROXIMATE LOAD CARRYING CAPACITY OF A SIMPLY SUPPORTED BEAM AT FINITE DEFLECTIONS (BENDING AND MEMBRANE THEORY)

Consider a rigid-plastic beam (Figure 3.2) of uniform rectangular cross-section width b and depth h, simply supported at the outer edges x = ± L and carrying a uniformly distributed lateral load of intensity P (force per unit length). The edge restraints are such that the ends of the beam at the centroidal axis are prevented from in-plane movements along the x-axis. Tensile axial forces N are induced in the beam due to the transverse deflection and increased length of the beam.

At the limit load the beam will tend to deform plastically according to the single-hinge mechanism of Figure 3.3. This mechanism, however, is known to be correct only at zero deflection when no membrane forces are

generated. Exact theoretical solutions when finite deflections are retained in the analysis are difficult to obtain, thus one has to resort to approximate solutions.

In developing an approximate method, we start by considering the single-hinge configuration of Figure 3.3 as a first approximation to the deformed shape of the beam during small but finite deflections. The membrane forces are no longer zero and must be considered in formulating the problem. In the following we shall apply the principle of virtual work to the determination of the limit load.

Consider the equilibrium configuration of the beam at the instant of plastic collapse (Figure 3.4). This mode of deformation has one degree of freedom defined by the rotation θ of each half of the beam. The angular displacement θ is thought of as an incremental displacement in the collapse state and is therefore a "small" quantity.

Let θ receive a variation $\delta\theta$ in the neighbourhood of the given configuration, Figure 3.4. Then observing that the hinge rotation at the central section is the sum of the rotations of the two portions of the beam, we have

$$\delta\psi = 2\delta\theta \tag{3.1}$$

where $\delta\psi$ is the increment of rotation at the hinge point as defined previously in Section 2.3.3.

Due to the increment $\delta\theta$, the length of the beam will receive a virtual extension $\delta\varepsilon$ given by

$$\delta\varepsilon = \delta(2L \sec\theta) = 2L \sec\theta \tan\theta \, \delta\theta \qquad (3.2)$$

For sufficiently small magnitudes of θ so that $\theta^2 << 1$, Equation (3.2) can be rewritten in the following simplified form

$$\delta\varepsilon = 2L\theta\delta\theta \qquad (3.3)$$

These internal deformations $\delta\psi$, $\delta\varepsilon$ are concentrated at the central plastic hinge section and are developed under a critical combination of axial force N and bending moment M at the hinge section.

The virtual work dissipated in the plastic hinge as a result of these deformations is

$$\delta W_{int} = N\delta\varepsilon + M\,\delta\psi \qquad (3.4)$$

As the plastic hinges always absorb work, no question of sign arises and we shall only be concerned with the numerical values of N, M and the corresponding deformations $\delta\varepsilon$, $\delta\psi$. It should be remarked in passing that in the theory of limit analysis it is customary to speak of rate of dissipation of energy rather than the internal energy itself. Since we are only concerned with small deformations, it is immaterial whether we speak of increment of deformation or of deformation rates. Thus, writing the internal energy absorbed in a virtual displacement of the beam is exactly equivalent to writing the rate of dissipation of energy at the plastic hinge.

In moving through the virtual displacement $\delta\theta$, the work done by the

applied uniform pressure P is

$$\delta W_{ext} = \delta\{\int_{-L}^{L} Pw(x)\, dx\} = P\delta S \tag{3.5}$$

where w(x) denotes the spatial distribution of deflection resulting from the assumed collapse mechanism, and S is the area swept by the deforming beam, so that

$$S = \int_{-L}^{L} w(x)\, dx \tag{3.6}$$

and for the mechanism of Figure 3.3

$$S = w_o L \tag{3.7}$$

where $w_o = w(x = 0)$ is the central deflection. Therefore δS which corresponds to the variation or virtual change in S can be written as:

$$\delta S = L\delta w_o \approx L^2\delta\theta \tag{3.8}$$

The theorem of virtual work thus furnishes the relation

$$\delta W_{int} = \delta W_{ext} \tag{3.9}$$

so that

$$N\delta\varepsilon + M\delta\psi = P^* \delta S \tag{3.10}$$

where P^* denotes the load carrying capacity of the beam at finite deflections.

It can easily be shown that Equation (3.10) is equivalent to writing the equilibrium equation of the beam in its deformed configuraiton.

Using the results of Equations (3.1), (3.3) and (3.8) in Equation (3.10) and observing that $\delta\theta$ is an arbitrary variation in the quantity θ, yields

$$P^* = \frac{2M_o}{L^2}\left(\frac{M}{M_o} + \frac{N}{M_o} w_o\right) \tag{3.11}$$

With reference to nomenclature used in Chapter 2 and Equations (2.4), (2.7) and (2.8), we have for a rectangular cross-section

$$\bar{r}_p = h/2 \quad ; \quad \bar{y}_e = e/2 \quad ; \quad N = 2\sigma_o\, b\, e \tag{3.12a,b,c}$$

$$N_o = \sigma_o\, b\, h \; ; \; M_o = \sigma_o\, b\, h^2/4 \tag{3.12d,e}$$

Upon substitution of the above quantities into Equation (2.6a), the yield condition for a rectangular section turns out to be

$$\frac{M}{M_o} = 1-\left(\frac{N}{N_o}\right)^2 \tag{3.13}$$

or using the dimensionless quantities defined by Equation (2.9)

$$\bar{m} = 1 - \bar{n}^2 \tag{3.13a}$$

Equation (3.13) can be represented by a pair of parabolic yield curves in a system of cartesian coordinates with $\frac{M}{M_o} = \bar{m}$ as abscissa and $\frac{N}{N_o} = \bar{n}$ as ordinate (Figure 3.5).

The flow rule (Equation (2.13)) appropriate to the parabolic yield function $f \equiv \bar{m} + \bar{n}^2 - 1$ requires that

$$\frac{N_o}{M_o} \frac{\delta\epsilon}{\delta\psi} = 2 \frac{N}{N_o} \tag{3.14}$$

provided that the zero stress axis lies within the beam cross-section.

From Equation s(3.1) and (3.3), the ratio $\delta\epsilon/\delta\psi$ is

$$\frac{\delta\epsilon}{\delta\psi} = L\theta = w_o \tag{3.15}$$

Thus, the flow rule as expressed by Equation (3.14) becomes

$$\frac{N}{N_o} = \frac{N_o}{M_o} \cdot \frac{w_o}{2} = \frac{2w_o}{h} \tag{3.16}$$

where the last step follows from Equations (3.12d,e). It is of passing interest to note that from the strained geometry of the hinge section (Figure 2.5d) $\delta\epsilon/\delta\psi = e$. This implies that for the collapse mechanism of Figure 3.3, the distance between the zero-stress axis and the central axis (which overlaps with the equal area axis for the symmetrical section considered) is also the vertical distance of the central axis from the original undeformed beam at the hinge point, (i.e. $w_o = e$).

Substitution of Equation s(3.16) and Equation (3.13) into (3.11) furnishes the relation

$$P^* = P_o \left[1 + 4 \left(w_o/h\right)^2\right] \qquad (3.17)$$

where $P_o = 2M_o/L^2$ is the load carrying capacity of the undeformed simply supported beam (for which $w_o = 0$), a result already obtained by the bending only theory in which the influence of finite deflections is ignored. Equation (3.17) establishes the load carrying capacity of the beam at a specified central deflection w_o. As the beam acquires a finite deformation, the axial force N increases in direct proportion according to Equation (3.16). A point is reached where the critical combination of N and M occurs at sections other than the central. This leads to a vioolation of the plasticity condition given by Equation (3.13). Therefore, the mechanism of Figure 3.3 is in effect, only at the onset of collapse or early stages of deformation when bending action is predominant. With increased transverse displacement in-plane tensile forces come into play, thereby causing a reduction in bending moment at the centre where the deflection is greatest. At points symmetrically located on either side of the midspan, however, the combination of moments induced by the axial force and the uniform pressure reaches a value sufficient to cause full plasticity in those regions. Consequently the assumed single degree of freedom system does not represent the actual mode of collapse of the beam whose change in geometry is permitted, and the corresponding central plastic hinge is fictitious. Since an approximate location rather than the exact location of the yield hinge has been used in the foregoing static analysis, P^* (as given by Equation (3.17)) must exceed the actual load carrying capacity of

the beam in accordance with the kinematic theorem of limit analysis, as defined in Section 2.3.5.

Of the three master conditions (2.14), only those of equilibrium and mechanism have so far been satisfied. A deformation shape has been guessed, and the writing of the virtual work equation ensured that equilibrium has been satisfied. The values of M and N must be corrected in successive stages of deformation until the conditions of mechanism, equilibrium and yield are satisfied simultaneously leading to an exact solution (i.e. coincidence of upper and lower bounds). The analysis of the assumed approximate model is considerably simpler than the exact analysis outlined above.

The preceding analysis is based on the assumption that the zero-stress axis remains within the beam cross-section (i.e. $e < h/2$) or what amounts to the same, the single hinge mechanism of Figure 3.3 is valid for maximum deflections not exceeding the half-depth of the beam (i.e. $w_o < h/2$). As the deflection w_o approaches $h/2$, the axial force N approaches its fully plastic limit N_o and the moment carrying capacity of all the sections along the beam reduces to zero. Thereafter the behaviour of the beam is governed by in-plane membrane forces $N = N_o$ and the associated deformation is essentially one of stretching. This corresponds to tensile yield stress across the whole cross-section of the beam, so that the distribution of normal stress is as shown in Figure 3.6a. No matter where the zero-stress axis may lie outside the beam surface, the fully plastic stress distribution consists of all fibres yielding in tension. Therefore, the state of stress is represented by the point $(\bar{n}, \bar{m}) \equiv (1,0)$ which we have already obtained as part of the interaction curve (Figure 3.5). Despite the fact that the moment is zero in this case, the section can still

rotate by an amount $\delta\psi$ as shown by the strained geometry of the section (Figure 3.6b). Since $e > h/2$, it follows that the rotation $\delta\psi$ can have any arbitrary magnitude satisfying the condition;

$$\delta\psi < \frac{2\delta\varepsilon}{h} \tag{3.18}$$

Equation (3.18) can also be obtained by considering the conditions set by the flow law at the point $(\bar{n}, \bar{m}) \equiv (1,0)$ of the yield curve. At such a corner point, the direction of the exterior normal to the curve cannot be uniquely defined and it may have any direction between the normals to the two portions of the parabola (lying above and below the $\bar{n}$ axis) at $(\bar{n}, \bar{m}) \equiv (1,0)$. Therefore, by geometry the slope of the deformation vector with components $(N_o\,\delta\varepsilon, M_o\,\delta\psi)$ is restricted to lie between the values $\pm 1/2$. i.e.

$$-\frac{1}{2} < \frac{M_o\delta\psi}{N_o\delta\varepsilon} < \frac{1}{2} \tag{3.19}$$

Recognizing that $M_o/N_o = h/4$ for a rectangular cross-section, Equation (3.19) can be rewritten as,

$$-\frac{2}{h} < \frac{\delta\psi}{\delta\varepsilon} < \frac{2}{h} \tag{3.20}$$

The next subsection is devoted to a purely membrane type analysis for predicting the load carrying capacity of the beam at moderately large deflection ($w_o > h/2$).

3.2.2 THE LOAD CARRYING CAPACITY OF BEAMS AT MODERATELY LARGE DEFLECTIONS (MEMBRANE ANALYSIS).

For the reasons outlined previously, we shall here consider the static response of a beam that carries the load substantially by the membrane force N_o. Such a structure, because of its initial curvature, can maintain a continuous distributed loading in equilibrium even though it has no bending stiffness and therefore simply utilizes its membrane strength. The structural behaviour of the beam at moderately large deflections (for which $w_o > h/2$, $(w')^2 << 1$) is therefore similar to that of a uniformly loaded perfectly flexible cable (i.e. bending moment at any point on the cable is zero) as shown in Figure 3.7. The equilibrium equation of the beam in this case may be obtained from Equation (3.10) by setting $M = 0$ and $N = N_o$, thus

$$N_o \, \delta\varepsilon = P^* \, \delta S \tag{3.21}$$

If the assumption of small deflection is retained (i.e. if the sag of the beam is small in proportion to its length) so that $(w')^2 << 1$, the virtual elongation of the beam irrespective of the shape of its deflected curve is

$$\delta\varepsilon = \delta\{\int_{-L}^{L} \frac{1}{2} (w')^2 \, dx\} = \int_{-L}^{L} w' \, \delta w' \, dx \tag{3.22}$$

Equation (3.22) when integrated by parts results in

$$\delta\varepsilon = \left[w' \, \delta w \right]_{-L}^{L} - \int_{-L}^{L} w'' \, \delta w \, dx \tag{3.23}$$

The first term in the above expression may be deleted by virtue of the kinematic boundary conditions of the problem. Making use of Equations (3.6) and (3.23), we can rewrite the equilibrium Equation (3.21) as

$$\int_{-L}^{L} \left[P^{*} + N_{o}\, w''(x) \right] \delta w(x)\, dx = 0 \qquad (3.21a)$$

Since $\delta w(x)$ is an arbitrarily imposed virtual displacement in the interval $-L < x < L$, we must have

$$N_{o} \frac{d^{2}w}{dx^{2}} = - P^{*} \qquad (3.24)$$

The solution of which leads to

$$w(x) = w_{o} - \frac{P^{*}}{2N_{o}}\, x^{2} \qquad (3.25)$$

Equation (3.25) defines the shape of the deflected membrane as being parabolic. At the edge supports, where $x = \pm L$ and $w = 0$ the foregoing equation reduces to

$$w_{o} = \frac{P^{*}}{2N_{o}}\, L^{2} \qquad (3.26)$$

Specialyzing to the case of a beam with rectangular cross-section, we can write Equation (3.26) as

$$P^* = \frac{8M_o}{L^2} \cdot \frac{w_o}{h} \tag{3.27}$$

The load carrying capacity P^* of a simply supported beam at finite deflections is therefore given by

$$P^*/P_o = \begin{cases} 1 + 4(\frac{w_o}{h})^2 & \text{for } w_o/h < 1/2, \text{ membrane and bending} \\ 4(\frac{w_o}{h}) & \text{for } w_o/h > 1/2, \text{ membrane only} \end{cases} \tag{3.28}$$

where $P_o = 2M_o/L^2$

A load-deflection curve is shown in Figure 3.8 based on the theoretical results of Equation (3.28). It shows that when the ends are fully constrained, the load rises rapidly above P_o especially as w_o approaches h/2. The limit load, as ordinarily computed from undeflected configuration, is highly conservative under these circumstances.

3.3 DYNAMIC ANALYSIS

The purpose of the present study is to predict the permanent deformation of a rigid-plastic simply supported beam (whose properties are specified in the previous section) acted on by a uniformly distributed loading with a rectangular time variation (i.e. instantaneous loading and unloading as shown in Figure 3.1). For the validity of the following rigid-plastic dynamic analysis, the duration of loading τ is restricted to

take on values in the approximate range (see Appendix A).

$$0.17\, P_o/P_m < \tau/T_e < 1$$

where T_e is the fundamental period of elastic vibration of the simply supported beam.

Deflections are considered to be in the range where both bending moments and membrane forces are important. This effect may be accounted for by considering the equilibrium of the beam in its deflected position. The equation of dynamic equilibrium of the beam is readily obtained simply by introducing the contribution of inertia terms into the equilibrium equation developed in the foregoing static analysis, i.e. Equation (3.10). If the mass per unit length of the beam is denoted by m the inertia load at any position x along the beam equals $-m\ddot{w}(x,t)$, by D'Alembert's principle, and the virtual work equation takes the form;

$$N\delta\epsilon + M\delta\psi = \int_{-L}^{L} [P(t) - m\ddot{w}(x,t)]\, \delta w(x,t)\, dx \qquad (3.29)$$

Equation (3.29) is independent of the mechanism of deformation and the cross-sectional shape of the beam. The discussion presented in the earlier sections reveals that dynamic plastic action will occur only if

$$P_m > P_o = 2M_o/L^2$$

For $P_m = P_o$ the beam yields indefinitely slowly and inertia forces do not

arise, and so time is measured from the first instant the above inequality is satisfied. In the following theoretical analysis, the single hinge mechanism of Figure 3.3 is assumed to hold if the peak pressure P_m falls in the medium range ($P_o < P_m < 3P_o$). It is known from the arguments given in the preceding section on static analysis that this mode of deformation violates the yield criterion (Equation (3.13)) when the influence of membrane forces is included in the analysis. Nevertheless, speaking from an engineering standpoint, the results can serve as good approximations to the real problem.

For high intensity loading ($P_m > 3P_o$) the travelling plastic hinge mechanism of Figure 2.12c is assumed to be valid. A development and full discussion of the governing equations of motion for both the travelling and static mechanism will be given in the following sections. In analogy to the static case in order to account for the influence of moderately large deflections ($w_o/h > 1/2$), a purely membrane analysis is also presented for both medium and high intensity loadings. It is assumed that the beam is initially unstrained ($w(x,0) = 0$) and at rest ($\dot{w}(x,0) = 0$).

3.3.1 MEDIUM LOAD ($P_o < P_m < 3P_o$)

Two phases must be distinguished in which the motion of the beam is governed by different equations.

Phase I ($0<t<\tau$)

a) Small deflections

If it is assumed that the shape of the displacement field in this case is the same as the deformation profile used for the corresponding static analysis, then

$$w(x,t) = w_o(t)\left[1-\frac{|x|}{L}\right] \quad \text{for } -L<x<L \tag{3.30}$$

where $w_o(t) = w(0,t)$ is the central deflection at any instant of time t. The prescribed boundary condition that w vanishes at $x = \pm L$ is satisfied by Equation (3.30) and the initial conditions will be satisfied if

$$w_o(0) = \dot{w}_o(0) = 0 \tag{3.31}$$

The substitution from Equation (3.30) into the dynamic equilibrium Equation (3.29), followed by an integration with respect to x from x = -L to x = L, results in

$$N\delta\varepsilon + M\delta\psi = \left[P(t) - \frac{2}{3}\, m\, \ddot{w}_o(t)\right]L\delta w_o(t) \tag{3.32}$$

This relationship is considered to hold for any arbitrary virtual displacement $\delta w_o = L\,\delta\theta$ imposed on the deflected configuration of the beam (Equation 3.30). On account of this and the geometrical relationships (3.1) and (3.3), Equation (3.32) becomes

$$Nw_o(t) + M = \frac{L}{2}^2\left[P(t) - \frac{2}{3}\, m\ddot{w}_o(t)\right] \tag{3.33}$$

Now the quantities N, M appearing in this equation are the critical stress resultants at the central hinge station and are therefore related by the interaction relation of Equation (3.13). The equilibrium Equation (3.33) in conjunction with the plasticity condition (3.13) and the flow rule (3.16) yields

$$M_o\left(1 + \frac{4}{h^2} w_o^2(t)\right) = \frac{L^2}{2} \left[P(t) - \frac{2}{3} m\ddot{w}_o(t)\right] \tag{3.34}$$

which upon rearrangement may be written

$$\ddot{w}_o(t) + \lambda w_o^2(t) = \frac{3}{2m}\left[P(t) - P_o\right] \tag{3.35}$$

where the parameter λ is given by

$$\lambda = \frac{6P_o}{mh^2} \tag{3.36}$$

Equation (3.35) is a nonlinear second order ordinary differential equation in terms of the time-dependent variable $w_o(t)$ which is yet to be determined. So far no restriction has been made upon the time history of the pressure P(t), thus implying that Equation (3.35) is applicable to a general load-time function satisfying the definition of blast-type loading (assumption iv). However, this equation can only be solved in analytic form if the load is a rectangular pulse. If we hereafter restrict ourselves to rectangular pulses only, our problem reduces to solving the differential equation

$$\ddot{w}_o + \lambda w^2{}_o = \nu \tag{3.37}$$

where

$$\nu = \frac{3}{2m}(P_m - P_o) \quad , 0 < \nu < \frac{3P_o}{m} \tag{3.38}$$

Equation (3.37) is satisfied during the pulse duration τ with ν = constant and is subject to initial conditions expressed by Equation (3.31).

Multiplying both sides of Equation (3.37) by $2\dot{w}_o$, we obtain

$$\frac{d}{dt}(\dot{w}_o)^2 + \frac{2\lambda}{3}\frac{d}{dt}(w_o)^3 - 2\nu\frac{d}{dt}(w_o) = 0$$

which after integration with respect to t yields the result

$$\dot{w}_o^2 + \frac{2\lambda}{3} w_o^3 - 2\nu\, w_o = \text{constant} \tag{3.39}$$

In order to fulfill the initial conditions of the problem (Equation 3.31) the constant of integration must vanish and Equation (3.39) can be re-written in the form

$$(\frac{dw_o}{dt})^2 = 2\nu w_o - \frac{2\lambda}{3} w_o^3$$

or

$$\frac{dw_o}{dt} = \sqrt{2\nu}\left[w_o - \frac{\lambda}{3\nu} w_o^3\right]^{1/2} \tag{3.40}$$

Separation of variables followed by an integration of Equation (3.40) leads to

$$t = \frac{1}{\sqrt{2\nu}} \int_0^{w_o} \frac{dw_o}{\left[w_o(1-w_o/\alpha^2) \right]^{1/2}} \tag{3.41}$$

where

$$\alpha^2 = \frac{3\nu}{\lambda} = \frac{3}{4} h^2 \left(\frac{P_m}{P_o} - 1 \right) ; \quad 0 < \alpha < \sqrt{3/2}\, h \tag{3.42}$$

Within the physical restrictions of the problem $0 < w_o < \frac{h}{2}$, i.e. $w_o < \alpha$. Therefore, with the substitution $w_o = \alpha \cos^2 \phi$ into Equation (3.41) we obtain after some algebraic manipulation

$$t = \sqrt{(\alpha/\nu)} \int_{\phi}^{\pi/2} \frac{d\phi}{\sqrt{(1 - \frac{1}{2} \sin^2\phi)}} \tag{3.43}$$

where the lower limit of the integral is restricted to be in the range given by

$$\cos^{-1} (1/6)^{1/4} < \phi < \frac{\pi}{2} \tag{3.43a}$$

The integral in Equation (3.43) can be evaluated explicitly, so that

$$t = \sqrt{(\alpha/\nu)} \left[K (1/\sqrt{2}) - F (1/\sqrt{2}, \phi) \right] \tag{3.44}$$

where

$$K (1/\sqrt{2}) \equiv K = \int_0^{\pi/2} \frac{d\xi}{\sqrt{(1-\frac{1}{2} \sin^2\xi)}}$$

is the complete ellipic integral of the first kind with modulus $1/\sqrt{2}$, and

$$F(1/\sqrt{2},\phi) = \int_0^{\phi} \frac{d\xi}{\sqrt{(1-\frac{1}{2}\sin^2\xi)}}$$

is the incomplete elliptic integral of the first kind with modulus $1/\sqrt{2}$, amplitude ϕ. A comprehensive study of elliptic integrals and functions is given by Byrd and Friedman (Reference 24). Equation (3.44) yields the time t required to reach a specific deflection $w_o(t)$. Upon regrouping the terms, Equation (3.44) becomes

$$F\ (1/\sqrt{2},\ \phi) = K - at \qquad (3.44a)$$

where

$$a^2 = \frac{\nu}{\alpha} = \frac{\sqrt{3}P_o}{mh}\left(\frac{P_m}{P_o} - 1\right)^{1/2} \qquad (3.45)$$

Let $u \equiv F\ (1/\sqrt{2},\ \phi)$, then we can express the inverse function of u as ϕ = am u = amplitude of u. Considered as a function of u,

$$\begin{aligned} \cos\phi &= \cos(\text{am } u) = \text{cn}(u) \\ \sin\phi &= \sin(\text{am } u) = \text{sn}(u) \\ \sqrt{(1-\tfrac{1}{2}\sin^2\phi)} &= d\phi/du = d(\text{amu})/du = \text{dn}(u) \end{aligned} \qquad (3.46)$$

where cn(u), sn(u) and dn(u) are Jacobian elliptic functions. These are of interest to us principally for the purpose of evaluating the elliptic integral F. Relevant information regarding the properties of these functions can be found in (Reference 24). Thus

$$w_o(t) = \alpha\, cn^2(u) = \alpha\, cn^2(K-at) \tag{3.47}$$

Differentiating Equation (3.47) with respect to time t gives

$$\dot{w}_o(t) = -a\frac{dw_o}{du} = 2a\alpha\, cn(u) \cdot sn(u) \cdot dn(u) \tag{3.48}$$

Equations (3.47) and (3.48) determine the displacement and velocity of the central point respectively as a function of time t. Since no energy is recoverable from a rigid-plastic beam, the motion continues until all the acquired kinetic energy is dissipated in plastic work. At this instant the entire beam comes to rest, i.e. $\dot{w}_o = 0$.

From the solution of Equation (3.48), it follows that the plastic deformation ceases at $t = t_f$ when

$$u_f = K - at_f = 0$$

where the subscript f designates the final state of the quantity to which it is attached. Hence, the instant at which the beam comes to rest is given by

$$t_f = K/a = K\sqrt{(mh/P_o)}\ \left\{\frac{1}{3(P_m/P_o - 1)}\right\}^{1/4} \qquad (3.49)$$

in which the numerical value of K = 1.854075 as obtained from the tables of elliptic integrals (Reference 24). The maximum deflection of the midpoint which is the final permanent deflection in a rigid-plastic theory is found by replacing t in expression (3.47) by t_f as given by Equation (3.49). Thus

$$w_o(t_f) = \delta_f = \alpha$$

or in non-dimensional form

$$\frac{\delta_f}{h} = \frac{\sqrt{3}}{2}\ \left(\frac{P_m}{P_o} - 1\right)^{1/2} \qquad (3.50)$$

It is seen that the final central deflection δ_f of the beam in this phase of motion (i.e. $0 < t < \tau$) is obtainable directly from the knowledge of the loading parameter P_m/P_o. In deriving the expression (3.50) we have assumed that the deformation finishes before the load application is completed, that is $t_f < \tau$ or $K < a\tau$. This situation arises due to the effect of axial constraints. When small lateral movements of the end supports are permitted as in the conventional first order bending analysis, the beam reaches its final position at $t_f = \frac{P_m}{P_o}\tau$ (References 10, 17). As a result, the duration of the beam response t_f is always greater than the

duration of the pressure pulse τ which implies that in this case the beam cannot cease moving so long as the applied load persists.

Within the framework of small deflection theory, Equation (3.50) holds for $\delta_f / h < 1/2$ or

$$1 < \frac{P_m}{P_o} < \frac{4}{3} \tag{3.51}$$

If inequality (3.51) is not satisfied (i.e. if $P_m/P_o > 4/3$), then the so-called "string stage" is reached whereby the behaviour of the beam is governed by in-plane membrane forces of constant magnitude N_o (Reference 11).

b) Moderately large deflections ($w_o/h > 1/2$) (membrane theory)

In view of the foregoing comments, the beam behaves as a perfectly flexible plastic membrane when the condition $w_o/h > 1/2$ is reached. For the latter case, the equilibrium equation of the beam may be obtained from Equation (3.29) by setting $M = 0$ and $N = N_o$, thus

$$N_o \, \delta\varepsilon = \int_{-L}^{L} \left[P(t) - m\ddot{w}(x,t) \right] \delta w(x,t) \, dx$$

Utilizing the same expression for $\delta\varepsilon$ as was used previously for the static analysis, i.e. Equation (3.23) and noting that $\delta w(x,t)$ is arbitrary in the interval $-L < x < L$, the above equation reduces to

$$N_o \frac{\partial^2 w}{\partial x^2} = m \frac{\partial^2 w}{\partial t^2} - P(t) \tag{3.52}$$

Equation (3.52) is the differential equation of motion of a simple membrane whose tensile resistance is N_o, and which is subjected to uniformly distributed transverse force P(t) per unit length. It is worth emphasizing that in deriving Equation (3.52) we have restricted our consideration to small (but finite) deflections in the sense that the relative change in arc length of the membrane at each point is small, that is, $(w')^2 << 1$. Equation (3.52) can also be interpreted as the differential equation governing the small vibrations of a "string" under the action of an applied force P(t) per unit length. Hence, this phase of motion is often referred to as the "plastic string" phase. Owing to its finite thickness, the beam does not strictly behave as a plastic string, so that although the moment carrying capacity of the beam is zero in this case, each cross-section undergoes an extension $\delta\varepsilon$ (at the central axis) as well as a rotation $\delta\psi$, the ratio of which $\delta\psi/\delta\varepsilon$ is limited to lie in the range given by Equation (3.20).

It follows from the results of the foregoing section, that if $a\tau > K$, and also $P_m/P_o > 4/3$, then the transition from beam to string behaviour occurs during the first phase of the beam motion when $0 < t < \tau$. Denoting by t_s, the instant at which the string phase is initiated, we have

$$w_o(t_s) = \alpha\, cn^2(K - at_s) = \alpha \cos^2\phi_s = \frac{h}{2} \qquad (3.53a)$$

where

$$\phi_s = \cos^{-1}\sqrt{(h/2\alpha)} = \cos^{-1}\left[\frac{1}{3\left(\frac{P_m}{P_o} - 1\right)}\right]^{1/4} \qquad (3.53b)$$

and from Equations (3.44) and (3.45)

$$t_s = \frac{1}{a}\left[K - F\left(1/\sqrt{2},\ \phi_s\right)\right] \tag{3.53c}$$

for $0 < t_s < t_f \left(= \frac{K}{a}\right) < \tau$

For convenience, we introduce the spatial coordinate transformation

$$x = x_o - L \tag{3.54}$$

where x_o is measured from the left-hand support. Thus, $x_o = 0,\ 2L$ at the left and right-hand supports, respectively, and $x_o = L$ at the beam centre (Figure 3.9).

If we take a new time origin corresponding to the instant t_s then the initial central displacement and initial centre point velocity using Equations (3.53a) and (3.40), are

$$\begin{aligned} w_o\,(t^* = 0) &= h/2 \\ \dot{w}_o\,(t^* = 0) &= \left[(3P_m - 4P_o)\ h/2m\right]^{1/2} \qquad \text{for } P_m/P_o > 4/3 \end{aligned} \tag{3.55}$$

where $t^* = t - t_s$.

Thus we arrive at the initial-boundary value problem

$$\text{D.E.}\quad \ddot{w}(x_o,\, t^*) = c^2 w''(x_o, t^*) + \begin{cases} P_n/m & \text{for } 0 < t^* < \tau - t_s \\ 0 & \text{for } \tau - t_s < t^* \end{cases} \qquad (3.56a,b)$$

$$\text{B. C.}\quad \begin{aligned} w(0, t^*) &= 0 \quad ; \; t^* > 0 \\ w(2L, t^*) &= 0 \quad ; \; t^* > 0 \end{aligned} \qquad (3.57)$$

$$\text{I.C.}\quad \begin{aligned} w(x_o,\, 0) &= w_o(0)\, \Phi(x_o) \quad ; \; 0 < x_o < 2L \\ \dot{w}(x_o,\, 0) &= \dot{w}_o(0)\, \Phi(x_o) \quad ; \; 0 < x_o < 2L \end{aligned} \qquad (3.58)$$

where

$$c = \sqrt{(N_o/m)} \qquad (3.59)$$

and

$$\Phi(x_o) = \begin{cases} x_o/L & \text{for } 0 < x_o < L \\ (2 - x_o/L) & \text{for } L < x_o < 2L \end{cases} \qquad (3.60)$$

and $w_o(0)$, $\dot{w}_o(0)$ are given by the first and second parts of Equation (3.55), respectively.

A formal solution of the problem satisfying the two boundary conditions of Equation (3.57) can be represented by an infinite series of the form

$$w(x_o, t^*) = \sum_{n=1,3,5,\ldots}^{\infty} \Psi_n(t^*) \sin\left(\frac{n\pi x_o}{2L}\right) \qquad (3.61)$$

where the even modes have been discarded owing to the symmetry of the problem. The coefficients $\Psi_n(t^*)$ appearing in the above summation are

unknown functions of time which must satisfy Equations (3.56) and (3.58).

It is convenient to divide the analysis into two stages such that during the first stage the load is still applied, and then a second stage throughout which the load has been removed (see Figure 3.9).

First Stage $t_s < t < \tau$

Substituting Equation (3.61) into Equation (3.56a) and recognizing that for a rectangular cross-section $4M_o/N_o = h$, we arrive at the following expression for $\Psi_n(t^*)$;

$$\Psi_n(t^*) = A_n \sin\left(\frac{n\pi c\, t^*}{2L}\right) + B_n \cos\left(\frac{n\pi c\, t^*}{2L}\right) + \left(\frac{2}{n\pi}\right)^3 \bar{P}h \qquad (3.62)$$

where A_n, B_n are arbitrary constants and $\bar{P}$ is the non-dimensional loading parameter defined as

$$\bar{P} = P_m/P_o \qquad (3.63)$$

Here P_o refers to the static collapse load for the simply supported beam as given by Equation (2.15). The initial conditions (Equation (3.58)), then lead to the requirements

$$w_o(0)\,\Phi(x_o) = \sum_{n=1,3,5,\ldots}^{\infty} [B_n + (2/n\pi)^3 \bar{P}h] \sin\left(\frac{n\pi x_o}{2L}\right)$$

$$\dot{w}_o(0)\,\Phi(x_o) = \sum_{n=1,3,5,\ldots}^{\infty} \left(\frac{n\pi c}{2L}\right) A_n \sin\left(\frac{n\pi x_o}{2L}\right) \qquad (3.64)$$

These are two Fourier sine series for the determination of the arbitrary constants A_n, B_n. Substituting Equations (3.55) and (3.60) into the Equation (3.64) and making use of the orthogonality of the sine function, we find that for odd values of n

$$B_n = h\,[\pm (2/n\pi)^2 - (2/n\pi)^3 \bar{P}] \qquad (3.65)$$

$$A_n = \pm h\,(2/n\pi)^3 \sqrt{(3\bar{P}-4)} \qquad (3.66)$$

where the + sign is to be used when n = 1,5,9,... and the - sign when n = 3,7,11,.... Using these values of A_n, B_n in Equation (3.62) yields the coefficients $\Psi_n(t^*)$ and hence the complete solution of the problem for $0 < x_o < L$, $t_s < t < \tau$. (It may be shown that due to the symmetry of the problem about $x_o = L$ only half the domain need to be considered). In particular the centrepoint deflection $w(x_o=L,t^*) = w_o(t^*)$ is given in nondimensional form by

$$w_o(t^*)/h = \sum_{n=1,3,5,\ldots}^{\infty} \Big\{ (2/n\pi)^3 \sqrt{(3\bar{P}-4)}\, \sin(n\omega) + (2/n\pi)^2 \cos(n\omega) \Big\} + (2/\pi)^3 \bar{P} \sum_{n=1}^{\infty} (-1)^{n+1} [1-\cos(2n-1)\omega] \qquad (3.67)$$

where

$$\omega = \pi c t^*/2L \quad ; \quad 0 \leq t^* \leq \tau - t_s \tag{3.68}$$

The plastic membrane acquires its maximum final deflection at $t^* = t^*_f$ when $\dot{w}(x_o, t^*_f) = 0$ or $\dot{w}_o(t^*_f) = 0$. Thus, setting the time derivative of Equation (3.67) equal to zero leads to the following expression

$$\sqrt{(3\bar{P} - 4)} \sum_{n=1,3,5,\ldots}^{\infty} \frac{1}{n^2} \cos(n\omega_f) - \frac{\pi}{2} \sum_{n=1,3,5,\ldots}^{\infty} \frac{1}{n} \sin(n\omega_f)$$

$$+ \bar{P} \sum_{n=1}^{\infty} (-1)^{n+1} \frac{\sin(2n-1)\omega_f}{(2n-1)^2} = 0 \tag{3.69}$$

where

$$\omega_f = \pi c t^*_f/2L \quad ; \quad 0 \leq t^*_f \leq \tau - t_s$$

Each of the infinite series appearing in the above expression are uniformly convergent and can be summed directly for a certain range of values of ω_f. Fuller details as to the development of the closed form summation of a wide class of Fourier series will be found in the book by Bromwich (Reference 25). For the sake of easy reference, some useful formulas that are applicable to the present study are given in Appendix B. In the following, frequent references will be made to these formulae.

From Equation (3.67) and the formulas (B.1), (B.2) and (B.3) it can be deduced that:

$$\omega_f = \begin{cases} \frac{\pi}{2}\,\frac{1-\sqrt{(3\bar{P}-4)}}{\bar{P}-\sqrt{(3\bar{P}-4)}} & \text{for } \frac{4}{3} < \bar{P} < \frac{5}{3} \;;\; 0 < \omega_f < \frac{\pi}{2} \\ \frac{\pi}{2}\,\frac{2\bar{P}-1+\sqrt{(3\bar{P}-4)}}{\bar{P}+\sqrt{(3\bar{P}-4)}} & \text{for } \frac{5}{3} < \bar{P} < 3 \;;\; \frac{\pi}{2} < \omega_f < \pi \end{cases} \tag{3.70}$$

Equation (3.70) furnishes the time t_f^* at which the deformation is completed. At this instant of time the membrane attains its maximum deflection. If Equation (3.70) is substituted into Equation (3.67) and use is made of the formulas (B.2), (B.4), (B.5) and (B.6), then we can obtain the maximum permanent deflection at the centre

$$\frac{\delta_f}{h} = w_o(t_f^*)/h = \begin{cases} \frac{1}{2} - \frac{1}{4}\,\frac{[1-\sqrt{(3\bar{P}-4)}]^2}{\bar{P}-\sqrt{(3\bar{P}-4)}} & \text{for } 4/3 < \bar{P} < 5/3 \\ \frac{1}{2}(1-\bar{P}) + \frac{1}{4}\,\frac{[2\bar{P}-1+\sqrt{(3\bar{P}-4)}]^2}{\bar{P}+\sqrt{(3\bar{P}-4)}} & \text{for } 5/3 < \bar{P} < 3 \end{cases} \tag{3.71}$$

Second Stage $\tau < t$

Throughout this stage the membrane is unloaded and the motion is governed by the homogenous Equation (3.56b). It is convenient to define a new time origin corresponding to the instant $t = \tau$ when the pulse has ceased to act. Let us define a new time parameter t^{**} as

$$t^{**} = t - \tau$$

or (3.72)

$$t^{**} = t^* - (\tau - t_s)$$

Then the general solution of Equation (3.56b) may be written in the following form

$$w(x_o, t^{**}) = \sum_{n=1,3,5,\ldots}^{\infty} \left\{ C_n \sin\left(\frac{n\pi c t^{**}}{2L}\right) + D_n \cos\left(\frac{n\pi c t^{**}}{2L}\right) \right\} \sin\left(\frac{n\pi x_o}{2L}\right) \tag{3.73}$$

where C_n, D_n are arbitrary constants.

The deflection w and velocity $\dot{w}$ at the beginning of this stage when $t^{**} = 0$ must match the values acquired by the membrane at the end of the first stage given by Equation (3.62) and its derivative at $t^* = \tau - t_s$. Therefore

$$C_n = A_n \cos(n\mu) - B_n \sin(n\mu)$$

$$D_n = A_n \sin(n\mu) + B_n \cos(n\mu) + \bar{P}h\ (2/n\pi)^3 \tag{3.74}$$

where A_n, B_n are given by Equations (3.65) and (3.66), and

$$\mu = \pi c(\tau - t_s)/2L \tag{3.75}$$

Using Equations (3.68), (3.72) and (3.75) we can write

$$\pi c t^{**}/2L = \omega - \mu \tag{3.76}$$

We now combine the Equations (3.73) - (3.76) and obtain

$$w(x_o,t^{**}) = \sum_{n=1,3,5,\ldots}^{\infty} \left\{ A_n \sin(n\omega) + B_n \cos(n\omega) \right.$$

$$\left. + \bar{P}h\,(2/n\pi)^3 \cos\,[n(\omega-\mu)] \right\} \sin\,(\frac{n\pi x_o}{2L}) \qquad (3.77)$$

Making use of Equations (3.65), (3.66) and (3.77), the deflection of the membrane at $x_o = L$ can be expressed in the following dimensionless form:

$$w_o/h = \sum_{n=1,3,5,\ldots}^{\infty} \left[(2/n\pi)^3\sqrt{(3\bar{P}-4)}\,\sin(n\omega) + (2/n\pi)^2 \cos(n\omega)\right]$$

$$+ \sum_{n=1}^{\infty} (-1)^{n+1}\,[2/(2n-1)\pi]^3\,\bar{P}\,[\cos[(2n-1)(\omega-\mu)]$$

$$- [\cos[(2n-1)\omega]] \qquad (3.78)$$

It will be convenient in later analyses to introduce a non-dimensional impulse parameter

$$\beta = \frac{I^2}{mhP_o} \qquad (3.79)$$

where

$$I = \int_0^{\tau} P(t)\,dt = P_m\,\tau \qquad (3.80)$$

is the total impulse (per unit length) applied to the beam.

With the above definitions and Equation (3.53c) we are now able to write down an expression for μ (Equation (3.75)) in terms of the basic non-dimensional parameters $\bar{P}$, β, as

$$\mu = \frac{\pi}{\sqrt{2}} \left\{ \frac{\sqrt{\beta}}{\bar{P}} - \left[\frac{1}{3(\bar{P}-1)}\right]^{1/4} \left[K-F(1/\sqrt{2}, \phi_s)\right] \right\} \tag{3.81}$$

where ϕ_s given by Equation (3.53b), is related to the parameter $\bar{P}$ by

$$\phi_s = \cos^{-1} \left[\frac{1}{3(\bar{P}-1)}\right]^{1/4} \tag{3.82}$$

We can also write

$$a_\tau = \sqrt{\beta}\left[3(\bar{P}-1)\right]^{1/4}/\bar{P} \tag{3.83}$$

It is important to realize that one of the conditions which ensures the transition from beam to string behaviour during the first phase of the beam motion is $t_s < \tau$ or $at_s < a\tau$. (The other condition to be satisfied is of course $4/3 < \bar{P} < 3$). If at_s and $a\tau$ are expresed in terms of $\bar{P}$ and β using Equations (3.53c) and (3.83), the latter requirement can be written as $\beta > \beta_m$ where

$$\beta_m = \bar{P}^2 \left[K - F(1/\sqrt{2}, \phi_s)\right]^2 / \sqrt{3(\bar{P} - 1)} \tag{3.84}$$

is the minimum value of the impulse parameter β beyond which the results of the preceding analyses is valid. It is evident that this value of β

corresponds to the particular case when the initiation of the string phase coincides with the termination of the load i.e. $\mu = 0$ when $\beta = \beta_m$.

Following the procedures which were developed for the analysis of the first stage we seek the instant of time $t^{**} = t_f^{**} = 2\omega_f L/\pi c$ at which the motion of the plastic membrane terminates. This is accomplished by finding the smallest root ω_f of the Equation $\dot{w}_o = 0 = \partial w_o/\partial\omega$, where w_o is given by Equation (3.78). Finally, making use of the formulas (B.1) to (B.3) it is a simple matter to show that the smallest root of the equation $\partial w_o/\partial\omega = 0$ which is associated with the maximum value of w_o, is

$$\omega_f = \begin{cases} \frac{\pi}{2}\left[1+(\bar{P}\zeta-1)/\sqrt{(3\bar{P}-4)}\right] & \text{for} \quad 0<\omega_f\leq\pi/2 \\ \frac{\pi}{2}\left[1+(\bar{P}\zeta-1)/[2\bar{P}+\sqrt{(3\bar{P}-4)}]\right] & \text{for} \quad \pi/2\leq\omega_f<\pi \end{cases} \tag{3.85}$$

where

$$\zeta = 2\mu/\pi = \sqrt{2}\left\{\frac{\sqrt{\beta}}{\bar{P}} - \left[\frac{1}{3(\bar{P}-1)}\right]^{1/4}\left[K-F(1/\sqrt{2},\phi_s)\right]\right\} \tag{3.86}$$

Upon substitution of the above expression for ω_f into Equation (3.78) and use of the formulas (B.2), (B.4) and (B.5), the maximum value of the transverse deflection $\delta_f = w_o(\omega_f)$ of the permanently deformed membrane can be obtained as

$$\frac{\delta_f}{h} = \frac{1}{4}\left[\sqrt{(3\bar{P}-4)} + 2\bar{P}\zeta - \bar{P}\zeta^2\right] + \begin{cases} \dfrac{1}{4}\dfrac{(\bar{P}\zeta-1)^2}{\sqrt{(3\bar{P}-4)}} & \text{for } 0 < \omega_f \leq \pi/2 \\ \dfrac{1}{4}\dfrac{(\bar{P}\zeta-1)^2}{2\bar{P}+\sqrt{(3\bar{P}-4)}} & \text{for } \pi/2 \leq \omega_f < \pi \end{cases} \tag{3.87}$$

where ζ is given by Equation (3.86) as a function of β, $\bar{P}$. It can readily be shown that for $\mu \equiv \mu(\beta, \bar{P}) < \mu_c$, where

$$\mu_c = \frac{\pi}{2}\,\frac{2\bar{P}-1+\sqrt{(3\bar{P}-4)}}{\bar{P}+\sqrt{(3\bar{P}-4)}} \tag{3.88}$$

the maximum response does not occur during the pulse application.

This concludes our analysis of Phase I.

Phase II ($t > \tau$)

a) Small deflections ($w_o/h < 1/2$)

If $a\tau < K$, then the beam in its unloaded state will continue to move in accordance with the single hinge mechanism of Figure 3.3, for $t > \tau$, until the kinetic energy generated during the load application is entirely absorbed in plastic flow. Determination of the final central displacement in this phase of motion is the principal object of the following analysis.

The governing differential equation of motion (3.35) after multiplying both sides by $\dot{w}_o(t)$ and integrating with respect to t, can be recast into the form

$$\frac{1}{2}(\dot{w}_o)^2 + \frac{\lambda}{3}w_o^3 + \frac{3}{2m}P_o w_o = \frac{3}{2m}\left[\int_0^{\tau} P(t)\,\dot{w}_o\,dt + \int_{\tau}^{t} P(t)\,\dot{w}_o\,dt\right]$$

Since presently we have $P(t) = 0$ for $t > \tau$ we may write the above as

$$\frac{1}{2}(\dot{w}_o(t))^2 + \frac{\lambda}{3}w_o^3(t) + \frac{3}{2m}P_o w_o(t) = \frac{3}{2m}P_m w_o(\tau) \qquad (3.89)$$

where

$$w_o(\tau) = \alpha\, cn^2(K - a\tau)$$

is the central displacement of the beam at the end of the first phase.

The final centrepoint deflection defined previously as $\delta_f = w_o(t_f)$ can readily be obtained from Equation (3.89) by setting $\dot{w}_o(t_f) = 0$. Thus, making use of Equation (3.89), we have

$$\frac{\lambda}{3}\delta_f^3 + \frac{3}{2m}P_o\delta_f = \frac{3}{2m}P_m\,\alpha\, cn^2(K - a\tau)$$

which after multiplying both sides by 1/h and using Equations (3.36), (3.42) and (3.63) can be written in the following non-dimensional form.

$$\frac{\delta_f}{h} + \frac{4}{3}\left(\frac{\delta_f}{h}\right)^3 = \frac{\sqrt{3}}{2}\,\bar{P}\sqrt{(\bar{P}-1)}\,\mathrm{cn}^2(K-a\tau) \qquad \text{for } a\tau < K \tag{3.90}$$

Letting

$$\chi = a\tau = \sqrt{\beta}\,\left[3(\bar{P}-1)\right]^{1/4}/\bar{P} \tag{3.91}$$

then it follows from the addition formulas of elliptic functions that

$$\mathrm{cn}\,(K-\chi) = k\,\mathrm{sn}(\chi)\mathrm{dn}(\chi)/\left[1-k^2\,\mathrm{sn}^2(\chi)\right] \tag{3.92}$$

where $k = 1/\sqrt{2}$ is the modulus of the elliptic integral K. Using the identities (3.46), we can rewrite Equation (3.92) as

$$\mathrm{cn}(K-\chi) = k\,\mathrm{sn}(\chi)/\mathrm{dn}(\chi) = \frac{1}{\sqrt{2}}\,\mathrm{sd}(\chi) \tag{3.93}$$

where $\mathrm{sd}(\chi) \equiv \mathrm{sn}(\chi)/\mathrm{dn}(\chi)$ is a Jacobian elliptic function.

Introducing into Equation (3.90) the relations of Equations (3.91) and (3.93) we have, in terms of $\bar{P}$ and β

$$\frac{\delta_f}{h} + \frac{4}{3}\left(\frac{\delta_f}{h}\right)^3 = \frac{\sqrt{3}}{4}\,\bar{P}\sqrt{(\bar{P}-1)}\,.\,\mathrm{sd}^2\left\{\sqrt{\beta}\,\left[3(\bar{P}-1)\right]^{1/4}/\bar{P}\right\} \tag{3.94}$$

which is valid so long as $\delta_f/h < 1/2$ and $a\tau < K \approx 1.854$

Putting

$$\gamma^2 = 4\left[\frac{\delta_f}{h} + \frac{4}{3}\left(\frac{\delta_f}{h}\right)^3\right] / \left[\bar{P}\sqrt{3(\bar{P}-1)}\right] \tag{3.95}$$

then Equation (3.94) can be inverted such that

$$\beta = \frac{\bar{P}^2}{\sqrt{3(\bar{P}-1)}}\left[sd^{-1}(1/\sqrt{2},\gamma)\right]^2 = \frac{\bar{P}^2}{\sqrt{3(\bar{P}-1)}}\left[F(1/\sqrt{2},\phi)\right]^2 \tag{3.96}$$

where

$$\phi = \sin^{-1}\sqrt{\{\gamma^2/(1+\gamma^2/2)\}} \tag{3.97}$$

Within the physical restrictions of the sine function $\gamma^2 \leq 2$. Equation (3.96) can be used to plot the nondimensional permanent deflection δ_f/h against the impulse parameter β for a specific value of $\bar{P}$. Figure (3.10) shows a family of such curves for constant values of $\bar{P}$ lying between 1 and 3. The figure also includes straight lines beyond the limiting curve $a\tau = K$, which represent the final deformations based on the small deflection analysis of Phase I (a), as indicated by Equation (3.50).

It may be observed from Figure (3.10) that for large values of β (such that $a\tau > K$) the response can be characterized by a single parameter $\bar{P}$ and becomes independent of the applied impulse I, a fairly obvious result that was to be expected.

It is interesting to note that in direct analogy with trigonometric circular functions, the elliptic functions $sn(\chi)$, $dn(\chi)$ (appearing as a quotient in $sd(\chi)$) can be represented by the following infinite polynomial series

$$sn(\chi) = \chi - (1+k^2)\chi^3/3! + (1+14k^2 + k^4)\chi^5/5!.... \qquad (3.98a)$$

$$dn(\chi) = 1 - k^2\chi^2/2! + (4+k^2)k^2\chi^4/4!.... \qquad (3.99b)$$

where $k = 1/\sqrt{2}$ and $\chi < K$.

Provided we are only interested in small values of $\chi = a\tau$, it is possible to truncate the series of Equation (3.98) at some suitable term, say χ^5. By truncating the series in this way we incur errors which are of the order of magnitude of χ^6 in comparison to the terms remaining in the series. Substituting the truncated series of Equation (3.98) into $sd(\chi) = sn(\chi)/dn(\chi)$ and using the binomial theorem yields

$$sd(\chi) \approx \chi \left(1 - \frac{1}{40}\chi^4\right) \qquad (3.99)$$

For $\chi = a\tau < 1$, this can further be simplified to $sd(\chi) \approx \chi$ and Equation (3.94) can approximately be written as

$$\frac{\delta_f}{h} + \frac{4}{3}\left(\frac{\delta_f}{h}\right)^3 \approx \frac{3}{4}\beta\left(1 - 1/\bar{P}\right) \qquad (3.100)$$

in which $a\tau < 1$ imposes the condition $\beta < \bar{P}^2/\left[3(\bar{P}-1)\right]^{1/2}$.

Figure (3.10) indicates the boundary $a\tau = 1$ below which the preceding approximation may be used with sufficient accuracy. The great simplification achieved in the form of the response equation is readily apparent.

b) Moderately large deflections ($w_o/h > 1/2$); membrane theory

If at $t_s > a\tau$ (i.e. $\beta < \beta_m$ or $\mu < 0$) and $w_o/h > 1/2$, the string phase is assumed to operate in which case the motion of the beam is governed by the differential Equation (3.56b). The analysis is along similar lines to that employed in Phase I(b) with the only difference that in the present case the initial conditions at the midpoint are

$$\begin{aligned} w_o(t^* = 0) &= h/2 \\ \dot{w}_o(t^* = 0) &= \sqrt{(2hP_o/m)}\,\Lambda \end{aligned} \tag{3.101}$$

where the last expression follows from Equation (3.89) with Λ defined by

$$\Lambda = \left[\frac{3\sqrt{3}}{8}\,\bar{P}\sqrt{(P-1)}\;sd^2(a\tau)-1\right]^{1/2} \tag{3.102}$$

and $t^* = 0$, as before, denotes the instant of time $t = t_s > \tau$ at which the string phase initiates (Figure 3.11).

It is an easy matter to show that in this case the formal solution for the central deflection $w(x_o = L, t^*) = w_o(t^*)$, is

$$w_o(t^*)/h = \sum_{n=1,3,5,\ldots}^{\infty} \left\{(4/n^2\pi^2)\cos(n\omega) + (16/n^3\pi^3)\,\Lambda \sin(n\omega)\right\} \tag{3.103}$$

where for notational consistency the nomenclature of Phase I(b) has been employed.

Our interest now centres on determining the permanent deflection at the midpoint, and for this information we turn to the evaluation of the time t_f^* when $\dot{w}_o = 0 = \partial w_o/\partial\omega$. With the aid of the formulas (B.1) and (B.2) it

may be shown that the membrane reaches its final position when

$$\omega_f = \pi c t_f^*/2L = \frac{\pi}{2}\left(1 - \frac{1}{2\Lambda}\right) \tag{3.104}$$

for $0 < \omega_f < \pi$ or $\Lambda > 1/2$.

The requirement that $\Lambda > 1/2$ demands a severe limitation on the values of α and hence on the values of the impulse parameter β for a fixed $\bar{P}$ lying in the range $4/3 < \bar{P} < 3$. It can be verified that those values of β which cause the transition from beam to string behaviour, violate the inequality $\Lambda > 1/2$. From an analytical point of view, these values of β lead to an impulsive change in the centrepoint velocity $\dot{w}_o$ from a positive to a negative value at $t^* = 0$. This abrupt change in velocity, which implies an instantaneous infinite acceleration at the midpoint, arises from the discontinuity of the slope of the initial deflected curve at $x_o = L$. In reality the plastic hinge which was assumed to be concentrated at the midpoint, extends over a finite plastic zone and the above singularities are essentially nonexistent. It may be shown that, for the particular shape of the initial displacement and velocity profiles considered here, the centrepoint velocity instantaneously (at $t^* = 0$) changes direction if $w_o(t^* = 0) < hc/2L$. We deduce that in this particular case the initial central deflection $w_o(t^* = 0) = h/2$ can be regarded as the maximum permanent deflection. The latter result, although important, is only valid for a small range of β beyond the transition from beam to string behaviour. We are mostly concerned with magnitudes of β that exceed this range and thus satisfy the inequality $0 < \omega_f < \pi$. In such cases we can uniquely

determine the value of ω_f and hence t_f^* from Equation (3.104). Upon substitution of Equation (3.104) into the Equation (3.103) and use of the formulas (B.2) and (B.4) we obtain the following expression for the final excursion of the midspan point in terms of the basic dimensionless parameters $\bar{P}$, β:

$$\frac{\delta_f}{h} = \begin{cases} \frac{1}{2} & \text{if } \Lambda < 1/2 \\ \frac{\Lambda}{2} + \frac{1}{8\Lambda} & \text{if } \Lambda > 1/2 \end{cases} \tag{3.105}$$

where $\Lambda \equiv \Lambda(\bar{P}, \beta)$ when the relation of Equation (3.83) is introduced into the definition of Λ given by Equation (3.102).

If a_τ is sufficiently small, the expression for Λ takes the simplified form

$$\Lambda \approx \left[\frac{9}{8}\left(1-\frac{1}{\bar{P}}\right)\beta - 1\right]^{1/2} \tag{3.106}$$

The relationship between δ_f/h and β for $\bar{P} = 2.0$ and 3.0 is depicted in Figure (3.12). The plateau observed in the diagram at $\delta_f/h = 0.5$ is a consequence of the sudden reversal in the direction of the initial centre-point velocity, as explained before. The width of this flat region decreases with increasing pressure, as seen on the diagram. In what follows we shall develop an alternative "approximate" approach which is simple to use and leads to results that are sufficiently accurate for engineering purposes.

Approximate Analysis of the String Phase

Thus far the analysis of the plastic string behaviour in both Phases I(b) and II(b) has been strictly based on the knowledge of the so called

"exact" (within the framework of our assumptions) deflection shape of the beam at the instant when the behaviour as a plastic string commences. However, the foregoing treatment introduces a great deal of mathematical difficulties particularly when the initial deflected curve is complicated as will be seen in the next section on high loads. It is therefore instructive to devise a simpler technique which can be more easily interpreted and used. We close this section with a brief description of the proposed "approximate" method of analysis of the string behaviour and simply quote the formulas that are furnished by this analysis without going into the details of the mathematics involved.

It has been suggested by Symonds and Jones (Reference 26) that the precise deflection curve at time $t = t_s$ or $t^* = 0$ (i.e. initial shape of the string) is not critical in as far as the subsequent motion of the string is concerned. For simplicity we assume the initial deflected shape to be sinusoidal with amplitude h/2, i.e.

$$\tilde{w}\,(x_o,\ t^* = 0) = \frac{h}{2} \sin\left(\frac{\pi x_o}{2L}\right) \ ;\ 0 < x_o < 2L \qquad (3.107)$$

where the tilda ~ indicates an approximate value.

Unlike the initial displacement profile, the initial velocity profile of the string plays a significant role in its subsequent motion. Let us assume that the initial velocity profile is also sinusoidal such that

$$\tilde{\dot{w}}\,(x_o,\ t^* = 0) = V_o \sin\left(\frac{\pi x_o}{2L}\right) \qquad (3.108)$$

where V_o is the amplitude of the assumed initial velocity profile.

In order to determine V_o we impose the condition that the total kinetic energy acquired by the beam at the end of the beam phase (i.e. at $t = t_s$ or $t^* = 0$) be equal to the kinetic energy represented by the approximate velocity field of Equation (3.108). This condition is satisfied if

$$\int_0^L \dot{w}^2 (x_o, 0)\, dx_o = \int_0^L V_o^2 \sin^2 (\frac{\pi x_o}{2L})\, dx_o$$

Hence:

$$V_o = \dot{w}_o(0) \left[\frac{2}{L} \int_0^L \Phi^2(x_o)\, dx_o\right]^{1/2} \qquad (3.109)$$

The motion beyond $t^* = 0$ is taken as governed by the differential Equation (3.56) and the boundary conditions of Equation (3.57) (where w and its derivatives are replaced by their corresponding approximate functions). It can be shown, using the orthogonality property of the sine function that the solution to this modified initial-boundary value problem is

$$\tilde{w}(x_o, t^*) = \Psi_1 (t^*) \sin(\frac{\pi x_o}{2L}) \qquad (3.110)$$

The simple analytical approach outlined above will now be applied to Phases I(b) and II(b) (Figure 3.13) in order to predict the approximate final central deflection $\tilde{\delta}_f$ during each of the aforementioned phases. Proceeding as before, we substitute Equation (3.110) into the appropriate Equation (3.56) and then use the initial conditions of Equations (3.107)

and (3.108) to completely determine the time-dependent function Ψ_1. Carrying out the differentiation with respect to t* on Ψ_1 (t*) and equating to zero gives the response duration $\tilde{t}_f^*$ which renders the deflection a maximum i.e. $\tilde{\delta}_f$. The results are given as follows:

Phase I(b)

i) First Stage: $0 < t^* < \tau - t_s$

The maximum permanent deflection is

$$\frac{\tilde{\delta}_f}{h} = \sqrt{(A_1^2 + B_1^2)} + (\frac{2}{\pi})^3 \bar{P} \qquad (3.111)$$

where

$$A_1 = \frac{2L}{\pi ch} V_o = \frac{1}{\pi}\left[\frac{2}{3}(3\bar{P} - 4)\right]^{1/2} \qquad (3.111a)$$

$$B_1 = \frac{1}{2} - (\frac{2}{\pi})^3 \bar{P} \qquad (3.111b)$$

The duration of response is given by

$$\tilde{t}_f^* = \frac{2L}{\pi c}\left[\tan^{-1}(A_1/B_1) + \pi\right] \quad \text{if } \bar{P} > \frac{\pi^3}{16} \approx 1.94$$

$$= \frac{2L}{\pi c}\tan^{-1}(A_1/B_1) \quad \text{if } \bar{P} < 1.94 \qquad (3.111c)$$

ii) Second Stage: $t^* > \tau - t_s$

The maximum permanent deflection is

$$\frac{\delta_f}{h} = \sqrt{(C_1^2 + D_1^2)} \tag{3.112}$$

where

$$C_1 = A_1 \cos \mu - B_1 \sin \mu \tag{3.112a}$$

$$D_1 = A_1 \sin \mu + B_1 \cos \mu + (\frac{2}{\pi})^3 \bar{P} \tag{3.112b}$$

and μ is defined by Equation (3.81). The critical value of $\mu = \mu_c$ above which the maximum response does not occur during the pulse application can be shown to be

$$\mu_c = \tan^{-1} (A_1/B_1) + \pi \quad \text{if } \bar{P} > 1.94$$

$$= \tan^{-1} (A_1/B_1) \quad \text{if } \bar{P} < 1.94 \tag{3.112c}$$

Thus, Equation (3.112) holds so long as $\mu < \mu_c$. When the latter inequality is violated, Equation (3.111) gives a prediction of the maximum response. The duration of response is

$$t_f^{**} = \frac{2L}{\pi c} \tan^{-1} (C_1/D_1) \tag{3.112d}$$

Phase II(b)

The final central deflection in this phase is given by

$$\frac{\tilde{\delta}_f}{h} = \left[\frac{1}{4} + \frac{8}{3\pi^2}\Lambda^2\right]^{1/2} \qquad (3.113)$$

where Λ is defined by Equation (3.102) with a_τ given by Equation (3.91).

The duration of the motion is found to be

$$\tilde{t}^*_f = \frac{2L}{\pi c}\tan^{-1}\left(\frac{4}{\pi}\Lambda\sqrt{2/3}\right) \qquad (3.113a)$$

Figure (3.14) shows how the final deflections predicted by the above method vary with the non-dimensional impulse parameter β when the parameter $\bar{P}$ is held constant. Also included are the deflections furnished by the small but finite deflection theory ($\delta_f/h \leq 1/2$) in which the bending moments interact with the axial forces. A comparison of the results of the "approximate" string phase analysis (Figure 3.14) with the corresponding "exact" results (Figure 3.12) reveals that the improvements achieved do not justify the labour involved in performing an exact analysis. Hereafter, for simplicity, we adopt the foregoing approximate technique whenever appropriate.

3.3.2 HIGH LOAD ($P_m > 3P_o$)

In this specific case of loading the motion of the beam consists of three phases. Because of the symmetry of the problem we refer only to the left half of the beam in what follows except for discussions on the pattern of motion.

Phase I $(0 < t < \tau)$

a) Small deflections $(w_o/h < 1/2)$

Instantaneously (at $t = 0^+$) the beam assumes the shape of a trapezium (Figure 2.12c) which is comprised of a central flat portion momentarily confined by two plastic hinges at a distance $[1 - \sqrt{(3/\bar{P})}]L$ from the centre (Reference 17). The axial forces come into play soon after the beam is set into motion thereby causing a violation of the plasticity condition in the neighbourhood of $x = \rho$. We must therefore expect that the plastic hinges travel along the beam during the loading interval $0 < t < \tau$. It appears reasonable to assume that the hinges move in toward the centre during this phase of motion. The velocity field meeting the above description, satisfying the boundary conditions and the appropriate kinematic requirement set forth by the second line of Equation (2.16) is

$$\dot{w}(x,t) = \begin{cases} \dot{w}_\rho(t) & \text{for } 0 \leq x \leq \rho(t) \\ \dot{w}_\rho(t)\,\dfrac{L-x}{L-\rho(t)} & \text{for } \rho(t) \leq x \leq L \end{cases} \qquad (3.114)$$

where, as before, $w_\rho(t)$ and $\dot{w}_\rho(t)$ are the transverse displacement and velocity at the hinge position, respectively, and are chosen so as to satisfy the initial conditions.

$$w_\rho(0) = \dot{w}_\rho(0) = 0 \qquad (3.115)$$

Differentiating the above with respect to time t permits the acceleration field to be written as

$$\ddot{w}(x,t) = \begin{cases} \ddot{w}_\rho(t) & \text{for } 0<x<\rho(t) \\ [\ddot{w}_\rho(t)+\dot{\rho}\dot{w}_\rho(t)/(L-\rho)]\,\dfrac{L-x}{L-\rho(t)} & \text{for } \rho(t)<x<L \end{cases} \tag{3.116}$$

This implies that the acceleration is discontinuous at the moving hinge with the amount of jump being given by

$$\ddot{w}(\rho^+,t) - \ddot{w}(\rho^-,t) = \dot{\rho}\,\frac{\dot{w}_\rho(t)}{L-\rho(t)}$$

$$\text{or} \quad [\ddot{w}_\rho] = \dot{\rho}\,\dot{w}_\rho/(L-\rho) \tag{3.117}$$

It follows from Equation (3.117) that the abrupt change in acceleration across the moving hinge is equal to the product of the velocity of the hinge along the beam and the angular velocity of the outer segment $\rho(t)<x<L$. This product is always negative since by hypothesis the central plane region is continually shrinking (i.e. $\dot{\rho} < 0$).

Having assumed the kinematically admissible acceleration field of Equation (3.116), we next write the dynamic equilibrium equations of the two segments to the right and left of the hinge. We adapt the same general approach used to derive the dynamic equilibrium equation of the single hinge mechanism (Section 3.3.1). Assuming that the central portion of the beam $0<x<\rho(t)$ remains rigid and resists the loads N,M without deformation, the expression for the dynamic equilibrium of the segment to the right of the hinge is found to be

$$\int_0^{\rho} [P(t) - m\ddot{w}_{\rho}(t)]\, \delta w(t)\, dx = 0 \qquad (3.118)$$

according to the principle of virtual displacements (Equation (3.29)).

Since the integral in Equation (3.118) vanishes for an arbitrary virtual disturbance δw and arbitrary x within the flat region $0 < x < \rho(t)$, the quantity inside the square brackets must be identically zero. Thus

$$m\ddot{w}_{\rho}(t) = P(t) \qquad (3.119)$$

The latter equation also follows from the fact that since the moment is maximum within the central region, the shear is zero and hence the load is solely supported by the inertia forces. Specializing to the rectangular pulse of Figure 3.1 we have for $0<x<\rho(t)$

$$\ddot{w}(x,t) = \ddot{w}_{\rho}(t) = \begin{cases} P_m/m & \text{for } 0<t<\tau \\ 0 & \text{for } t>\tau \end{cases} \qquad (3.120)$$

Since all the deformation consisting of both bending and stretching occurs in the outer segment of the beam $\rho(t) < x < L$, the dynamic equilibrium equation of this segment is similar to that of the single hinge mechanism of Figure (3.3) for the medium load range. Equation (3.34) can therefore be made to apply in this case by merely replacing L, $w_o(t)$ and $\ddot{w}_o(t)$ by $L-\rho(t)$, $w_{\rho}(t)$ and $\ddot{w}_{\rho}(t) + \dot{\rho}\,\dot{w}_{\rho}(t)/(L-\rho(t))$ respectively. As a result of such replacement, for the loading interval $0<t<\tau$, the equilibrium

equation of the segment just to the left of the hinge for the general case of blast loading can be written as

$$M_o(1 + 4w_\rho^2/h^2) = \frac{1}{2}(L-\rho)^2 \left[P(t) - \frac{2}{3} m \left(\ddot{w}_\rho + \dot{\rho}\dot{w}_\rho/(L-\rho)\right)\right]$$

or upon substitution of Equation (3.119)

$$M_o (1+ 4w^2{}_\rho/h^2) = \frac{1}{6}(L-\rho)^2 P(t) - \frac{1}{3} m\dot{w}_\rho\dot{\rho}(L-\rho) \qquad (3.121)$$

for $\rho(t) < x \leq L$.

From Equation (3.119) and the initial conditions (3.115) it follows by repeated integration that

$$m\dot{w}_\rho(t) = \int_0^t P(\xi)\, d\xi \quad ; \quad 0 < t < \tau \qquad (3.122)$$

$$mw_\rho(t) = \int_0^t (t-\xi)\, P(\xi)\, d\xi \quad ; \quad 0 < t < \tau \qquad (3.123)$$

where ξ, as before, is a dummy integration variable.

Introducing Equations (3.122) and (3.123) into the general equation of motion (3.121) yields a first order ordinary differential equation in terms of the time variable $\rho(t)$. Specializing once again to a pulse of rectangular shape we have

$$m\dot{w}_\rho(t) = P_m t$$

$$mw_\rho(t) = P_m t^2/2 \qquad (3.124)$$

Using these results in Equation (3.121) and collecting terms, we obtain

$$\frac{6M_o}{P_m}\left[1 + \left(\frac{P_m}{mh}\right)^2 t^4\right] = (L-\rho)^2 - 2t\dot{\rho}(L-\rho)$$

which can also be written in the form

$$t\frac{dr^2(t)}{dt} + r^2(t) = g(t) \qquad (3.125)$$

where

$$r(t) = \left[L-\rho(t)\right] \qquad (3.125a)$$

and

$$g(t) = 6M_o\left[1 + (P_m/mh)^2 t^4\right]/P_m \qquad (3.125b)$$

Integration of Equation (3.125) gives

$$r^2(t) = \frac{1}{t}\int_0^t g(\xi)\, d\xi$$

which finally leads to

$$r(t) = L-\rho(t) = L\sqrt{(3/\bar{P})}\left[1 + \frac{1}{5}\left(\frac{P_m}{mh}\right)^2 t^4\right]^{1/2} \qquad \text{for } 0 \leq t \leq \tau \qquad (3.126)$$

Equation (3.126) gives the instantaneous location of the plastic hinge throughout the interval $0 \leq t \leq \tau$ while the load remains constant at P_m. It can readily be seen from the above result that the distance of the hinge from the support increases with time t as hypothesized before. The initial position of the hinge at the onset of loading is determined by setting t = 0 in Equation (3.126). Thus

$$\rho(0) = \rho_o = L[1 - \sqrt{(3/\bar{P})}] \qquad (3.127)$$

as before.

It can be surmized from Equation (3.124) that the beam cannot cease moving in this phase of motion (i.e. for $0 < t < \tau$). However, the beam can start behaving as a plastic string if

$$w_o(t) = w_\rho(t) = P_m t^2/2m \geq h/2 \quad \text{for} \quad 0 < t < \tau$$

The latter case is treated separately in the following sub-section on moderately large deflection analysis.

This concludes the small (but finite) deflection analysis of the first phase of motion.

b) Moderately large deflections; membrane theory

The plastic string stage is reached when

$$t = t_s = \sqrt{(mh/P_m)} < \tau$$

The subsequent motion for $t > t_s$ takes place according to the string Equation (3.56a). The latter equation is to be satisfied subject to the following initial conditions at the centre (where $x = 0$ or $x_o = L$)

$$w_o(t^* = 0) = h/2$$

$$\dot{w}_o(t^* = 0) = P_m t_s / m = \sqrt{(P_m h/m)} \tag{3.128}$$

Owing to the complicated nature of the initial displacement shape, we resort to the approximate technique developed at the end of Section 3.3.1 in order to study the behaviour of the beam in the string mode. According to our earlier assumption the velocity profile is linear (Equation (3.114)) and its spatial distribution at the onset of the string phase is given by:

$$\Phi(x_o) = \begin{cases} x_o/r(t_s) & \text{for} \quad 0 < x_o < r(t_s) \\ 1 & \text{for } r(t_s) < x_o < L \end{cases} \tag{3.129}$$

where $r(t_s)$ is obtained from Equation (3.126) after replacing t by t_s, i.e.

$$r(t_s) = L - \rho(t_s) = \sqrt{6/5}\ \sqrt{(3/\bar{P})}\ L$$

Substituting from Equation (3.129) into Equation (3.109) and carrying out the integration yields:

$$V_o = \dot{w}_o(0)\ \left[2 - 4\sqrt{2}\ /\ \sqrt{(5\bar{P})}\right]^{1/2}$$

where $\dot{w}_o(0)$ is given by the second line of Equation (3.128) (Figure 3.15). Proceeding in a manner similar to that described for the case of medium range load we divide the analysis up into two stages; load era (first stage) and free era (second stage).

i) First Stage: $0 < t^* < \tau - t_s$

It may be shown that the maximum transverse deflection of the permanently deformed membrane is in this case given by

$$\frac{\tilde{\delta}_f}{h} = \sqrt{(A_1^2 + B_1^2)} + \left(\frac{2}{\pi}\right)^2 \bar{P} \qquad (3.130)$$

where

$$A_1 = \frac{2}{\pi}\left[\bar{P} - 2\sqrt{(2\bar{P}/5)}\right]^{1/2} \qquad (3.130a)$$

$$B_1 = \frac{1}{2} - \left(\frac{2}{\pi}\right)^3 \bar{P} \qquad (3.130b)$$

The duration of response of the membrane is

$$t_f^* = \frac{2L}{\pi c}\left[\tan^{-1}\left(A_1/B_1\right) + \pi\right] \qquad (3.130c)$$

Second Stage: $t^* > \tau - t_s$

During this stage the maximum permanent deflection is

$$\frac{\tilde{\delta}_f}{h} = \sqrt{(C_1^2 + D_1^2)} \tag{3.131}$$

where

$$C_1 = A_1 \cos \eta - B_1 \sin \eta \tag{3.131a}$$

$$D_1 = A_1 \sin \eta + B_1 \cos \eta + (\frac{2}{\pi})^3 \bar{P} \tag{3.131b}$$

and η which represents the same physical quantity as μ in the medium pressure range is defined by

$$\eta = \frac{\pi}{\sqrt{2}} [\sqrt{\beta}/\bar{P} - 1/\sqrt{\bar{P}}] \tag{3.132}$$

Equation (3.131) predicts the maximum response until η reaches its critical value η_c given by

$$\eta_c = \tan^{-1} (A_1/B_1) + \pi \tag{3.131c}$$

For those combinations of β, $\bar{P}$ which result in $\eta > \eta_c$ the final deflection of the membrane is attained during the load application (i.e. first stage) and its magnitude is determined by Equation (3.130). The duration of motion measured from the instant the load ceases to act is

$$t_f^{**} = \frac{2L}{\pi c} \tan^{-1} (C_1/D_1) \qquad (3.131d)$$

The analysis outlined above holds for $t_s < \tau$, where t_s is given by Equation (3.128). That is to say, the permanent centrepoint deflection δ_f/h predicted by Equations (3.130) and (3.131) are valid so long as $(t_s/\tau)^2 = \bar{P}/\beta < 1$.

Phase II ($\tau < t < T$)

a) Small deflections : combined bending and membrane theory

During this phase of motion the width of the central flat region continues to decrease from $\rho(\tau)$ to $\rho(T) = 0$. From this instant on (i.e. for $t > T$), the hinge remains at the midspan point and a new phase of motion, Phase III, ensues. The following analysis is concerned with the determination of T and the value of the central velocity and displacement at this instant of time.

Throughout the second phase the beam is unloaded so that $P(t) = 0$ for $0 < x < L$ and $\tau < t < T$. This expresses the fact that in this interval of time the transverse acceleration of the central segment is given by

$$\ddot{w}_\rho(t) = 0 \qquad \text{for} \quad \tau < t < T \qquad (3.133)$$

The Equation of motion of the outer segment is again valid in this phase provided that we set $P(t) = 0$ in Equation (3.121). Thus, we may write

$$M_o (1 + 4w_\rho^2/h^2) = -\frac{1}{3} m\dot{w}_\rho \dot{\rho} (L-\rho) \qquad (3.134)$$

Since $w(x,t)$, $\dot{w}(x,t)$ are piecewise continuous in x,t, the deflection $w_\rho(t)$ and velocity $\dot{w}_\rho(t)$ must match the values acquired by the beam at the end of the first phase given by Equations (3.115) and (3.116) with $t = \tau$. Hence, with the aid of Equations (3.133) and (3.80), we have for the rectangular pulse

$$\dot{w}_\rho(t) = P_m\tau/m = I/m \tag{3.135}$$

$$w_\rho(t) = I(t-\tau/2)/m \qquad ; \qquad t>\tau \tag{3.136}$$

Substituting these expressions into Equation (3.134) we obtain

$$\frac{6M_o}{I}\left[1+4\left(\frac{I}{mh}\right)^2(t-\tau/2)^2\right] = \frac{d}{dt}\left[L-\rho(t)\right]^2 \quad ; \quad t>\tau \tag{3.137}$$

The general solution of Equation (3.137) can be found by direct integration. Utilizing the value $L-\rho(\tau)$ given by Equation (3.126) at the end of the first stage as the initial condition in this case, yields the following expression for the determination of the hinge position in the interval $\tau<t<T$

$$\left[L-\rho(t)\right]^2 = \frac{6M_o}{I}\left\{t + \frac{4}{3}\left(\frac{I}{mh}\right)^2 (t-\tau/2)^3 + \frac{1}{30}\left(\frac{I}{mh}\right)^2\tau^3\right\} \tag{3.138}$$

Since $\rho(T) = 0$ by the definition of T, Equation (3.138) finally yields

$$T + \frac{4}{3}\left(\frac{I}{mh}\right)^2 (T-\tau/2)^3 = \frac{I}{3P_o} - \frac{1}{30}\left(\frac{I}{mh}\right)^2 \tau^3 \qquad (3.139)$$

The time T when the plastic hinge arrives at the beam centre is determined from the solution of the above cubic equation and in turn the centrepoint velocity and deflection at time T are given by

$$\dot{w}_\rho(T) = \dot{w}_o(T) = I/m \qquad (3.140)$$

$$w_\rho(T) = w_o(T) = I(T-\tau/2)/m \qquad (3.141)$$

Since the transverse velocity at the hinge is constant (see Equation (3.135)) right up to the centre, the motion of the beam cannot stop in the interval $\tau<t<T$. However, a transition to string phase can occur if the deflection w_ρ is of the order of the half-depth of the beam. The maximum permanent deflection when the beam behaves as a one-dimensional membrane, is given in the following.

b) Moderately large deflections; membrane theory

At the initiation of the string stage

$$w_o(t_s) = \frac{I}{m}(t_s - \tau/2) = h/2 \qquad (3.142)$$

which implies that

$$t_s = \frac{1}{2}(mh/I + \tau) \qquad \text{where } \tau < t_s < T \tag{3.143}$$

The analysis in this case is essentially the same as in Phase II(b) described earlier except that the initial condition on the velocity is now

$$\dot{w}(x_o, t_s) = \frac{I}{m}\Phi(x_o) = \frac{I}{m} \begin{cases} x_o/r(t_s) & \text{for } 0 < x_o < r(t_s) \\ 1 & \text{for } r(t_s) < x_o < L \end{cases} \tag{3.144}$$

where $r(t_s) = L - \rho(t_s)$ is given by Equation (3.138) with t replaced by t_s (Figure 3.15). The result is

$$r(t_s) = L - \rho(t_s) = L\left[2/\beta + 3/(2\bar{P}) + \frac{1}{10}(\beta^2/\bar{P}^3)\right]^{1/2} \tag{3.145}$$

It is then a simple matter to show that the maximum transverse deflection of the membrane is

$$\frac{\tilde{\delta}_f}{h} = \sqrt{(A_1^2 + B_1^2)} \tag{3.146}$$

where

$$A_1 = \frac{2L}{\pi ch} \quad V_o = \frac{2}{\pi}\sqrt{\beta}\left[1 - \frac{2}{3}\frac{r(t_s)}{L}\right]^{1/2} \tag{3.146a}$$

$$B_1 = \frac{1}{2} \tag{3.146b}$$

The duration of motion is

$$\tilde{t}_f^* = \tan^{-1}(A_1/B_1) \qquad (3.146c)$$

The above analysis is appropriate only if $t_s > \tau$ and $r(t_s) = L - \rho(t_s) < L$, or what amounts to the same if the inequalities $\bar{P} > \beta$ and $2 + \frac{3}{2}(\beta/\bar{P}) + \frac{1}{10}(\beta/\bar{P})^3 < \beta$ are simultaneously satisfied.

Phase III $t > T$

a) Small deflections ($w_o/h < 1/2$)

During this third phase of motion, the beam deforms in accordance with the single hinge mechanism. If we assume that the deflections are sufficiently small so that the permanent distortion in the two halves of the beam do not affect the formulation, then the motion of the beam beyond the time T is governed by the differential equation

$$\ddot{w}_o(t) + \lambda w_o^2(t) + \frac{3}{2m} P_o = 0 \qquad (3.147)$$

subject to the initial conditions of Equations (3.140), (3.141). Integrating Equation (3.147) after multiplying both sides by $\dot{w}_o(t)$ leads to

$$\frac{1}{2}\dot{w}_o^2(t) + \frac{\lambda}{3} w_o^3(t) + \frac{3}{2m} P_o w_o(t) = \frac{1}{2}\left(\frac{I}{m}\right)^2 + \frac{\lambda}{3}\left(\frac{I}{m}\right)^3 (T-\tau/2)^3 + \frac{3}{2m} P_o \left(\frac{I}{m}\right)(T-\tau/2) \qquad (3.148)$$

for $t > T$, where the right hand side (i.e. the constant of integration) has been determined from the initial conditions at $t = T$. The beam finally comes to rest at time t_f when $\dot{w}_o(t_f) = 0$. Using Equations (3.148) and (3.36), the final centrepoint deflection δ_f can be expressed as

$$\frac{\delta_f}{h} + \frac{4}{3}\left(\frac{\delta_f}{h}\right)^3 = \frac{I^2}{3mhP_o} + \frac{4}{3}\left(\frac{I}{mh}\right)^3 (T-\tau/2)^3 + \left(\frac{I}{mh}\right)(T-\tau/2) \tag{3.149}$$

Now Equation (3.139) can be recast into the following form:

$$(T-\tau/2) + \frac{4}{3}\left(\frac{I}{mh}\right)^2 (T-\tau/2)^3 = \frac{I}{3P_o} - \frac{1}{2}\tau - \frac{1}{30}\left(\frac{I}{mh}\right)^2\tau^3 \tag{3.139a}$$

Combining Equations (3.139a) and (3.149) to eliminate T provides the following equation, which determines δ_f/h once the pressure pulse and the beam properties are defined:

$$\frac{\delta_f}{h} + \frac{4}{3}\left(\frac{\delta_f}{h}\right)^3 = \frac{2}{3}\frac{I^2}{mhP_o} - \frac{I}{2mh}\tau - \frac{1}{30}\left(\frac{I}{mh}\right)^3\tau^3 \tag{3.150}$$

In terms of the dimensionless parameters of our problem β, $\bar{P}$ defined by Equations (3.79) and (3.63), Equation (3.150) can be rewritten as

$$\frac{\delta_f}{h} + \frac{4}{3}\left(\frac{\delta_f}{h}\right)^3 = \frac{2}{3}\beta - \frac{1}{2}(\beta/\bar{P}) - \frac{1}{30}(\beta/\bar{P})^3 \tag{3.151}$$

which is valid so long as $\delta_f/h < 1/2$.

If interest lies in very small values of $\chi = a\tau$ such that terms of the order of χ^4 and higher can be neglected, we can write Equation (3.151) approximately as

$$\frac{\delta_f}{h} + \frac{4}{3}\left(\frac{\delta_f}{h}\right)^3 \approx \frac{2}{3}\beta\left(1 - \frac{3}{4\bar{P}}\right) \tag{3.152}$$

It is noticeable that we have already implicitly neglected terms of similar order in the derivation of the approximate Equation (3.100), so that the truncation error committed is consistent. It is also evident that for small deflections, $\delta_f/h < 1/2$ Equations (3.100) and (3.152) yield the same response at $\bar{P} = 3$ (i.e. at the transition from medium to high loading range). From these observations we conclude that for $\chi^4 << 1$:

$$\frac{\delta_f}{h} + \frac{4}{3}\left(\frac{\delta_f}{h}\right)^3 \approx \begin{cases} \frac{3}{4}\beta\left(1 - \frac{1}{\bar{P}}\right) & \text{for } 1 < \bar{P} < 3 \\ \\ \frac{2}{3}\beta\left(1 - \frac{3}{4\bar{P}}\right) & \text{for } \bar{P} > 3 \end{cases} \tag{3.153}$$

provided that $\delta_f/h < 1/2$.

It can be observed that if the non-linear term, $(\delta_f/h)^3$, in Equation (3.153) is eliminated the linearized equation described by Symonds (see Equation (10) of (Reference 27) for beams with no axial constraints, will once more be obtained.

Finally Equation (3.151) reduces to the impulsive loading case when we take the limit $\bar{P} \to \infty$, so that

$$\frac{\delta_f}{h} + \frac{4}{3}\left(\frac{\delta_f}{h}\right)^3 = \frac{2}{3}\beta_o \qquad (3.154)$$

where

$$\beta_o = \frac{I_o^2}{mhP_o}$$

and I_o is the ideal impulse (corresponding to a Dirac delta function) which causes the same central deflection δ_f/h as the equivalent rectangular pressure pulse. Equation (3.154) is identical to that obtained by Symonds and Mentel (see Equation (25) of Reference 11 or Equation (14) of Reference 27) to predict the central deflection of a simply supported axially constrained beam subjected to a uniformly distributed initial velocity, I_o/m.

b) Moderately large deflections; membrane theory

If during this third phase of motion the central deflection exceeds h/2, the beam starts behaving as a one-dimensional membrane before it comes to a stop.

The initial condition on velocity is in this case:

$$\dot{w}(x_o, t^* = 0) = \dot{w}_o(0)\frac{x_o}{L} \quad \text{for} \quad 0 \leq x_o \leq L \qquad (3.155)$$

in which $\dot{w}(0)$ is given by the following expression

$$\dot{w}_o\,(t^* = 0) = \dot{w}_o(0) = \frac{I}{m}\sqrt{(3/\beta)}\left[\frac{2}{3}(\beta-1)\right.$$

$$\left. - \frac{1}{2}(\beta/\bar{P}) - \frac{1}{30}(\beta/\bar{P})^3\right]^{1/2} \qquad (3.155a)$$

In view of the difficulties involved in using the precise initial deflected shape, we employ the approximate technique (Figure 3.15) developed previously to obtain the final central deformation of the membrane as

$$\frac{\tilde{\delta}_f}{h} = \sqrt{(A_1^2 + B_1^2)} \qquad (3.156)$$

where

$$A_1 = \frac{2L}{\pi ch} V_o = \frac{2}{\pi}\left[\frac{2}{3}(\beta-1) - \frac{1}{2}(\beta/\bar{P}) - \frac{1}{30}(\beta/\bar{P})^3\right]^{1/2} \qquad (3.156a)$$

$$B_1 = \frac{1}{2} \qquad (3.156b)$$

The time to reach this maximum deflection is given by

$$\tilde{t}_f^* = \tan^{-1}(A_1/B_1) \qquad (3.156c)$$

Clearly the above formulation is valid for $\bar{P} > \beta$ and $2 + \frac{3}{2}(\beta/\bar{P}) + \frac{1}{10}(\beta/\bar{P})^3 > \beta$.

In Figure 3.16 are shown curves of the final deflection ratio δ_f/h as function of the impulse parameter β for some typical values of the

pressure parameter $\bar{P}$ in the range $\bar{P} > 3$.

This concludes our finite deflection analysis of a simply supported beam subjected to a rectangular pressure pulse of arbitrary intensity and duration.

3.4 SUMMARY OF RESULTS, INCLUDING THE SOLUTION FOR BEAMS WITH CLAMPED ENDS

In this section we outline the solution for the dynamic plastic deformation of an axially constrained fixed-ended beam (one whose edge constraints prevent axial in-plane displacements as well as transverse displacements and rotations) loaded by a uniformly distributed rectangular pulse. The results are then given in a tabular form against the corresponding predictions for the simply suported beam analysed in the previous sections.

At collapse, the fixed-ended beam carries the load in the manner of a simply supported beam. The displacement configurations are therefore similar in each case, but resisting moments of critical magnitude M act at both ends of the former beam. This necessitates an increase in the total plastic work dissipation and the Equation (3.4) representing the internal virtual work now becomes:

$$\delta W_{int} = N\delta\varepsilon + 2M\delta\psi \qquad (3.157)$$

since in this case both axial strain and curvature change take place at the fixed end as well as at the centre. Evidently, the results of a simply supported beam (given in detail in the preceding sections) can be made to apply to a beam with fixed ends by merely replacing the critical moment M

by 2M whenever it occurs in each equation (this also includes the replacement of M_o; the critical bending moment in the absence of axial load; by $2M_o$).

In accordance with the above modification the flow rule (Equation (3.16)) takes the form

$$\frac{N}{N_o} = \frac{N_o w_o}{4M_o} = \frac{w_o}{h} < 1 \qquad (3.158)$$

It can be seen that the beam solution is now valid for central deflections smaller than the full depth of the beam, as opposed to half-depth of the beam in the simply supported case. In view of this, it may be shown that the various results for the simply-supported beam given in the previous sections reduce to the corresponding results for clamped beams when the appropriate parameters are selected from Table 3.1

The subsequent tables (Tables 3.2 and 3.3) serve to summarize the predictions of the permanent central deformation of simply supported and fully clamped beams according to the complete theory of this thesis. The comparison between predictions of final deflections of various theoretical models and the test results, in the limiting case of an impulsive load, are shown in Figure 3.17 for fully clamped axially restrained beams.

3.5 DISCUSSION OF RESULTS

From the results of the analysis presented in this chapter (Figures 3.14 and 3.16) it can be seen in general that two basic parameters are needed to adequately represent the influence of the rectangular pressure pulse on the permanent deflections, namely the impulse parameter β and the pressure parameter $\bar{P}$. Replacement of the pressure pulse by an ideal

impulse; which represents only a single parameter β, may therefore lead to unsatisfactory results. This is especially true for small values of $\bar{P}$. As $\bar{P}$ increases the deflection-impulse (i.e., δ_f/h vs. β) variations become progressively stronger in resemblance to that of an ideal impulse. One may observe from Figure 3.14 that for values of β and $\bar{P}$ to the right of the cross-hatched boundary the maximum deflections do not depend on β. Consequently in this region the response can be characterized by the single parameter $\bar{P}$. This is equivalent to replacement of the pressure pulse by a step load.

It can be inferred from Figure 3.17 that the results of the present "approximate" plastic string analysis compare favourably with the experimental values observed on fully clamped beams subjected to impulsive loads. The linearized solution which neglects the effects of geometry changes, is of course too crude to give a true indication of the beam's behaviour, as can be observed from Figure 3.17 for the extreme case of an impulsive load. The same is also true for dynamic loads with finite durations. Owing to its unrealistic predictions, we shall not consider the results of the linear bending - only theory as means of comparison in our further discussions.

The analysis presented in this chapter can be expected to give good results for impulse parameters in the approximate range given by the inequality (A.9) (see Appendix A). Nevertheless it is believed that the present solution represents the behaviour of beams with constrained ends closely enough for many practical situations (where the ratio L/h is not too small).

In all the preceding analysis a plastic hinge was assumed to be concentrated at a point, however, in reality where the stresses become

critical, a plastic zone of finite curvature extends out from either sides of the hinge point. This spreading out of the plastic deformation, which is not accounted for in the rigid-plastic analysis, plays a significant role in the reduction of deflections. The inclusion of strain hardening and strain-rate effects also tends to reduce the final deflections and must be taken into account for less conservative and more realistic results.

Table 3.1

Comparison of various parameters used in the analysis of simply supported and fully clamped beams

Parameter	Simply Supported Beam	Clamped Beam
P_o	$2M_o/L^2$	$4M_o/L^2$
$\bar{P}$	P_m/P_o	P_m/P_o
β	I^2/mhP_o	I^2/mhP_o
a^2	$\frac{P_o}{mh}\left[3(\bar{P}-1)\right]^{1/2}$	$\frac{P_o}{2mh}\left[3(\bar{P}-1)\right]^{1/2}$
$a\tau$	$\sqrt{\beta}\left[3(\bar{P}-1)\right]^{1/4}/\bar{P}$	$\sqrt{(\beta/2)}\left[3(\bar{P}-1)\right]^{1/4}/\bar{P}$
β_m	$\bar{P}^2\left[K-F(1/\sqrt{2}, \phi_s)\right]^2/\left[3(\bar{P}-1)\right]^{1/2}$	$2\bar{P}^2\left[K-F(1/\sqrt{2}, \phi_s)\right]^2\left[3(\bar{P}-1)\right]^{1/2}$
$r(t_s)$ [Phase II(b)]	$L\left[2/\beta + 3/2\bar{P} + \frac{1}{10}(\beta^2/\bar{P}^3)\right]^{1/2}$	$L\left[4/\beta + 3/2\bar{P} + \frac{1}{40}(\beta^2/\bar{P}^3)\right]^{1/2}$

Table 3.2

Theoretical prediction of final central deflection of simply supported and fully clamped beams: Medium load $1 < \bar{P} < 3$

		Simply-supported Beam	Clamped Beam
Phase I(a)	$1 < \bar{P} \quad 4/3$ $a\tau > K$	$\frac{\delta_f}{h} = \frac{\sqrt{3}}{2}\left[\bar{P}-1\right]^{1/2}$	$\frac{\delta_f}{h} = \sqrt{3}\left[\bar{P}-1\right]^{1/2}$
Phase I(b)	$4/3 < \bar{P} < 3$ $\beta > \beta_m$		
	i) First stage	$\frac{\delta_f}{h} = \sqrt{(A_1^2 + B_1^2)}+(\frac{2}{\pi})\ \bar{P}$	$\frac{\delta_f}{h} = 2\sqrt{(A_1^2+B_1^2)}+2(\frac{2}{\pi})^3\ \bar{P}$
	ii) Second stage	$\frac{\delta_f}{h} = \sqrt{(C_1^2 + D_1^2)}$	$\frac{\delta_f}{h} = 2\sqrt{(C_1^2 + D_1^2)}$
Phase II(a)	$1 < \bar{P} < 4/3$ $a\tau < K$	$\frac{\delta_f}{h} + \frac{4}{3}(\frac{\delta_f}{h})^3 = \frac{2}{3}(\Lambda^2+1)$	$\frac{\delta_f}{h} + \frac{1}{3}(\frac{\delta_f}{h})^3 = \frac{4}{3}(\Lambda^2+1)$
Phase II(b)	$4/3 < \bar{P} < 3$ $\beta < \beta_m$	$\frac{\delta_f}{h} = \left[\frac{1}{4} + \frac{8}{3\pi^2}\ \Lambda^2\right]^{1/2}$	$\frac{\delta_f}{h} = \left[1 + \frac{32}{3\pi^2}\ \Lambda^2\right]^{1/2}$

A_1, B_1 are given by Equations (3.111a, b)

C_1, D_1 are given by Equations (3.112a, b) where it is understood that the appropriate parameters are selected from Table 3.1

Table 3.3

Theoretical prediction of final central deflection of simply supported and fully clamped beams: High load $\bar{P} > 3$

	Simply-supported Beam	Clamped Beam	
Phase I(a)	No permanent deformation	No permanent deformation	
Phase I(b)†			
i) First stage	$\frac{\delta_f}{h} = \sqrt{(A_1^2+B_1^2)}+(\frac{2}{\pi})^2\bar{P}$	$\frac{\delta_f}{h} = 2\sqrt{(A_1^2+B_1^2)}+2(\frac{2}{\pi})^2\bar{P}$	$\bar{P}<\beta$ / $\bar{P}<\beta/2$
ii) Second stage	$\frac{\delta_f}{h} = \sqrt{(C_1^2 + D_1^2)}$	$\frac{\delta_f}{h} = 2\sqrt{(C_1^2 + D_1^2)}$	
Phase II(a)	No permanent deformation	No permanent deformation	
Phase II(b)	$\frac{\delta_f}{h} = [(\frac{2}{\pi})^2\beta\ [1-\frac{2}{3}\frac{r(t_s)}{L}\ + \frac{1}{4}\ ]^{1/2}$	$\frac{\delta_f}{h} = [2(\frac{2}{\pi})^2\beta\ [1-\frac{2}{3}\frac{r(t_s)}{L}\ +1\ ]^{1/2}$	$\bar{P}>\beta$ / $\bar{P}>\beta/2$; $r(t_s)<L$
Phase III(a)	$\frac{\delta_f}{h} + \frac{4}{3}(\frac{\delta_f}{h})^3 = \frac{2}{3}\beta - \frac{1}{2}(\beta/\bar{P}) - \frac{1}{30}(\beta/\bar{P})^3$	$\frac{\delta_f}{h} + \frac{1}{3}(\frac{\delta_f}{h})^3 = \frac{2}{3}\beta - \frac{1}{2}(\beta/\bar{P}) - \frac{1}{120}(\beta/\bar{P})^3$	

Table 3.3

Theoretical prediction of final central deflection of simply supported and fully clamped beams: High load $\bar{P} > 3$ (Continued)

	Simply-supported Beam	Clamped Beam
Phase III(b)	$\frac{\delta_f}{h} = \{(\frac{2}{\pi})^2 [\frac{2}{3}(\beta-1) - \frac{1}{2}(\beta/\bar{P}) - \frac{1}{30}(\beta/\bar{P})^3] + \frac{1}{4}\}^{1/2}$ $\bar{P}>\beta$ $r(t_s)>L$	$\frac{\delta_f}{h} = \{2(\frac{2}{\pi})^2 [\frac{2}{3}(\beta-2) - \frac{1}{2}(\beta/\bar{P}) - \frac{1}{120}(\beta/\bar{P})^3] + 1\}^{1/2}$ $\bar{P}>\beta/2$ $r(t_s)>L$

It is understood that the various parameters appearing in the above are appropriately selected from Table 3.1

†A_1, B_1, C_1 and D_1 are given by Equations (3.130a, b) and (3.131 a,b)

CHAPTER IV

CONSTRUCTION OF ISODAMAGE CURVES

4.1 INTRODUCTION

A useful way of representing the response of a structure to a specific pulse shape is to establish the appropriate structural "isoresponse" curve. The latter are the locus of combinations of peak pressure and impulse that produce the same response, in this case the maximum displacement of the structure. For a plastic structure undergoing a given permanent deformation or damage, the corresponding curve is called an "isodamage" curve. The object of this chapter is to convert the complete solution obtained in the previous chapter into a form suitable for the generation of isodamage curves. the variables (or parameters) that control each damage mechanism will also be distinguished. Following a pattern somewhat similar to that established in the preceding sections, we shall consider here two distinct levels of damage typified by small damage ($\delta_f/h < 0.5$) and large damage ($\delta_f/h > 0.5$).

4.2 SMALL DAMAGE ($\delta_f/h < 0.5$)

We proceed to find a relationship between the dimensionless pressure parameter $\bar{P}$ and the dimensionless impulse parameter β by treating the level of damage δ_f/h as a fixed quantity. The following equations for β result from Equations (3.94) and (3.151) when we keep the quantity δ_f/h at a constant level. Thus

$$\beta = \frac{\bar{P}^2}{\sqrt{3(\bar{P}-1)}}\left[F(1/\sqrt{2}, \phi)\right]^2 \quad \text{for} \quad 1 < \bar{P} < 3 \qquad (4.1)$$

where $\phi = \phi\ (\bar{P};\ \delta_f/h)$ is given by the combination of Equations (3.95) and (3.97). Beyond the above pressure range (i.e. for $\bar{P} > 3$) the impulse parameter β is given by the smallest positive real root of the polynomial equation.

$$\frac{1}{30}\ (\beta/\bar{P})^3 + (\beta/\bar{P})\left[\frac{1}{2} - \frac{2}{3}\bar{P}\right] + \frac{\delta_f}{h} + \frac{4}{3}\left(\frac{\delta_f}{h}\right)^3 = 0 \quad \text{for } \bar{P} > 3 \tag{4.2}$$

Equations (4.1) and (4.2) give the $\bar{P}$ - β combinations that produce the same final deflection δ_f/h. These combinations are plotted in Figure 4.1 for $\delta_f/h = 0.25$ and 0.5. At the lower end (horizontal part) of the curves, the response can be characterized by a single parameter, namely the pressure parameter $\bar{P}_c$ given by

$$\bar{P}_c = 1 + \frac{4}{3}\left(\frac{\delta_f}{h}\right)^2 ; \quad 1 < \bar{P}_c < 4/3 \tag{4.3}$$

which follows from Equations (3.50).

The value of the impulse parameter β beyond which the dynamic pulse can be characterized by a step load, is given by the root of Equation $a\tau = K$, or

$$\beta_c = \frac{\bar{P}_c^{\,2}\ K^2}{\sqrt{3(\bar{P}_c - 1)}} = \frac{K^2}{2}\left[1 + \frac{4}{3}\left(\frac{\delta_f}{h}\right)^2\right]^2 \Big/ \frac{\delta_f}{h} \tag{4.4}$$

The upper part of the isoresponse curves are asymptotic to an impulse parameter β_o given by

$$\beta_o = \frac{3}{2}\left[\left(\frac{\delta_f}{h}\right) + \frac{4}{3}\left(\frac{\delta_f}{h}\right)^3\right] \qquad (4.5)$$

In the intermediate dynamic loading realm (knee of the curve), both parameters β and $\bar{P}$ influence the permanent deflections. Hence we must know the entire time history of the loading. Points on this part of the curve are described by Equations (4.1) and (4.2).

4.3 SEVERE DAMAGE ($\delta_f/h > 0.5$)

Our discussion so far has been limited to small permanent deflections in which effects of flexure and stretching are coexistent. However, as mentioned earlier, for moderately large deflections the beam offers no resistance to bending and behaves as a flexible one-dimensional membrane (so-called string behaviour). In what follows we shall be concerned with the determination of $\bar{P}$ - β curves that are governed by the latter phenomenon. For simplicity we use the results of the approximate analysis (developed at the end of Section 3.3.1) based on the dissipation of the initial kinetic energy into the kinetic energy associated with an equivalent sine-shape velocity profile.

It can be seen from the results of the previous chapter, Figure 3.14 and Equation (3.111), that pressures in the medium range, $1 < \bar{P} < 3$, do not contribute to damage δ_f/h greater than $\delta_f/h \approx 1.42$. For the sake of clarity we construct the pressure-impulse curves separately according to whether the damage quantity δ_f/h is greater or less than $\delta_f/h \approx 1.42$.

i) $0.5 < \delta_f/h < 1.42$

The value of the pressure parameter $\bar{P}_c$ is in this case given by Equation (3.111) as

$$\bar{P}_c = \frac{\left(\frac{\delta_f}{h}\right)^2 - \frac{1}{4} + \frac{2}{3}\left(\frac{2}{\pi}\right)^2}{\frac{1}{2}\left(\frac{2}{\pi}\right)^2 - \left(\frac{2}{\pi}\right)^3 + 2\left(\frac{2}{\pi}\right)^3 \frac{\delta_f}{h}}, \quad 4/3 < \bar{P}_c < 3 \qquad (4.6)$$

The corresponding value of the impulse parameter β_c required to achieve the same central deflection δ_f/h can be obtained from Equation (3.81) and (3.112c) as

$$\beta_c = \bar{P}_c^2 \left\{ \frac{\sqrt{2}}{\pi} \mu_c + \left[\frac{1}{3(\bar{P}_c - 1)}\right]^{1/4} \left[K - F(1/\sqrt{2}, \phi_s)\right] \right\} \qquad (4.7)$$

where ϕ_s and μ_c are defined by Equations (3.82) and (3.112c) with $\bar{P}$ replaced by $\bar{P}_c$. As the pressure is increased from $\bar{P}_c$ to $\bar{P} = 3$ (i.e. within the medium range of dynamic loading) the pressure-impulse relationship can be described by Equations (3.112) and (3.113) when they are converted into the form $\beta \equiv \beta(\bar{P}; \delta_f/h)$ with δ_f/h being a fixed parameter. Performing the above conversion leads to the following $\beta - \bar{P}$ relationships:

$$\beta = \bar{P}^2 \left\{ \frac{\sqrt{2}}{\pi} \mu + \left[\frac{1}{3(\bar{P} - 1)}\right]^{1/4} \left[K - F(1/\sqrt{2}, \phi_s)\right] \right\} \qquad (4.8)$$

for $\bar{P}_c < \bar{P} < 3$ and $\beta > \beta_m$ or $\mu > 0$, where

$$\mu = \sin^{-1}\left\{\frac{Q}{\sqrt{(A_1^2 + B_1^2)}}\right\} - \sin^{-1}\left\{\frac{B_1}{\sqrt{(A_1^2 + B_1^2)}}\right\} \qquad (4.8a)$$

In the above the inverse sine is an angle between $\frac{-\pi}{2}$ and $\frac{\pi}{2}$ with A_1 , B_1 given by Equations (3.111a) and (3.111b) respectively and Q defined as

$$Q = \frac{\pi^3}{16\bar{P}}\left[\left(\frac{\delta_f}{h}\right)^2 - \left(A_1^2 + B_1^2\right) - \left(\frac{2}{\pi}\right)^6 \bar{P}^2\right] \qquad (4.8b)$$

If $\bar{P}$ is increased to a level that renders the quantity μ negative (i.e. $\mu < 0$ or $\beta < \beta_m$) then the results of Phase II(b) prevails (i.e. Equation 3.113) and the $\beta - \bar{P}$ relationship becomes

$$\beta = \frac{\bar{P}^2}{\sqrt{3}(\bar{P}-1)}\left[F(1/\sqrt{2}, \phi)\right]^2 \text{ for } \bar{P}_c < \bar{P} < 3 \text{ and } \beta < \beta_m \qquad (4.9)$$

where ϕ is given by Equation (3.97) in which

$$\gamma^2 = \{\pi^2\left[\left(\frac{\delta_f}{h}\right)^2 - \frac{1}{4}\right] + \frac{8}{3}\} \; / \; \left[\bar{P}\sqrt{3}(\bar{P}-1)\right] \qquad (4.9a)$$

To construct the remaining part of the $\bar{P} - \beta$ curve beyond $\bar{P} = 3$ we proceed to rewrite the results of the high load membrane analysis in the form $\beta \equiv \beta\,(\bar{P};\, \delta_f/h)$. In doing so we make use of Equations (3.131), (3.146) and (3.156). Elementary though somewhat lengthy analysis leads to the following expressions for the impulse parameter β.

$$\beta = \bar{P}^2\left[\frac{\sqrt{2}}{\pi}\eta + \frac{1}{\sqrt{\bar{P}}}\right] \qquad (4.10)$$

for $\bar{P} > 3$ and $\beta > \bar{P}$ or $\eta > 0$, where

$$\eta = \sin^{-1}\left\{\frac{Q}{\sqrt{(A_1^2+B_1^2)}}\right\} - \sin^{-1}\left\{\frac{B_1}{\sqrt{(A_1^2+B_1^2)}}\right\} \qquad (4.10a)$$

the inverse sine being an angle between $\frac{-\pi}{2}$ and $\frac{\pi}{2}$ with A_1, B_1 given by Equations (3.130a,b). The quantity Q is again defined by Equation (4.8b), however the A_1 appearing in that expression is now given by Equation (3.130a).

If the quantity η (Equation 4.10a) becomes negative as a consequence of increase in pressure, two different cases arise according to whether the plastic hinges are within the half-span (i.e. $0 < \rho < L$) or at the midspan (i.e. $\rho = 0$) prior to the onset of string phase (Equations (3.146) and (3.156)). The value of β as a function of $\bar{P}$ and the fixed parameter δ_f/h are in each of the above cases given by the roots of the following polynomial equations:

$$\frac{2}{45\bar{P}^3}\beta^4 + \left(\frac{2}{3\bar{P}} - 1\right)\beta^2 + \left[\frac{8}{9} + \frac{\pi^2}{2}\left(\left(\frac{\delta_f}{h}\right)^2 - \frac{1}{4}\right)\right]\beta$$

$$- \frac{\pi^4}{16}\left[\left(\frac{\delta_f}{h}\right)^2 - \frac{1}{4}\right]^2 = 0 \qquad (4.11)$$

for $\bar{P} > 3$, $\bar{P} > \beta$ and $2 + \frac{3}{2}(\beta/\bar{P}) + \frac{1}{10}(\beta/\bar{P})^3 < \beta$

$$\frac{1}{30\bar{P}^3}\beta^3 + \left(\frac{1}{2\bar{P}} - \frac{2}{3}\right)\beta + \frac{2}{3} + \frac{\pi^2}{4}\left[\left(\frac{\delta_f}{h}\right)^2 - \frac{1}{4}\right] = 0 \qquad (4.12)$$

for $\bar{P} > 3$, $\bar{P} > \beta$ and $2 + \frac{3}{2}(\beta/\bar{P}) + \frac{1}{10}(\beta/\bar{P})^3 > \beta$

For a given δ_f/h, as the pressure is increased indefinitely (i.e. $P \to \infty$), the magnitude of β necessary to maintain the given deflection (or damage) δ_f/h may be shown to be

$$\beta_o = 1 + \frac{3\pi^2}{8}\left[\left(\frac{\delta_f}{h}\right)^2 - \frac{1}{4}\right] \tag{4.13}$$

provided $\beta_o < 2$ or $\frac{\delta_f}{h} < 0.72$ and

$$\beta_o = \frac{1}{2}\left[b_1 + \sqrt{(b_1^2 - 4c_1)}\right] \tag{4.14}$$

for $0.72 < \frac{\delta_f}{h} < 1.42$, where

$$b_1 = \frac{8}{9} + \frac{\pi^2}{2}\left[\left(\frac{\delta_f}{h}\right)^2 - \frac{1}{4}\right] \tag{4.14a}$$

$$c_1 = \frac{\pi^4}{16}\left[\left(\frac{\delta_f}{h}\right)^2 - \frac{1}{4}\right]^2 \tag{4.14b}$$

Equations (4.13) and (4.14) define the location of the vertical asymptotes in the $\bar{P} - \beta$ space and represent the value of the ideal impulse which produces the same damage δ_f/h as the rectangular pulses. Figure 4.2 illustrates a complete picture of the relationship that must exist between the pressure and impulse (in nondimensional form) to provide a given central damage $0.5 < \delta_f/h < 1.42$.

ii) $\delta_f/h > 1.42$

As mentioned before the medium range of pressure intensity (i.e $\frac{4}{3} < \bar{P} < 3$) makes no contribution to the damages δ_f/h that exceed 1.42. Under

these circumstances the isodamage curves emanate from a different starting pressure $\bar{P}_c$ given by

$$\bar{P}_c = \frac{q}{s} + \left[\left(\frac{q}{s}\right)^2 - \frac{1}{s} \left\{ \left(\frac{\delta_f}{h}\right)^2 - \frac{1}{4} \right\} \right]^{1/2} \qquad (4.15)$$

where

$$s = \left[\left(\frac{2}{\pi}\right)^2 - \left(\frac{2}{\pi}\right)^3 + 2 \left(\frac{2}{\pi}\right)^3 \frac{\delta_f}{h} \right]^2 \qquad (4.15a)$$

and

$$q = \sqrt{s} \left[\left(\frac{\delta_f}{h}\right)^2 - \frac{1}{4} \right] + \frac{4}{5} \left(\frac{2}{\pi}\right)^4 \qquad (4.15b)$$

The impulse parameter β_c, beyond which the response is insensitive to impulse and depends primarily on the pressure magnitude, is given by Equation (4.10) with $\bar{P}$ replaced by $\bar{P}_c$ defined above. The points with coordinates $(\beta, \bar{P})$ that describe the dynamic and impulsive parts of the isoresponse curve can once again be obtained from Equations (4.11) to (4.13). In Figure 4.3 are shown curves of the pressure as a function of impulse, for some typical values of the permanent deflection ratio $\delta_f/h > 1.42$.

4.4 DISCUSSION OF RESULTS

The general shape of the isodamage curves, which is approximately hyperbolic, remains unaltered with increasing deflections. In the vicinity of the vertical asymptote, changes in load magnitude for a given impulse

cause relatively small deviations from the isodamage curve, but changes in impulse for a given load magnitude cause relatively large departures. The location of these critical load curves changes considerably with increasing deflection δ_f/h. For a particular value of δ_f/h the corresponding isodamage curves predicted by the linear bending theory always lie to the left of the present curves, the amount of shift being proportional to the square of the given deflection $(\delta_f/h)^2$. These pure bending isodamage curves, which can be drawn for a specific value of δ_f/h using the linear part of Equation (3.153), clearly lead to overconservative predictions of the beam response and have therefore been excluded from the present diagrams.

The isodamage curves presented in this chapter are particularly useful for preliminary design where a gross picture of the structure response is desired prior to undergoing a costly program in terms of computer time to analyze the structure through numerical methods. The validity of the present results, however, must rely upon experimental results.

CHAPTER V

CONCLUSIONS

5.1 CONCLUDING REMARKS ON THE THEORY AND ITS APPLICABILITY

An analytical procedure, which includes the effects of finite geometry changes, has been developed herein to predict permanent deformations of rigid-plastic symmetrically supported beams subjected to uniformly distributed blast-type loadings. In the general formulation of the problem distinct deflection modes have been assumed for various ranges of load intensity. A closed-form solution has been derived for the simplest case, that of a rectangular beam acted on by a rectangular pressure pulse of arbitrary magnitude and duration. The dependence of the permanent central deflection on peak pressure and impulse has been emphasized.

However there were some experimental results available for the case of impulsive loading. This case has been obtained as a special case from the general formulas derived herein. It is encouraging to note that these results for the case of a fully clamped beam are in better agreement with the corresponding experimental values (Figure 3.17) than are the estimates obtained by Symonds and Mentel (Reference 11). The theoretical predictions cannot be compared with experimental results since (to the author's knowledge) no test data seem to have been reported for the response of beams to dynamic loads of finite durations. Moreover, due to the lack of relevant uniqueness or bounding theorems it is impossible to assess whether the present predictions are smaller or larger than the exact solution. An assessment of the validity of the various approximations made in the theory outlined herein must await information from experiments

and/or numerical elasto-plastic solutions.† Nevertheless until such supporting confirmation of the theory are obtained the predictions suggested here are believed to be sufficiently accurate to enable designers to make preliminary design decisions. The final results presented as structural isodamage curves are particularly useful in predicting the characteristics of the rectangular pulse required to cause a specified permanent deformation of the beam. These isodamage plots provide a simple presentation of the theoretical results and are extremely important in planning experiments.

It is thought that the method suggested herein could in principle be used to analyze beams having other cross-sectional geometries (restricted to sections with at least one axis of symmetry) by incorporating the appropriate yield condition of the cross-section and its associated flow rule. Such an extension of the theory is now under investigation at UBC.

The mathematical model and its formulation presented here can be applied to any arbitrary pulse shape that satisfies the definition of blast-type loading. In most cases, however, owing to their nonlinear character, the differential equations of motion have to be solved by a numerical technique. Only in the particular case of a rectangular pulse can the equations be integrated in analytic form.

The intent of all the theoretical work presented in this thesis was to obtain the permanent deflection of the beam as a measure of the likelihood of failure. It is felt, however, that information from experiments

---

† This is currently under study at UBC.

is needed to clarify this point since failure may occur due to rupture, fracture or breakage at some point in the material before the permanent deformation is reached.

5.2 FUTURE AREAS OF RESEARCH

The topic presents many interesting areas for further detailed investigations. The following is intended to briefly outline a few of these areas of research that are needed to improve or extend the existing theoretical procedure.

The lack of experimental results in the dynamic realm (when the intensity and duration of the pressure pulse are finite) is readily apparent from a survey of the literature. These results are of prime importance in validating the analytically predicted behaviour of axially restrained beams. Experiments are needed for loads with time durations that are comparable to the natural period of the beam, since the present rigid-plastic solutions are only valid for durations of loading well removed from the natural period. For more realistic results, the elasto-plastic, strain hardening and strain rate effects on the transient dynamic response of beams should be studied. The complete solution in this case requires involved numerical computations. Further research is also required to investigate the effect of different load-time histories on final plastic deformation. Correlation parameters need to be established in order to eliminate the dependence of the response on the pulse shape. To provide a valid correlation over a wide range of load durations, particularly those near the natural period of the structure response these correlation parameters should be checked out on elastic-plastic models. Using these parameters, the isodamage curves obtained here for rectangular pulses can be made to apply to various other

forms of pulse shapes.

Another useful contribution to the existing literature would be to study the influence of "partial" as opposed to "full" end restraints against in-plane movements. Prevention of axial motion at the ends is obviously critical; this is evident from the enormous difference in the deflection predicted by the bending-only theory and from those theories that also take account of axial forces arising from the in-plane end contraints. In practice, however, full end fixity cannot be provided and a small amount of slipping usually occurs at the edge supports. In view of this, it would be informative to have a knowledge of the final deflections acquired by the beam when the axial end restraints are relaxed slightly.

In situations where the size of the beam is significant relative to the stand-off distance from the explosion, the distribution of pressure can no longer be taken as uniform. It would therefore be of value to have theoretical techniques at hand which could account for pressures that are non-uniformly distributed over the beam length.

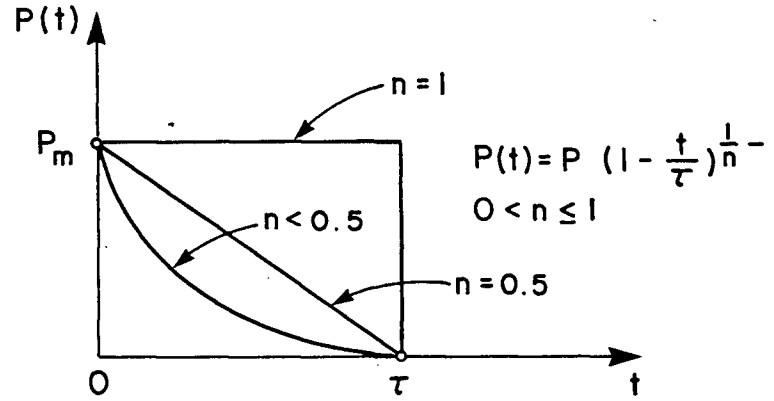

Fig.2.1 Blast-type pulse shapes

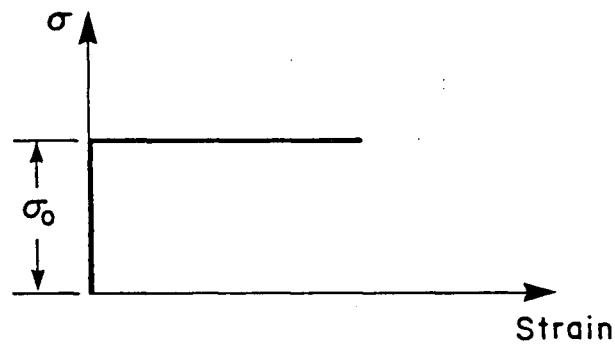

Fig.2.2 Idealized stress-strain diagram: Rigid-perfectly plastic

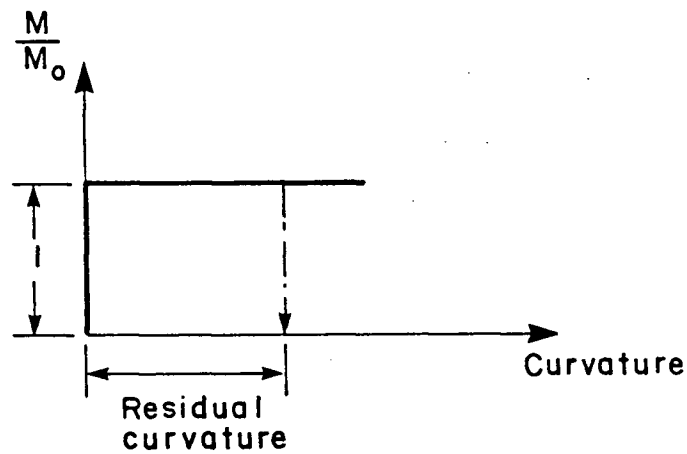

Fig.2.3 Idealized moment-curvature diagram: Rigid-perfectly plastic

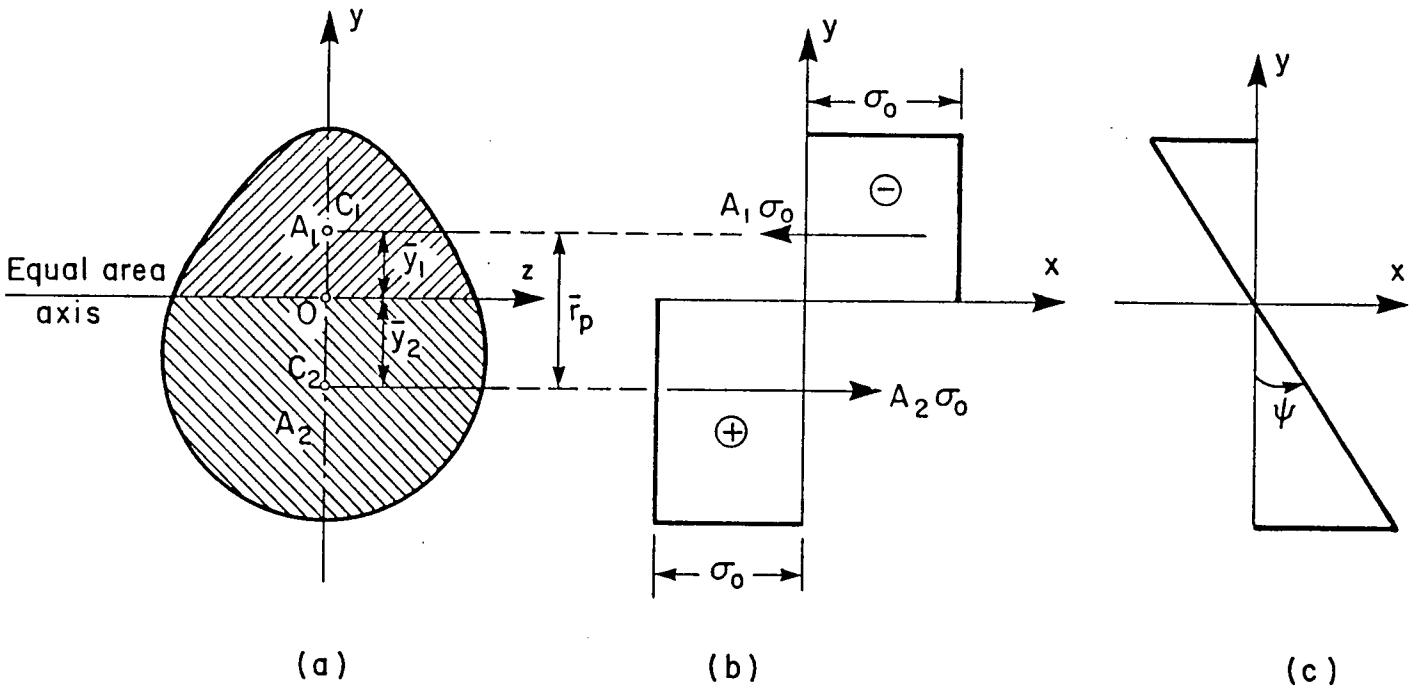

Fig.2.4 Pure bending of a beam of a general cross-section having one axis of symmetry:Fully plastic state

(a) general cross-section with single axis of symmetry
(b) fully plastic stress distribution
(c) strained geometry of section

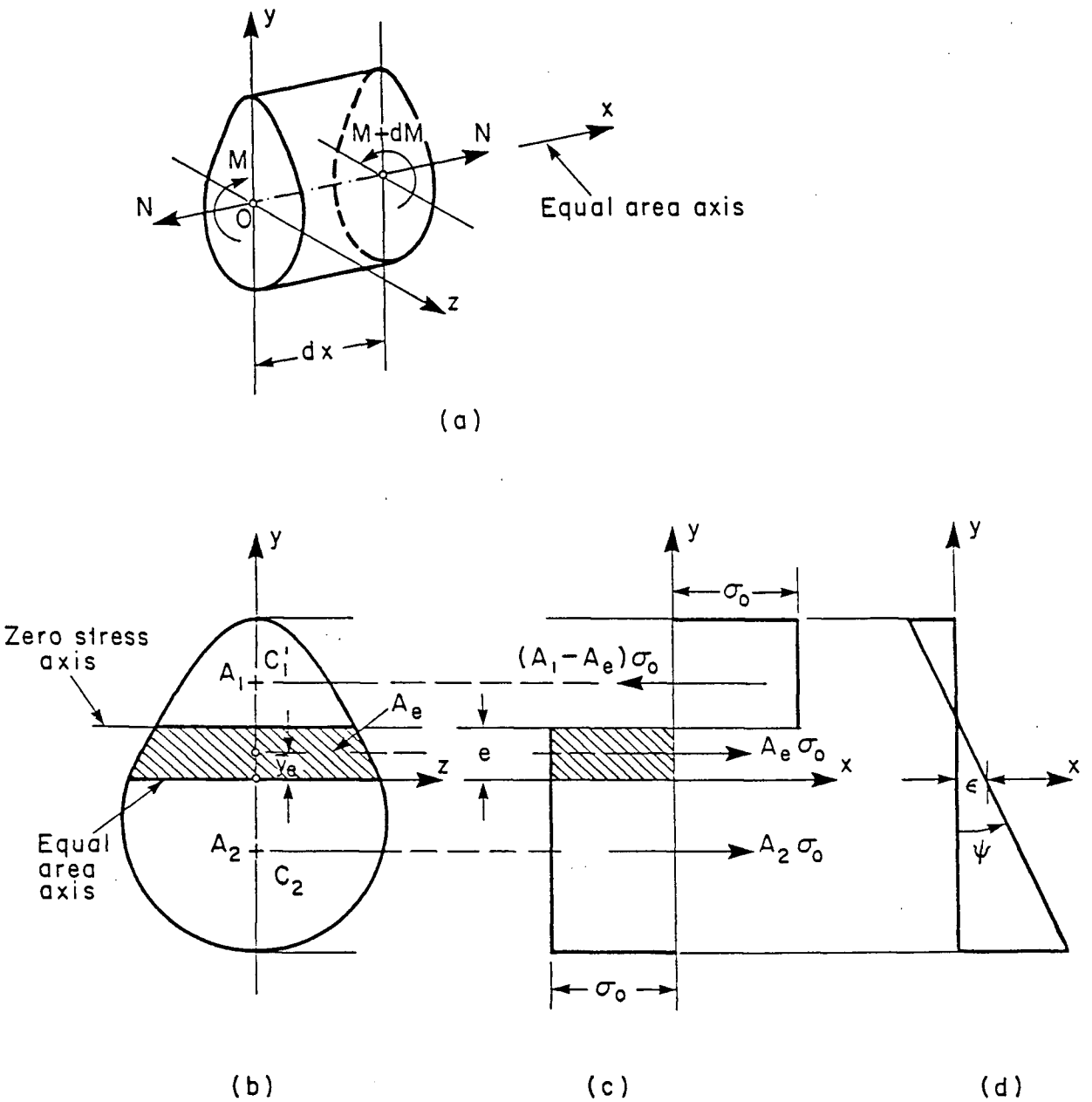

Fig.2.5 Combined tension and bending of a beam of a general cross-section having one axis of symmetry:Fully plastic state

(a) bending moment and axial load as viewed on a beam element
(b) cross-section
(c) fully plastic stress distribution
(d) strained geometry of section

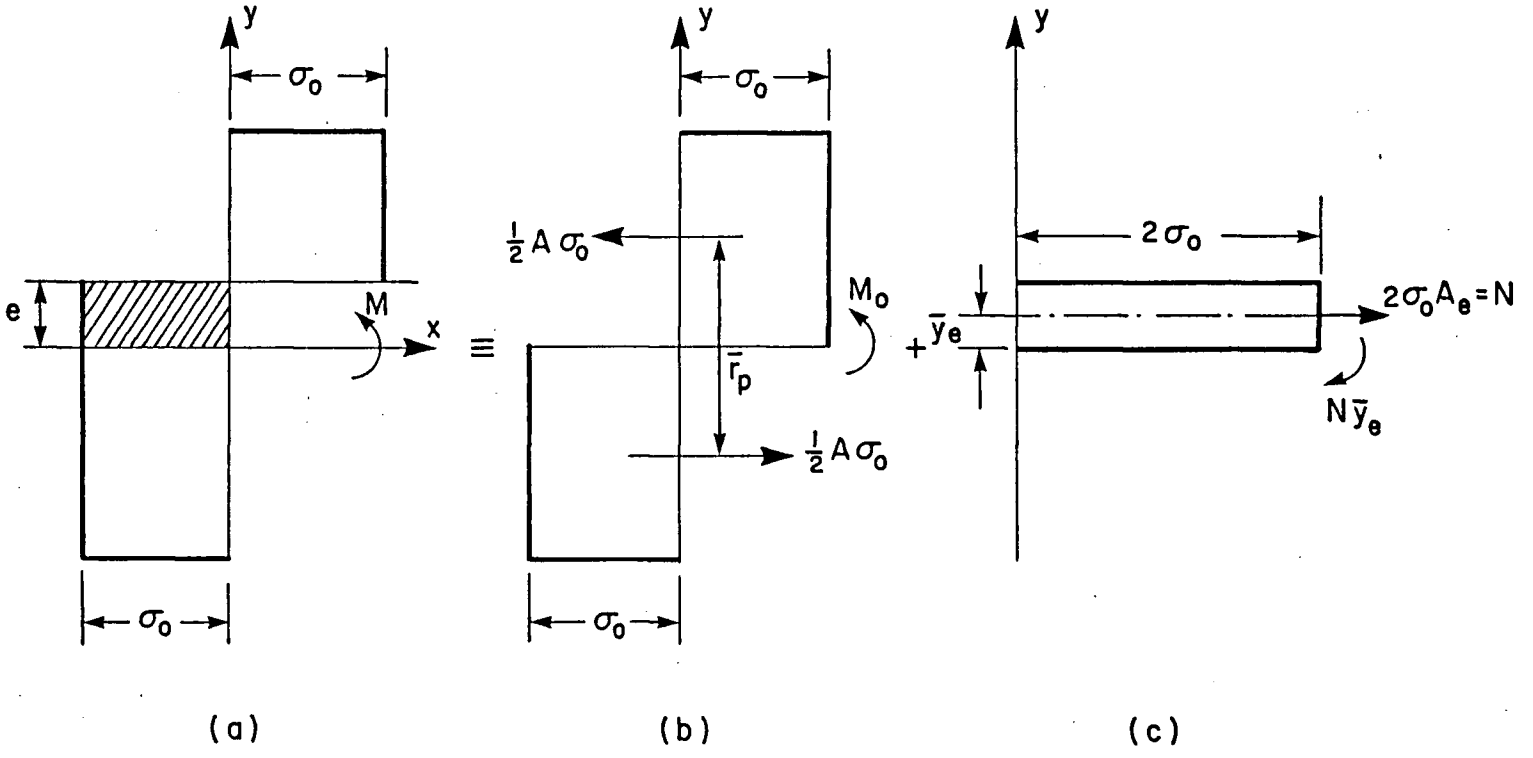

Fig.2.6 Resolution of the fully plastic stress distribution

(a) fully plastic stress distribution
(b) fully plastic stress distribution in the absence of axial load
(c) fictitious stress distribution

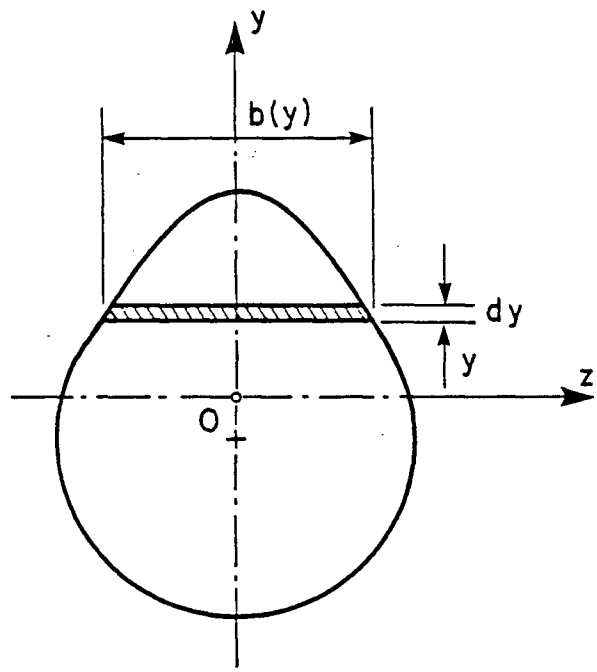

Fig.2.7 Schematic of the cross-section showing a typical differential element

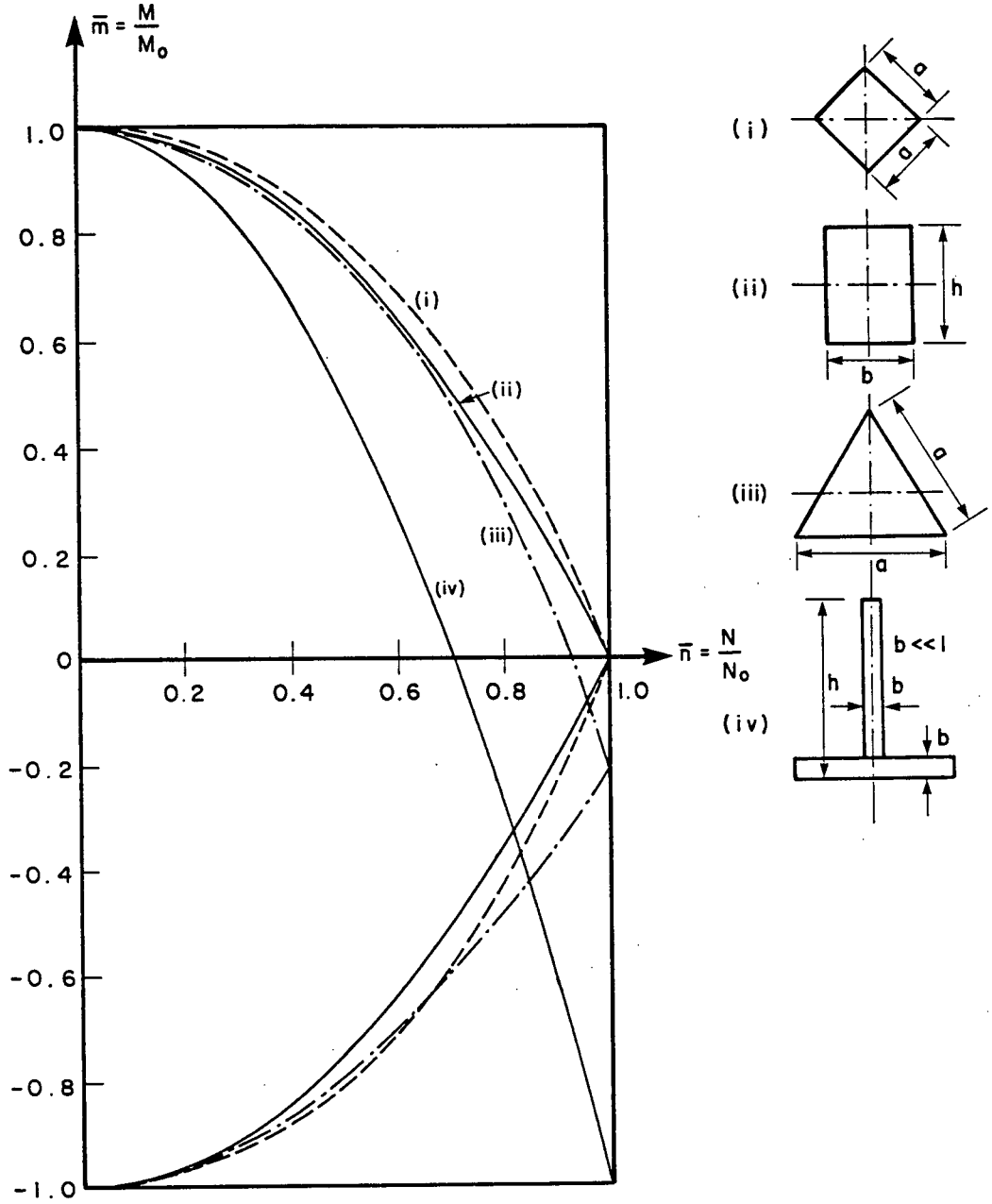

Fig.2.8 Yield curves for some typical cross-section geometries

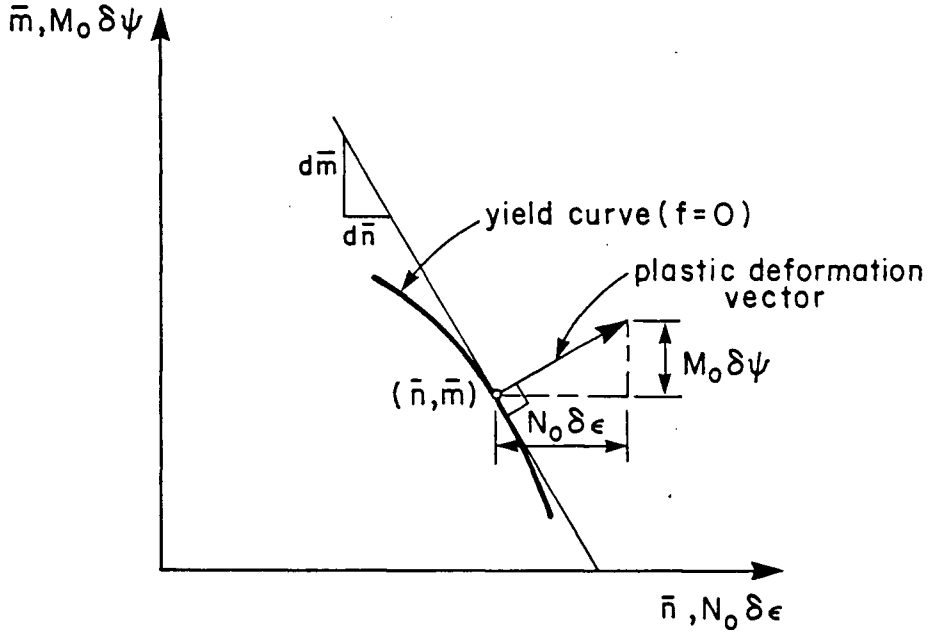

Fig.2.9 Yield curve and the associated normal deformation vector

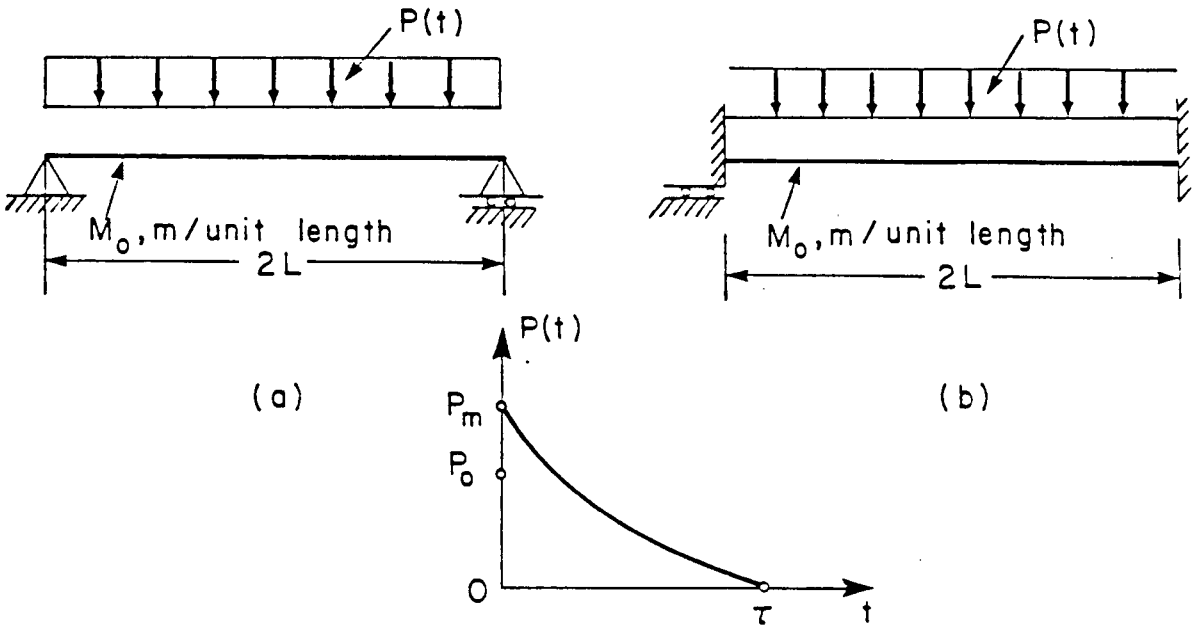

Fig.2.10 Symmetrically supported beams subjected to uniformly distributed blast-type loading

(a) simply supported beam (no axial constraints)
(b) clamped beam (no axial constraints)
(c) general pressure-time history

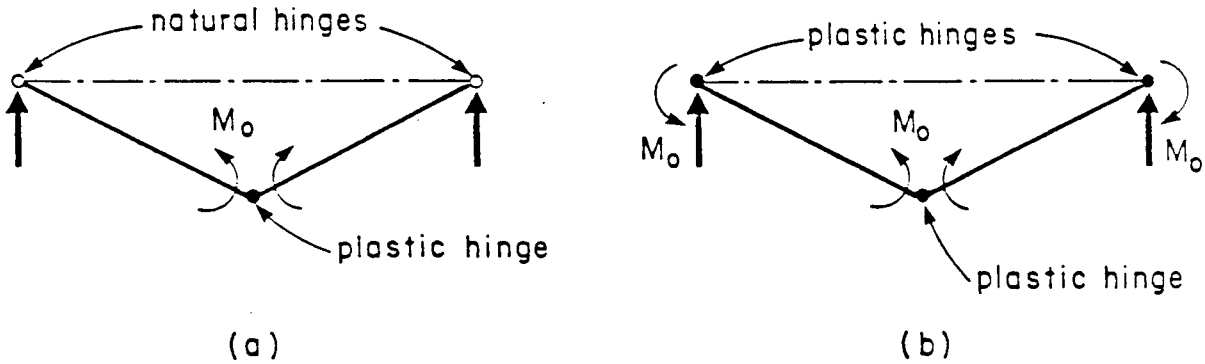

Fig.2.11 Static collapse mechanisms

(a) simply supported beam
(b) clamped beam

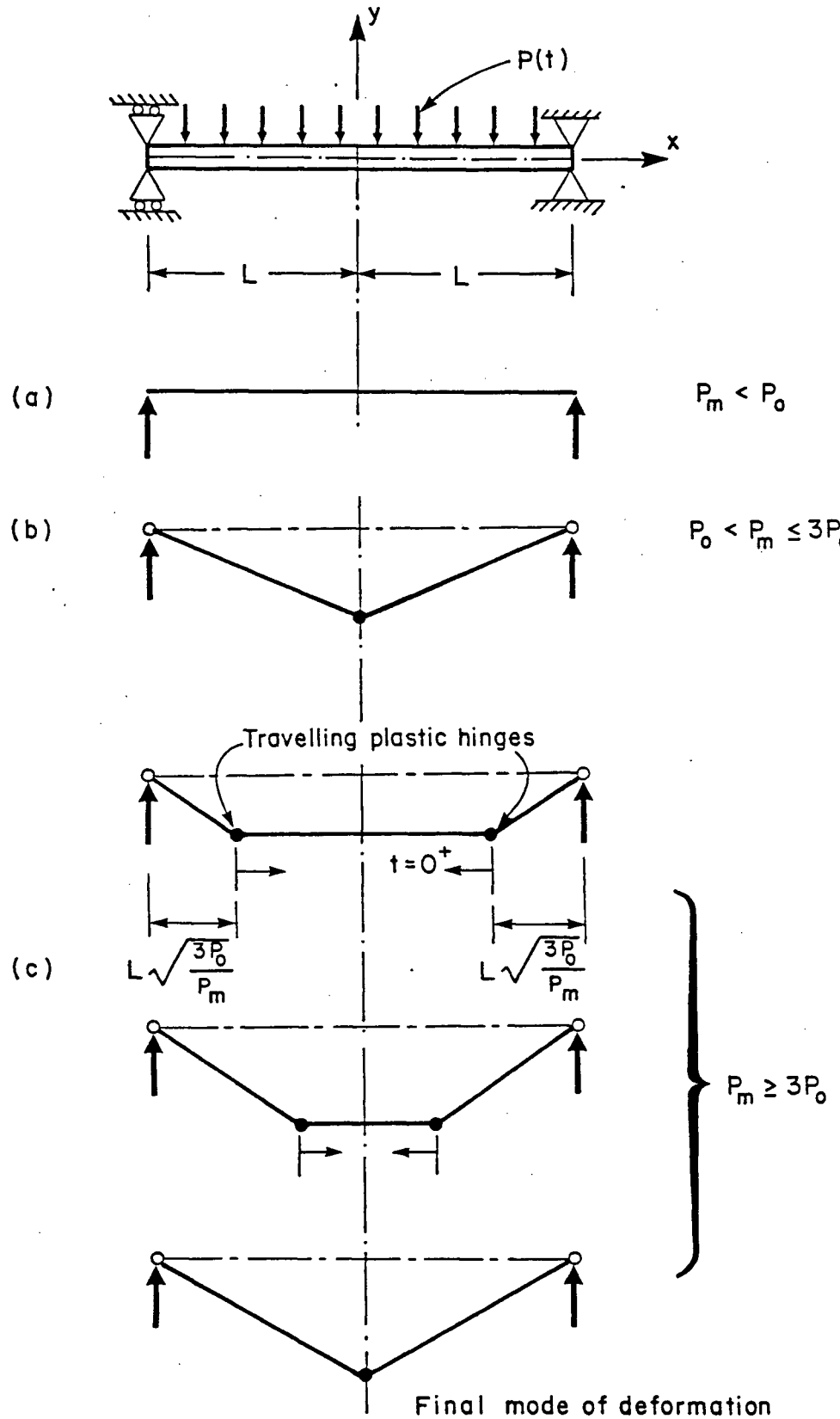

Fig.2.12 Process of deformation

(a) low pressure range (b) medium pressure range (c) high pressure range

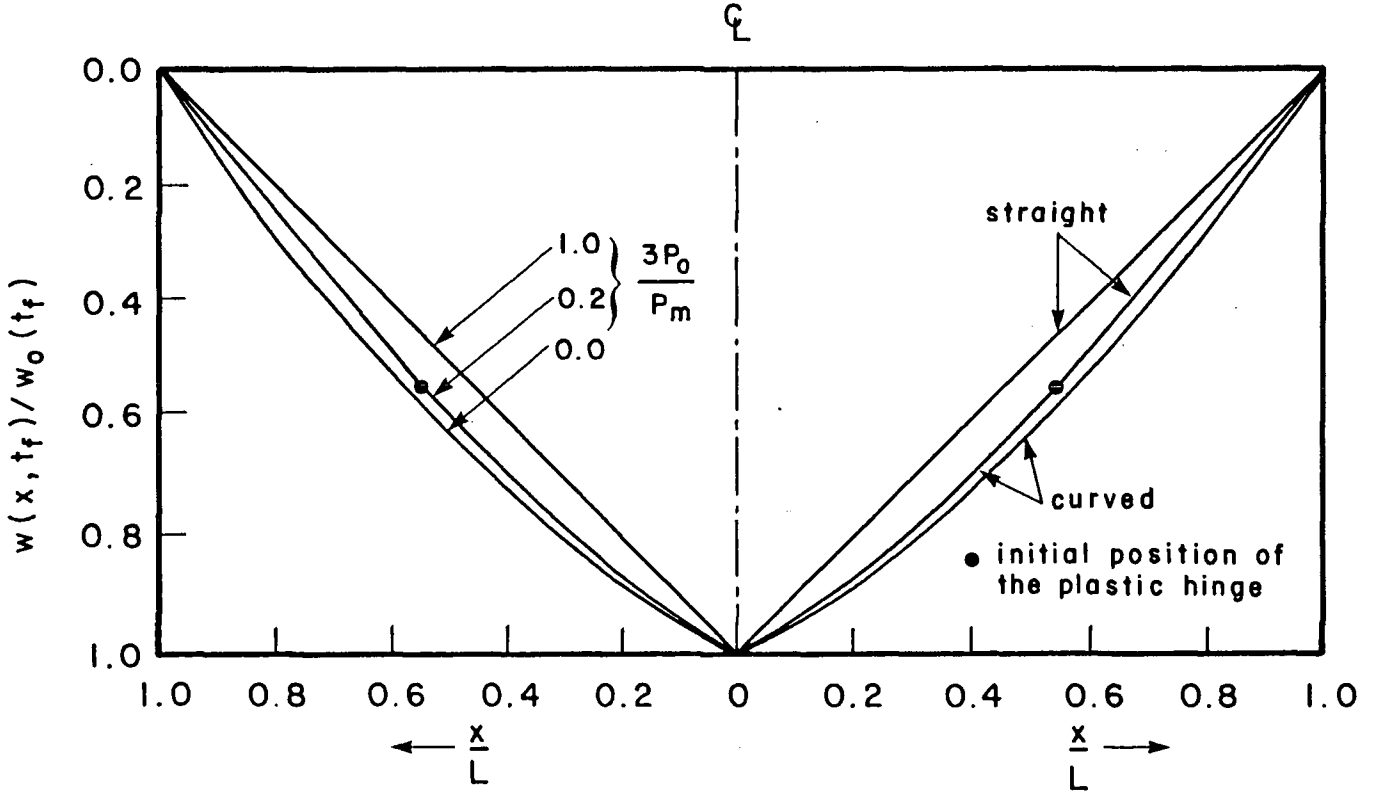

Fig.2.13 Variation of final deflection profile, expressed in terms of central deflection, with pressure intensity (Linear bending theory of Reference 17)

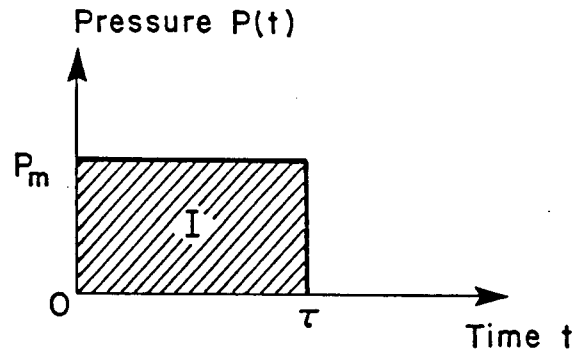

Fig.3.1 Rectangular pressure pulse

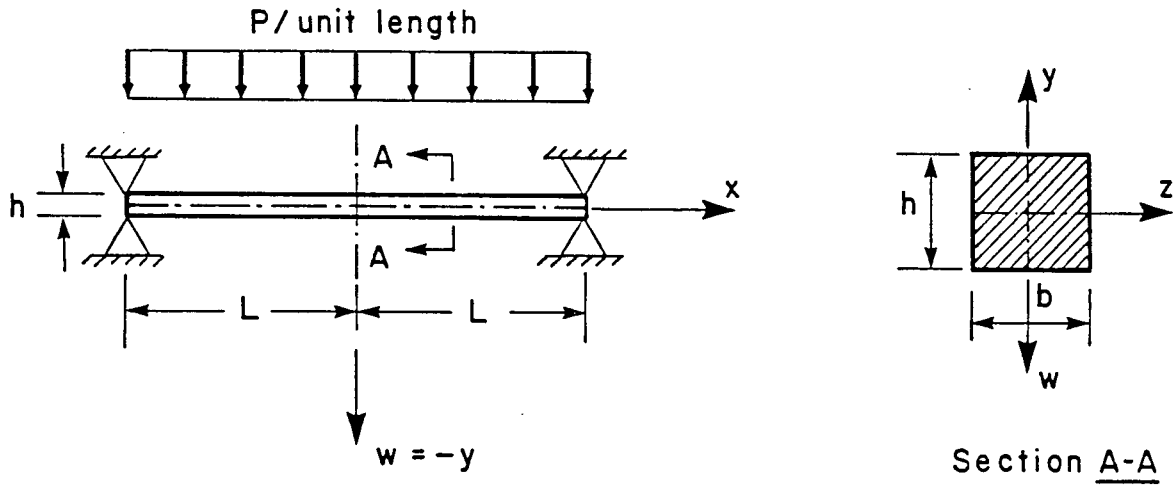

Fig.3.2 Simply supported axially constrained beam carrying a uniformly distributed load

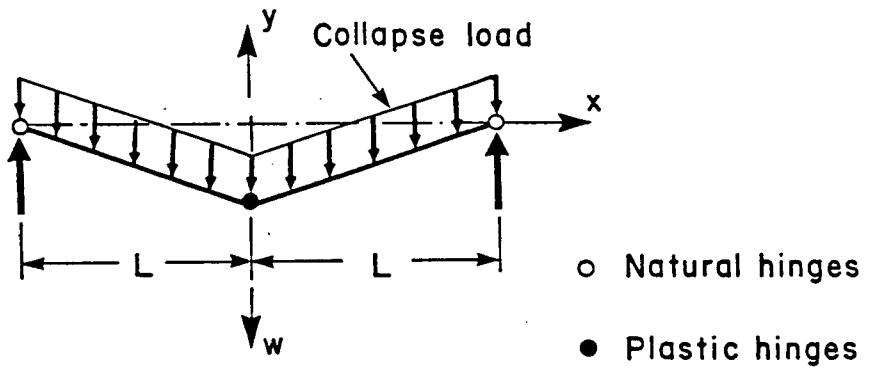

Fig.3.3 Configuration of the simply supported beam after development of a central plastic hinge

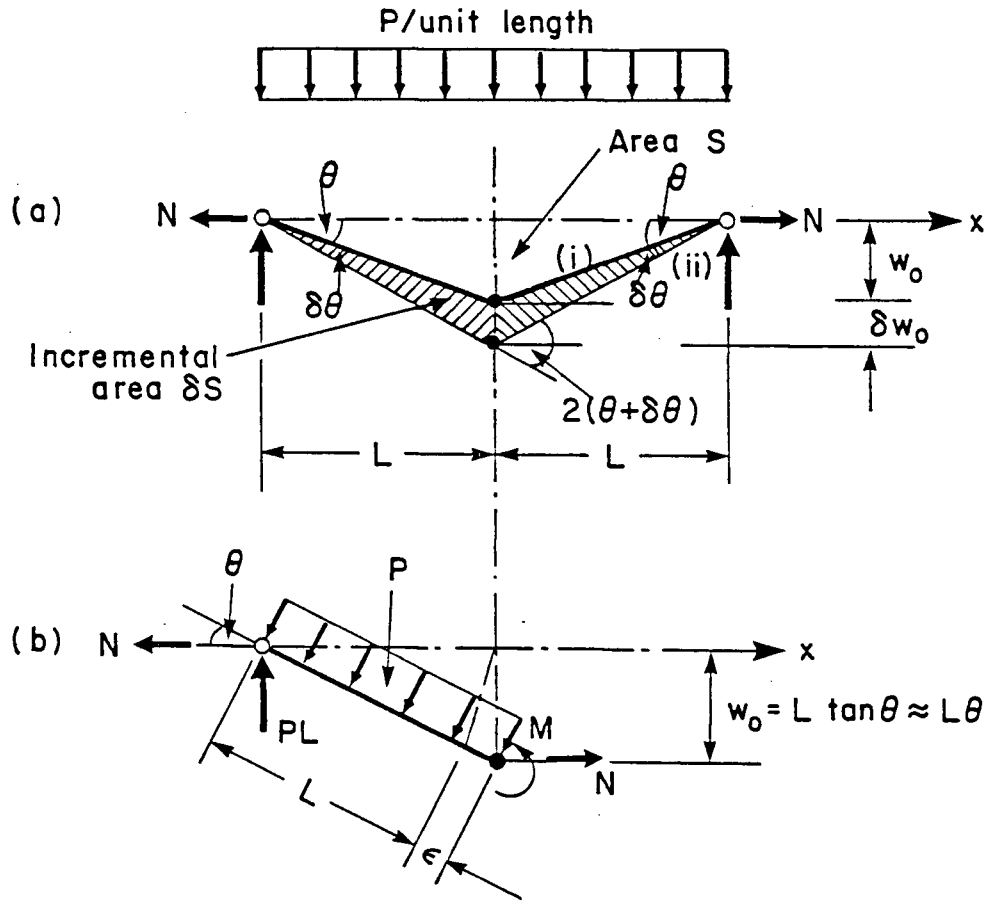

Fig.3.4 Nomenclature and free body diagram for a static analysis of the simply supported beam

(a) (i) Deflected form during collapse
(ii) Virtually disturbed configuration

(b) Free body diagram

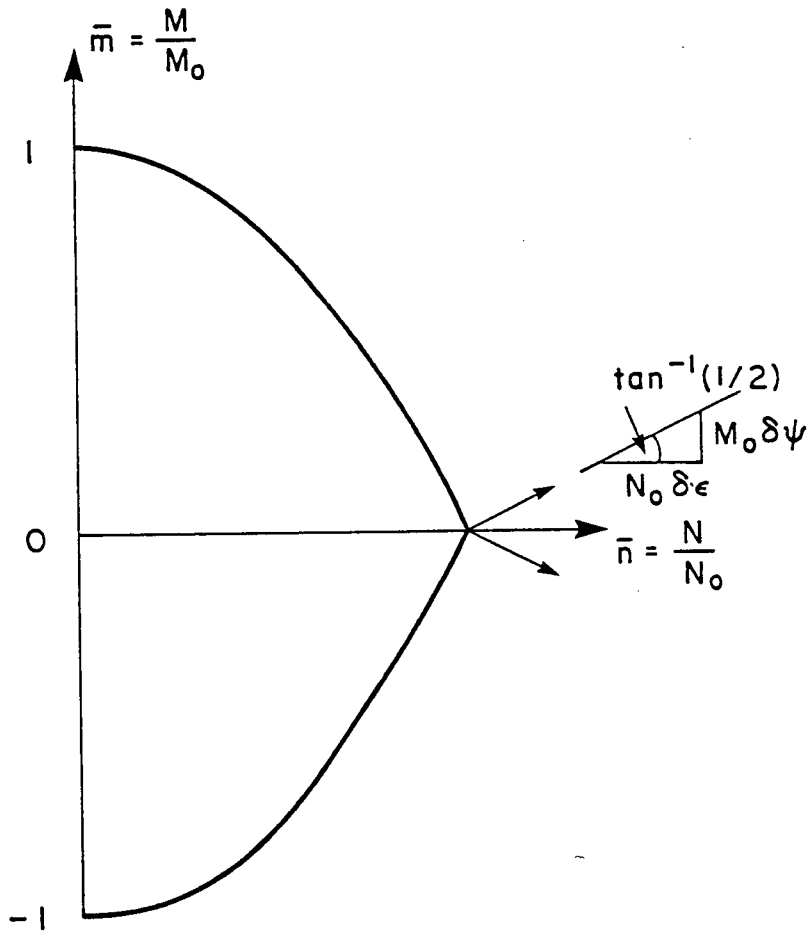

Fig.3.5 Parabolic yield surface for a rectangular cross-section

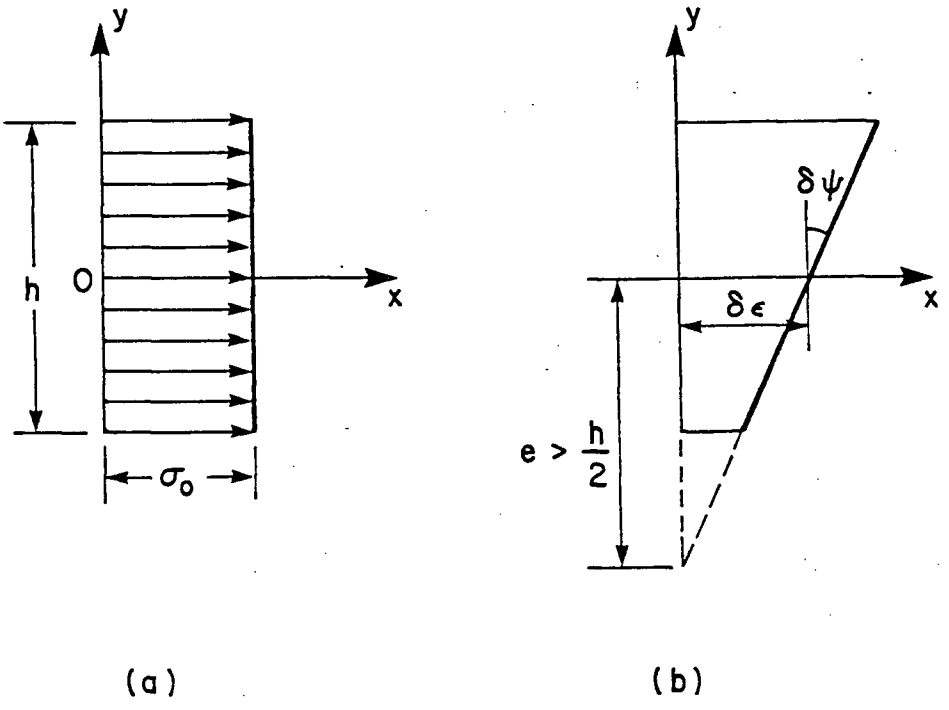

Fig.3.6 Stress and strain diagrams after the axial load reaches its fully plastic limit N_o

(a) tensile yield stress distribution across the whole cross-section

(b) strained geometry of the section

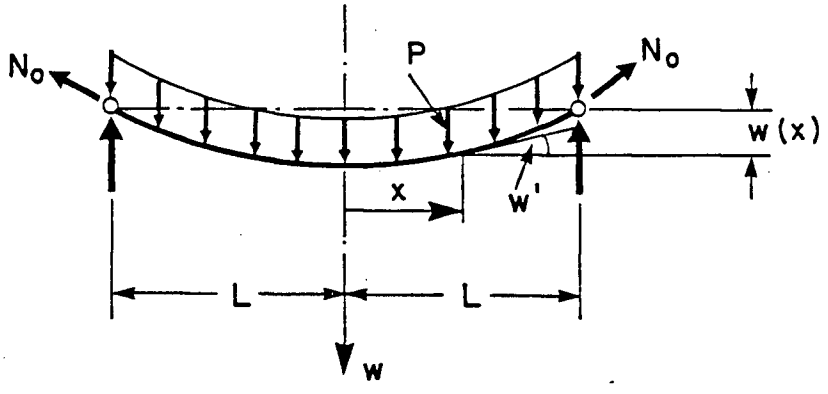

Fig.3.7 Perfectly flexible cable carrying the load by the membrane force N_o

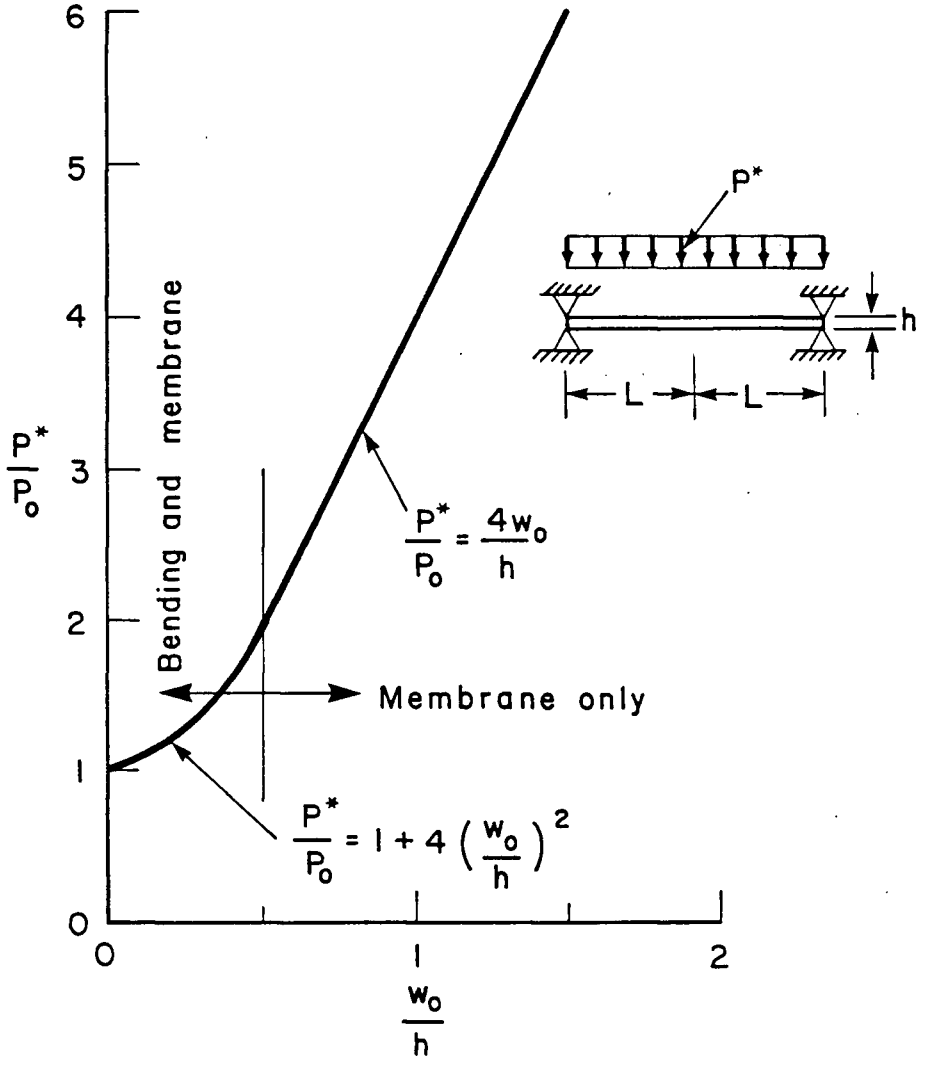

Fig.3.8 Variation of static load carrying capacity with deflection for a simply supported beam with axially constrained ends

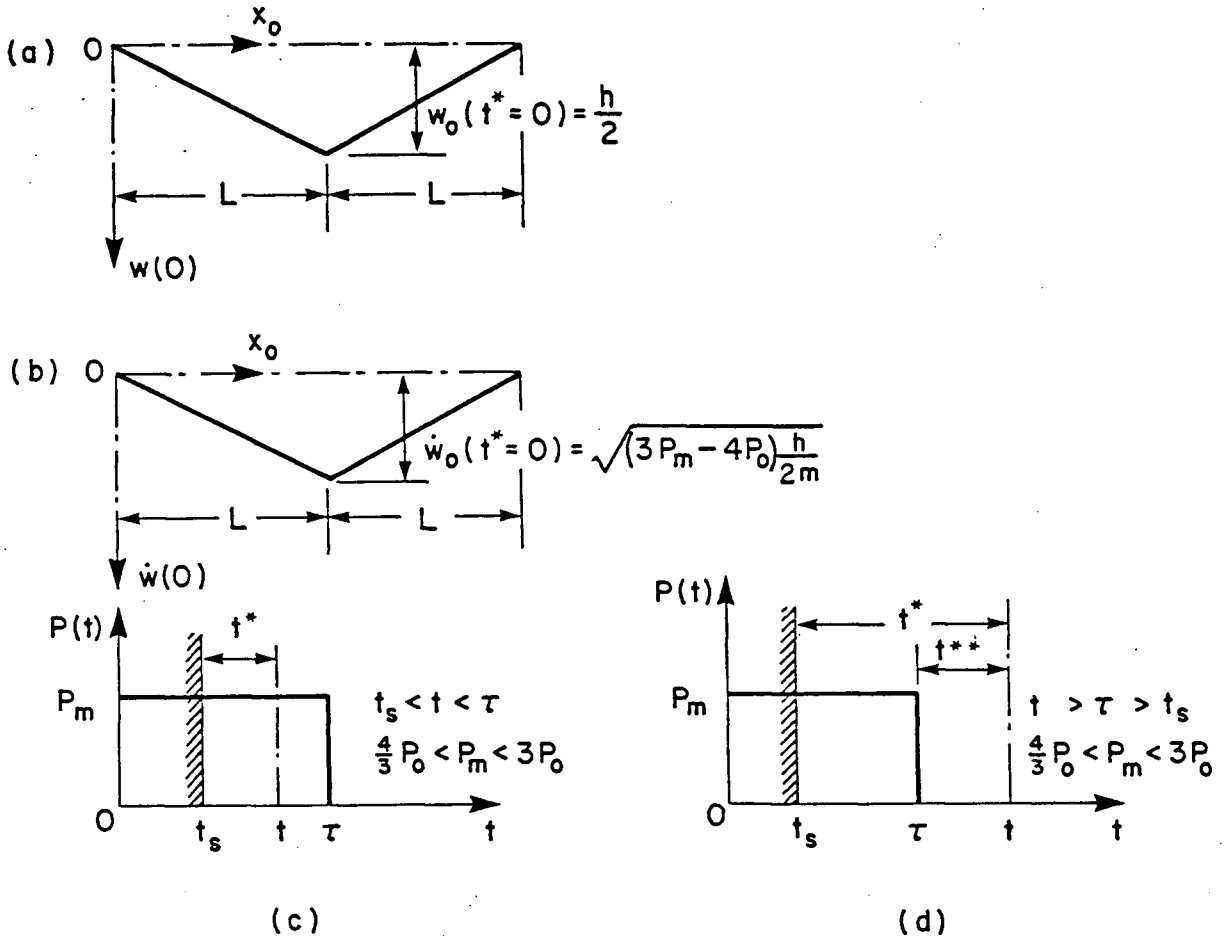

Fig.3.9 Initial displacement and velocity profiles for an "exact" plastic membrane analysis: Medium load;Phase I(b)

(a) initial displacement profile
(b) initial velocity profile
(c) first stage;loading era
(d) second stage;free era

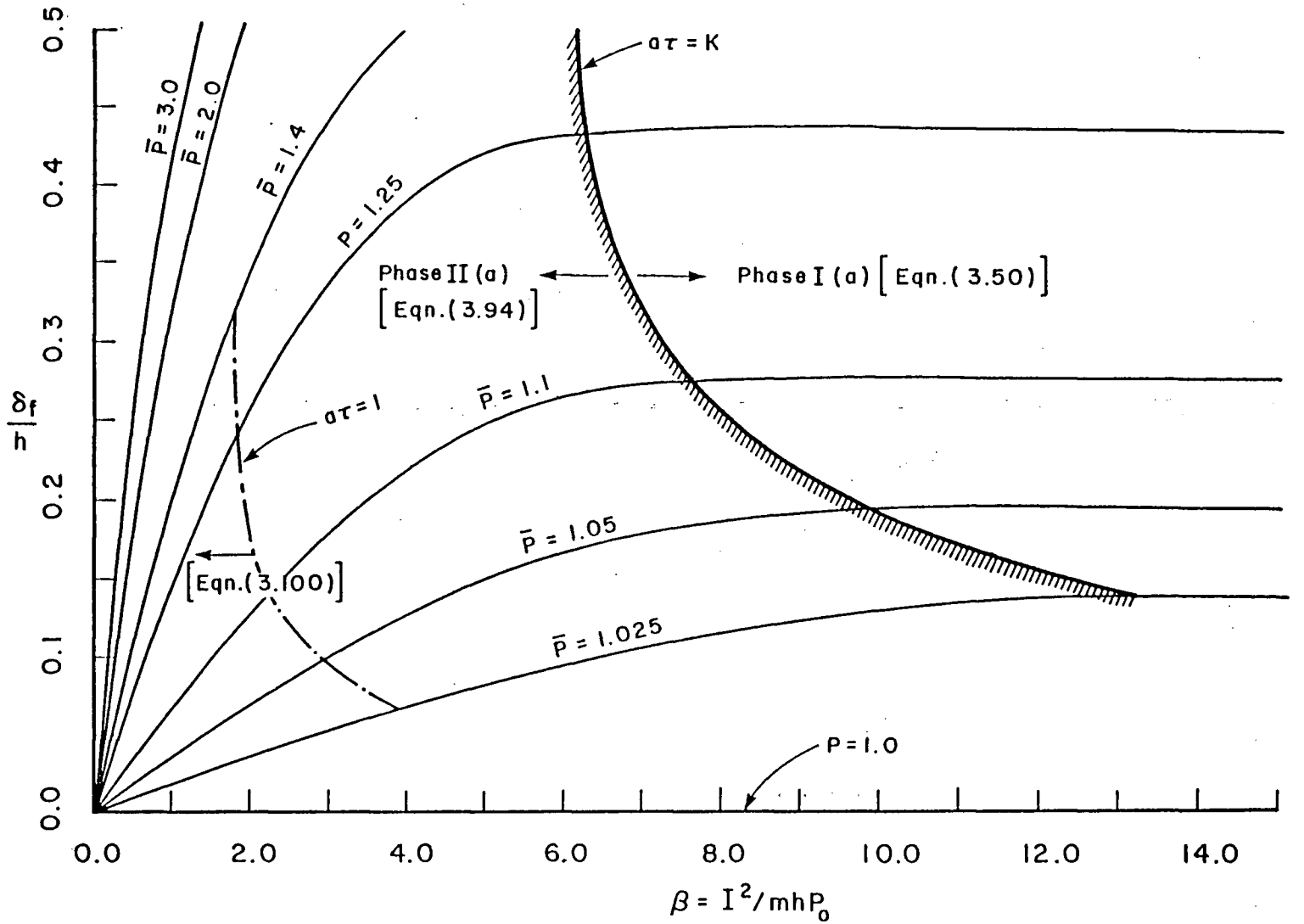

Fig.3.10 Variation of δ_f/h vs. β predicted by the small deflection theory (no string phase) for various values of $\bar{P}$ in the medium range of loading

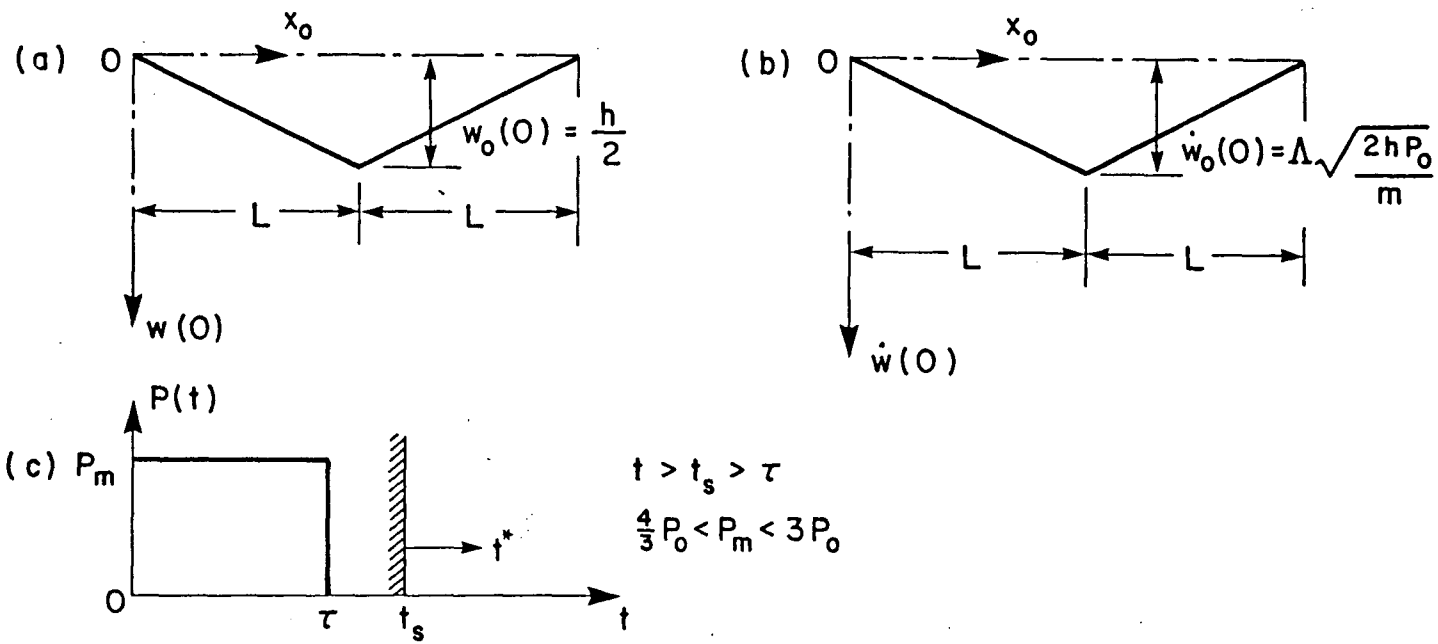

Fig.3.11 Initial displacement and velocity profiles for an "exact" plastic membrane analysis: Medium load;Phase II(b)

(a) initial displacement profile
(b) initial velocity profile
(c) initiation of string phase referred to load-time distribution

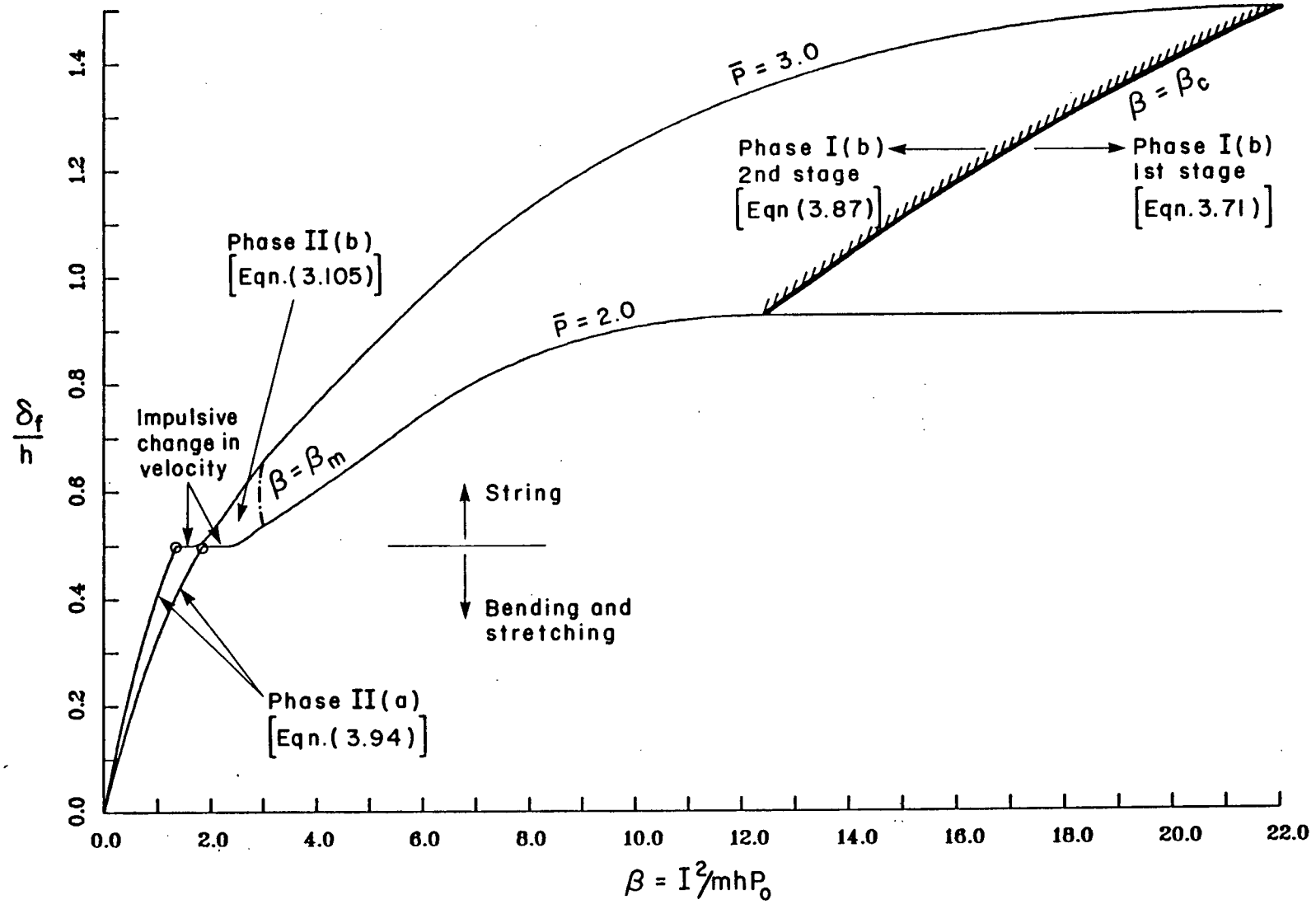

Fig.3.12 Variation of δ_f/h vs. β predicted by the exact plastic membrane analysis for $\bar{P}=2.0$ and 3.0 ; medium load

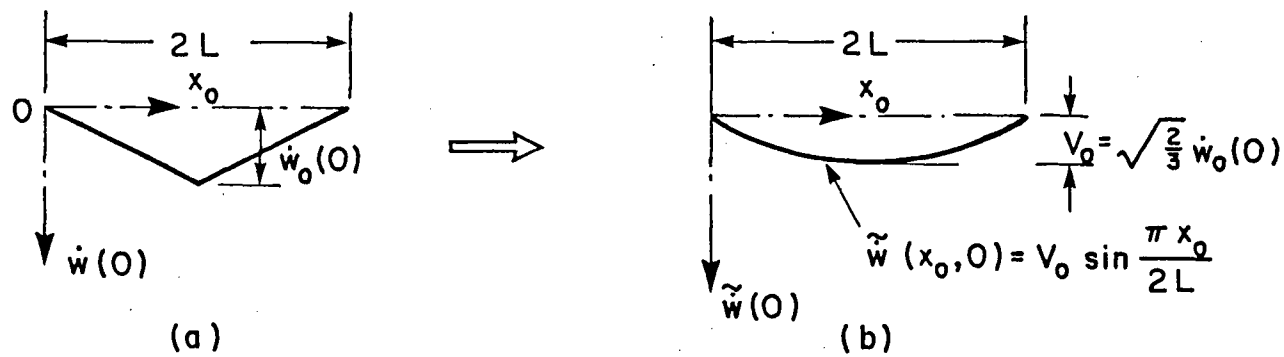

Fig.3.13 Assumed kinematically admissible initial velocity field for the approximate plastic membrane analysis of Phases I(b) and II(b);Medium load

(a) original initial velocity profile
(b) equivalent velocity field representing the same K.E. as (a)

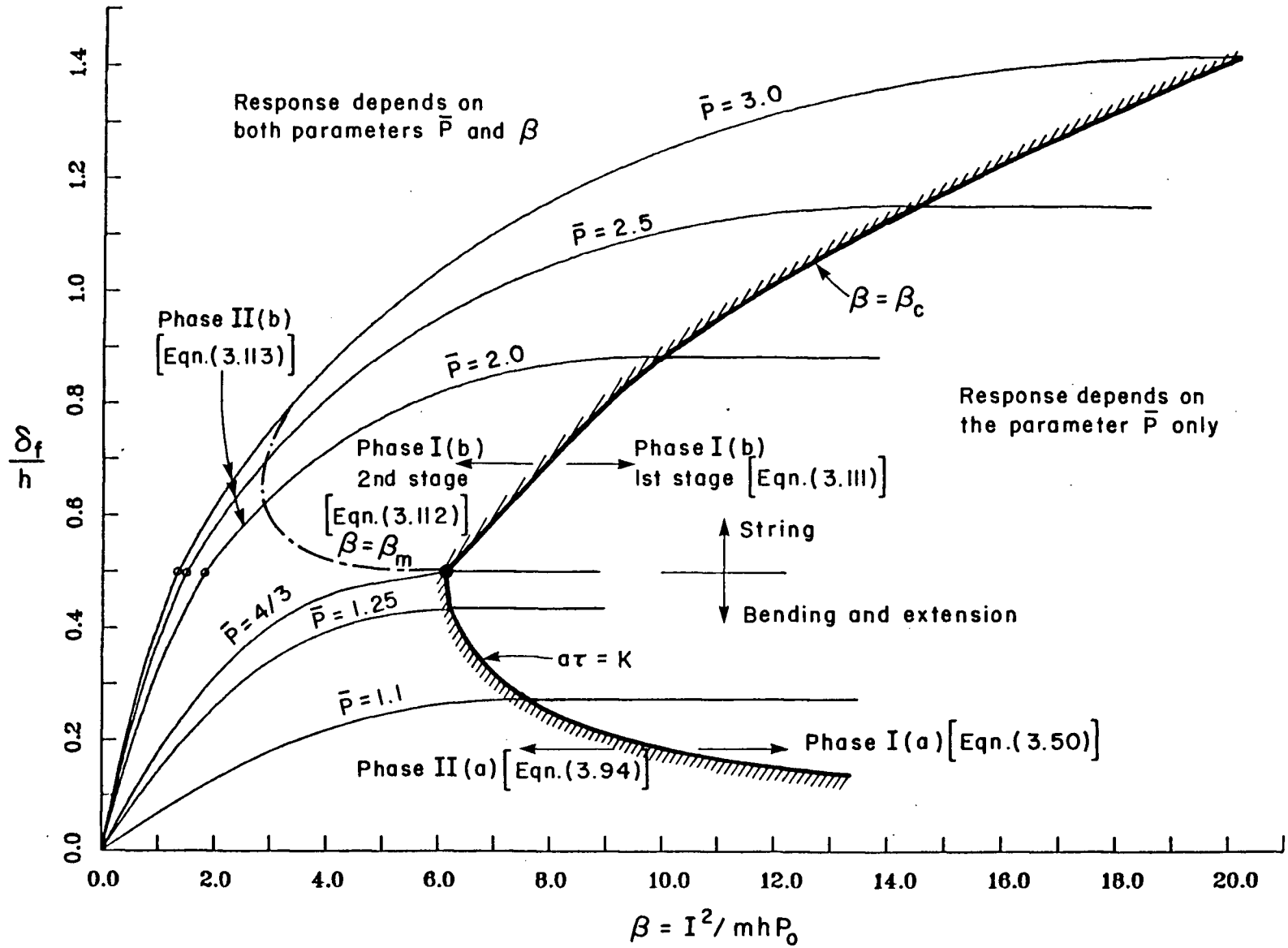

Fig.3.14 Variation of δ_f/h vs. β predicted by the complete analysis of the medium load case(approximate plastic string solution)

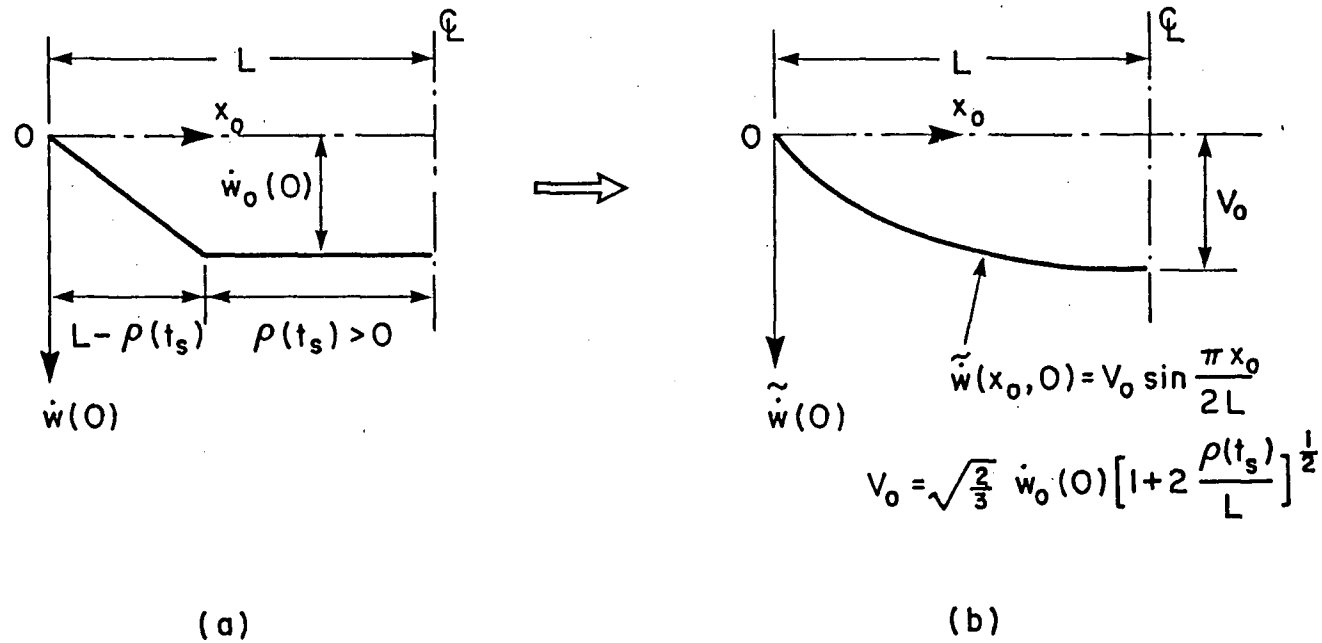

Fig.3.15 Assumed kinematically admissible initial velocity field for the approximate plastic membrane analysis of Phases I(b) and II(b);High load

(a) original initial velocity profile
(b) equivalent velocity field representing the same K.E. as (a)

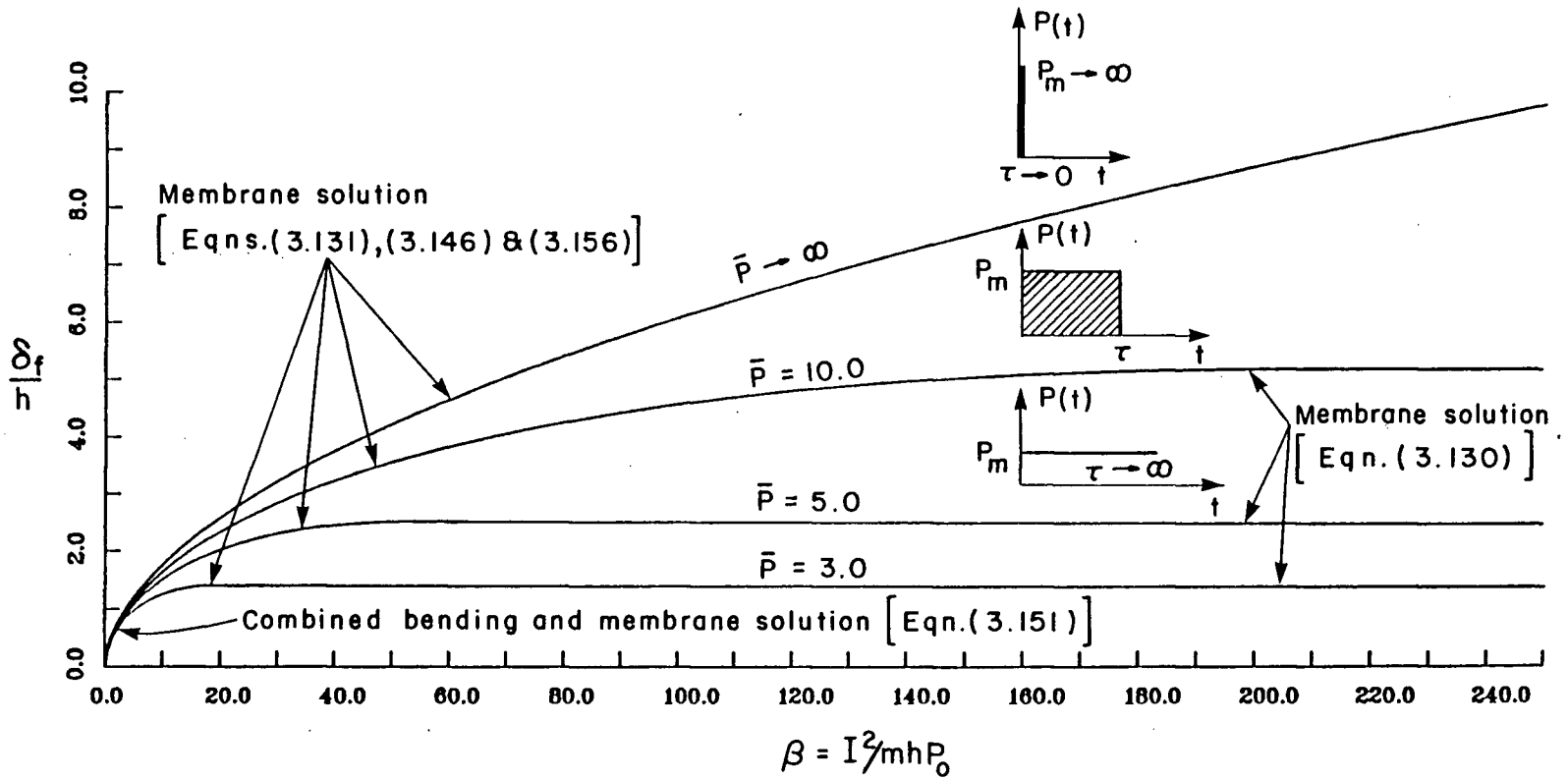

Fig.3.16 Variation of δ_f/h vs. β predicted by the complete analysis of the high load case

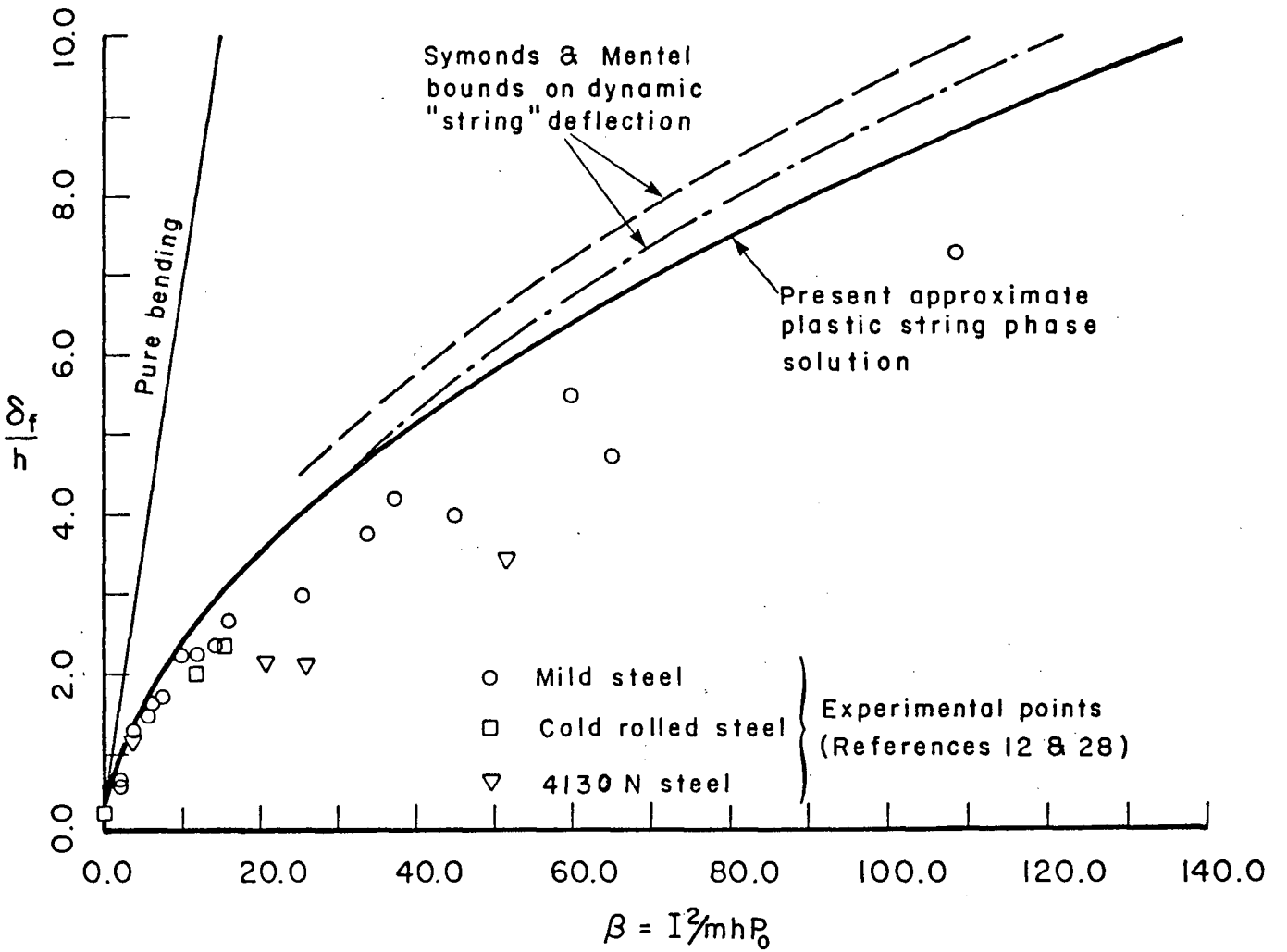

Fig.3.17 Comparison of experimental results and theoretical predictions of the maximum permanent deflections of impulsively loaded beams fully clamped at both ends

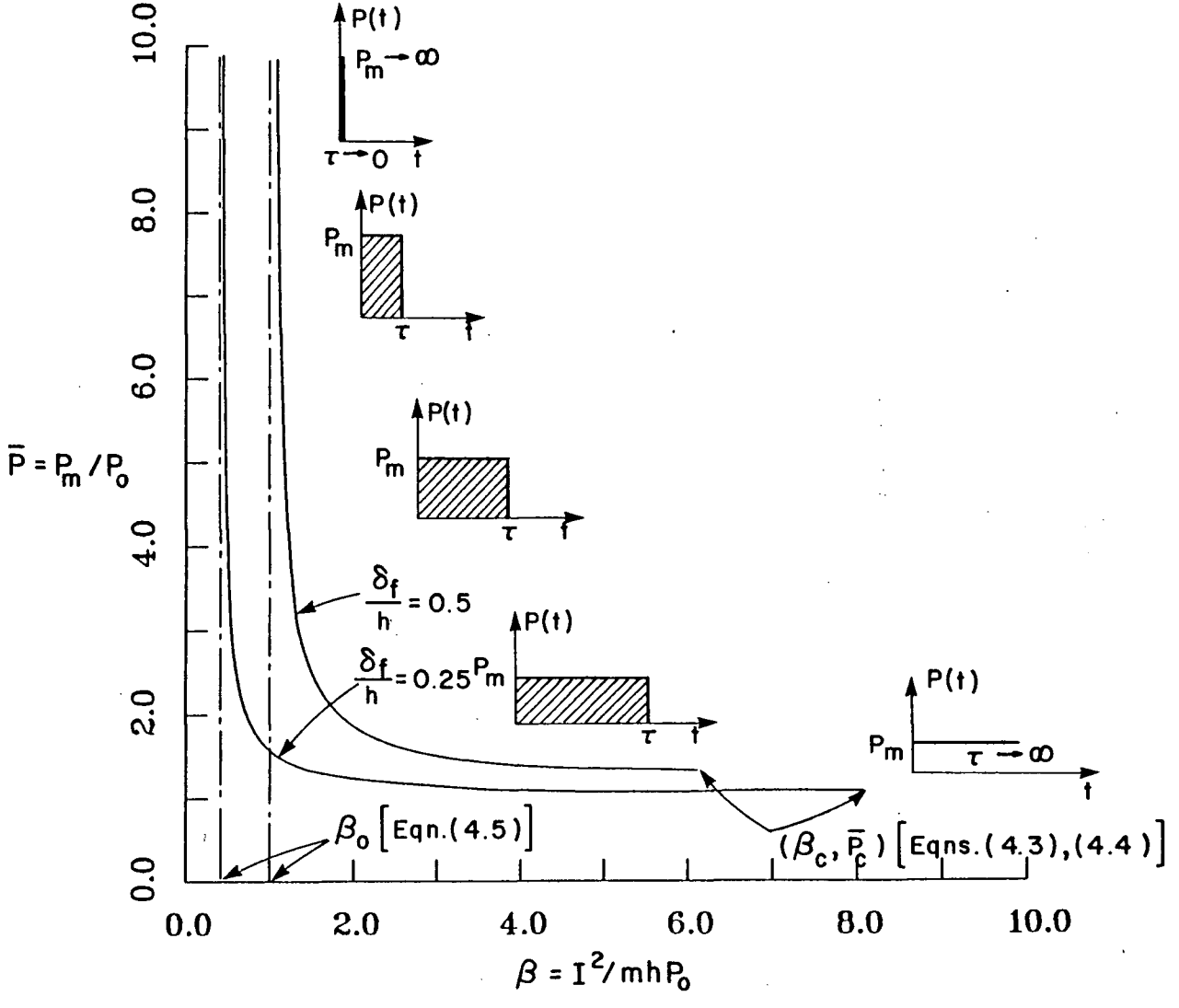

Fig.4.1 Theoretical Pressure-Impulse isodamage curves for small damage parameters δ_f/h = 0.25 and 0.5

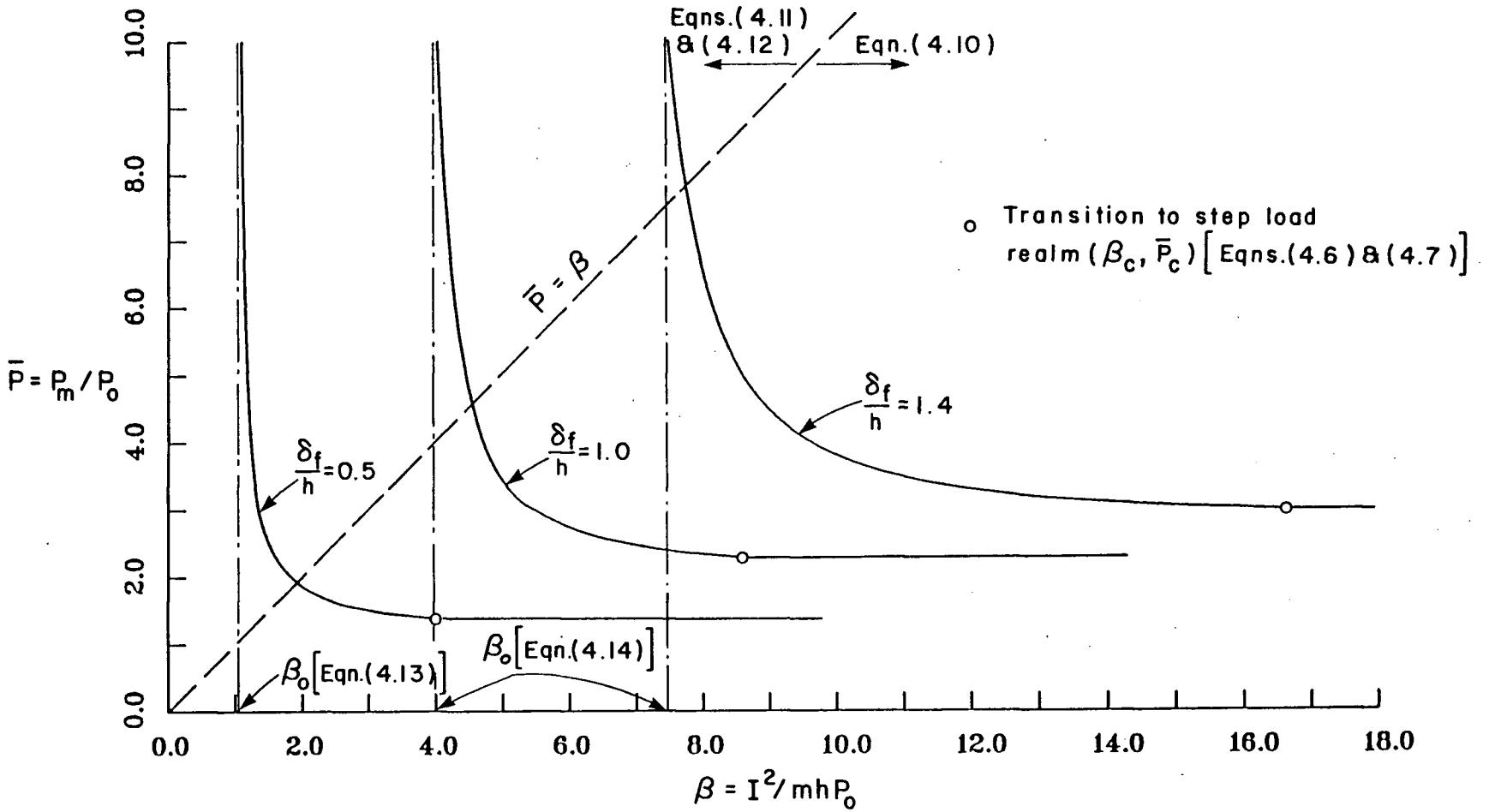

Fig.4.2 Theoretical Pressure-Impulse isodamage curves for moderately severe damage parameters δ_f/h = 0.5 , 1.0 and 1.4

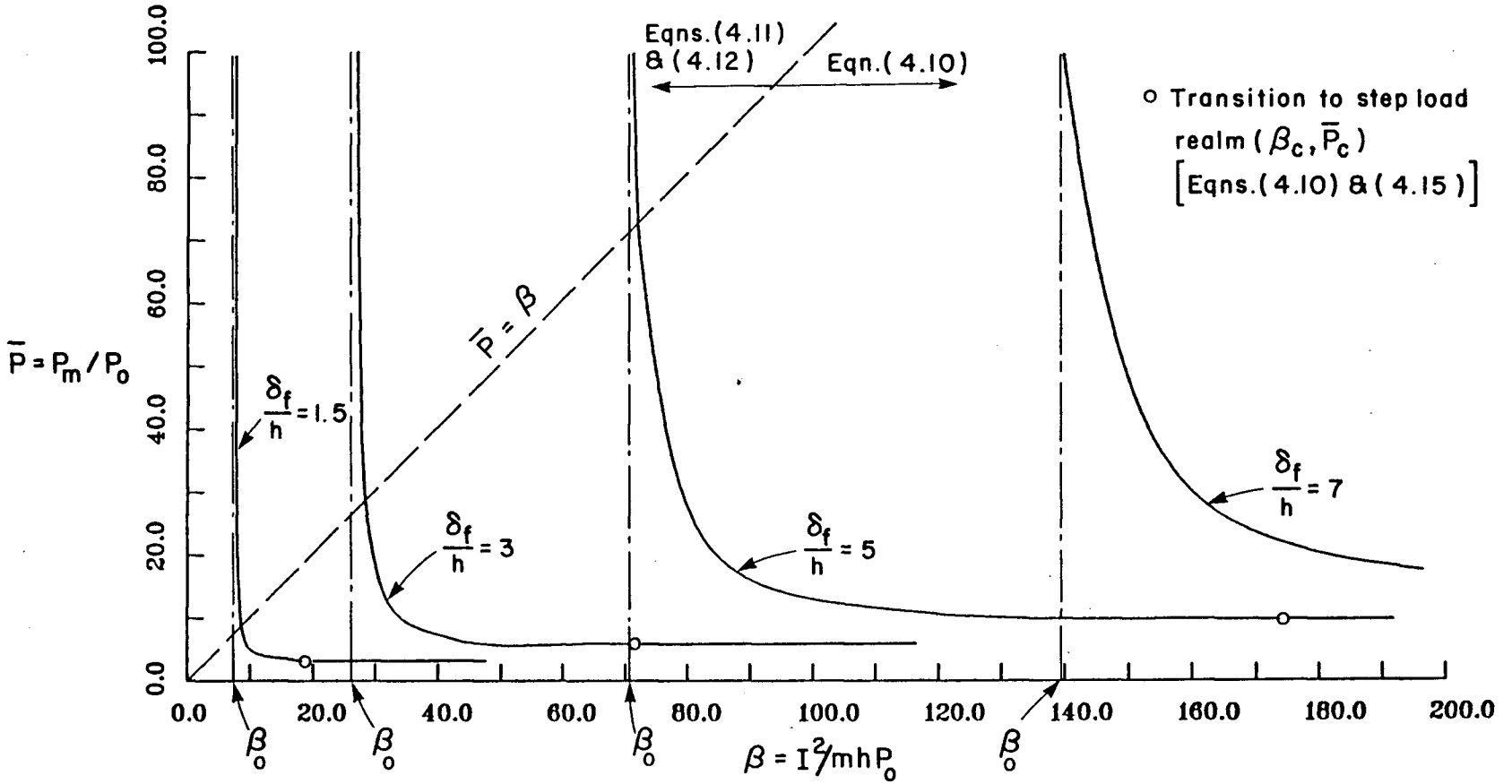

Fig.4.3 Theoretical Pressure-Impulse isodamage curves for severe damage parameters δ_f/h = 1.5,3,5 and 7

REFERENCES

1. Menkes, S.B. and Opat, H.J., "Broken Beams; Taring and Shear Failures in Explosively Loaded Clamped Beams", Exp. Mechanics, Vol. 13, 1973, pp 480-486.

2. Jones, N., "A Literature Review of the Dynamic Plastic Behaviour of Structures", Shock and Vibration Digest, Vol. 7, August 1975, pp 89-105.

3. Jones, N., "Recent Progress in the Dynamic Plastic Behaviour of Structures", Part 1 and 2, Shock and Vibration Digest, Vol. 10, September 1978, pp 21-33 and October 1978, pp 13-19.

4. Jones, N., "Recent Progress in the Dynamic Plastic Behaviour of Structures", Shock and Vibration Digest, Part 3, Vol. 13, October 1981, pp 3-16.

5. Baker, W.E., "Approximate Techniques for Plastic Deformation of Structures Under Impulsive Loading, III", Shock and Vibration Digest, Vol. 14, November 1982, pp 3-11.

6. Ari-Gur, J., Anderson, D.L. and Olson, M.D., "Air-Blast Response of Beams and Plates", Structural Research Series, Report No. 30, Dept. of Civil Engineering, University of British Columbia, Vancouver, Canada, June 1983.

7. Lee, E.H. and Symonds, P.S., "Large Plastic Deformations of Beams Under Transverse Impact", J. of Applied Mechanics, Trans, ASME, Vol. 74, 1952, pp 308-313.

8. Baker, J.F., "A Review of Recent Investigations into the Behaviour of Steel Frames in the Plastic Range", J. Inst. Civil Engrs, Vol. 31, 1949, pp 188.

9. Symonds, P.S., "Dynamic Load Characteristics in Plastic Bending of Beams", J. of Applied Mechanics, Vol. 20, 1953, pp 475-482.

10. Symonds, P.S., "Large Plastic Deformations of Beams Under Blast Type Loading", Proc. of the 2nd U.S. National Congress of Applied Mechanics, ASME, 1954, pp 505-515.

11. Symonds, P.S. and Mentel, T.J., "Impulsive Loading of Plastic Beams with Axial Constraints", J. of the Mechanics and Physics of Solids, Vol. 6, 1958, pp 186-202.

12. Humphreys, J.S., "Plastic Deformation of Impulsively Loaded Straight Clamped Beams", J. of Applied Mechanics, Vol. 22, Trans, ASME, March 1965, pp 7-10.

13. Chen, M.M., Hsu, P.T. and Pian, T.H.H., "Impulsive Loading of Rigid-plastic Curved Beams", Proc. of the 4th U.S. National Congress of Applied Mechanics, ASME, 1962, pp 1039-1045.

14. Nonaka, T., "Some Interaction Effects in a Problem of Plastic Beam Dynamics, Part I - III", J. of Applied Mechanics, Trans. of the ASME, Vol. 34, September 1967, pp 623-643.

15. Jones, N., "Influence of Strain-Hardening and Strain-Rate Sensitivity on the Permanent Deformation of Impulsively Loaded Rigid-Plastic Beams", Int. J. Mech. Sci., Vol. 9, 1967, pp 777-796.

16. Jones, N., "A Theoretical Study of the Dynamic Plastic Behaviour of Beams and Plates with Finite-Deflections", Int. J. of Solids and Structures, Vol. 7, 1971, pp 1007-1029.

17. Krajcinovic, D., "Dynamic Response of Rigid-Plastic Beams - General Case of Loading". J. Struct. Mech., Vol. 3, 1975, pp 439-457.

18. Symonds, P.S., "Survey of Methods of Analysis for Plastic Deformation of Structures Under Dynamic Loadings", Brown University, Report BU/NSRDC/1-67, 1967.

19. Seiler, J.A., Cotter, B.A. and Symonds, P.S., "Impulsive Loading of Elastic-Plastic Beams", J. of Applied Mechanics, Vol. 33, 1957, pp 515-521.

20. Witmer, E.A., Balmer, H.A., Leech, J.W. and Pian, T.H.H., "Large Dynamic Deformations of Beams, Rings, Plates and Shells", AIAA J., Vol. 1, 1963, pp 1848-1857.

21. Abrahamson, G., and Lindberg, H.E., "Peak Load-Impulse Characterization of Critical Pulse Loads in Structural Dynamics", Proceedings of a Symposium held at Stanford Univesity, California, Edited by Herrmann, G. and Perrone, N., June 1971, pp 31-53.

22. Bonder, S.R. and Symonds, P.S., "Experimental and Theoretical Investigation of the Plastic Deformation of Cantilever Beams Subjected to Impulsive Loading", J. of Applied Mechanics, Vol. 29, 1962, pp 719-728.

23. Perrone, N., "On a Simplified Method of Solving Impulsive Loaded Structures of Rate-Sensitive Materials", ASME J. of Applied Mechanics, Vol. 32, September 1965, pp 489-492.

24. Byrd, P.F. and Friedman, M.D., "Handbook of Elliptic Integrals for Engineers and Physicists", Springer-Verlag, 1954.

25. Bromwich, T.J.I'A., "Introduction to the Theory of Infinite Series", Macmilland & Co. Ltd., 1965.

26. Symonds, P.S. and Jones, N., "Impulsive Loading of Fully Clamped Beams with Finite Plastic Deflections and Strain-Rate Sensitivity", Int. J. of Mechanical Sciences, Vol. 14, 1972, pp 49-69.

27. Ari-Gur, J., Anderson, D.L. and Olson, M.D., "Review of Air-Blast Response of Beams and Plates", 2nd Int. Conf. on Recent Advances in Structural Dynamics, U. of Southampton, Southampton, England, April 1984.

28. Jones, N., Griffin, R.N. and Van Duzer, R.E., "An Experimental Study into the Dynamic Plastic Behaviour of Wide Beams and Rectangular Plates", Int. J. of Mechanical Sciences, Vol. 13, August 1971, pp. 721-735.

APPENDIX A

Validity of the Dynamic Rigid-Plastic Analysis: Bounds on the Pulse Duration

It was stated in Section 2.2 that the rigid, ideal plastic theory can be expected to give satisfactory results if conditions are such that the input energy greatly exceeds the maximum amount of energy that could be stored in the beam in the form of elastic strain energy. As a general rule of thumb it appears that for simple beams a factor of at least 3 is desirable (Reference 22). If this energy ratio is denoted by R, the above criterion is

$$R = \frac{\text{Input kinetic energy}}{\text{Strain energy at incipient yield}} > 3 \qquad (A.1)$$

For the simply supported beams of Figure 2.10a the bending moment distribution at incipient yield (i.e. when the outermost fibres of the beam at the midsection start yielding), is

$$M(x) = M_y \left(1 - \frac{x^2}{L^2}\right) \qquad (A.2)$$

where $M_y = \frac{1}{6} \sigma_o b h^2$ is the bending moment at which the yield stress, σ_o is first attained in the extreme fibres.

If for simplicity we neglect the strain energy stored in the beam due to stretching we can write an expression for the maximum elastic strain energy (of the half-beam) as

$$(\Omega \text{ bending})_{max} = \int_0^L \frac{(M^2(x))_{max}}{2EI_s} dx = \frac{16}{5} \frac{M_y^2 L}{bh^3} \qquad (A.3)$$

where $I_s = bh^3/12$ is the second moment of area of the beam cross-section and E is the modulus of elasticity of the beam material.

Also the input kinetic energy for half of the beam can be written as

$$K.E. = \frac{1}{2} \frac{I^2 L}{m} \qquad (A.4)$$

where $I = P_m \tau$ is the applied impulse per unit length and m is the mass per unit length of the beam. The inequality of A.1 can be expressed in non-dimensional form in terms of the fundamental period of elastic vibration of the simply supported beam, which is given by

$$T_e = \frac{8L^2}{\pi} \sqrt{(m/EI_s)} \qquad (A.5)$$

Using Equations (A.3) to (A.5) in (A.1) and noting that $M_y = 2M_o/3 = P_o L^2/3$, yields

$$\left(\frac{\tau}{T_e}\right) > \frac{\pi}{6\sqrt{10}} \frac{P_o}{P_m} \approx \frac{1}{6} \frac{P_o}{P_m} \qquad (A.6)$$

For a given beam and a given value of the maximum pressure, this sets a lower limit on the duration of the pulse for which the rigid-plastic analysis can be expected to be reasonably accurate.

An additional limitation suggested by Symonds (Reference 20) is that the duration τ of the dynamic pressure pulse must be small compared with the natural period of elastic vibration of the beam. This provides an upper bound on the pulse duration and consequently the admissible range of τ is given by the following inequality

$$\frac{1}{6}\,\frac{P_o}{P_m} < \frac{\tau}{T_e} < 1 \qquad (A.7)$$

Let us investigate the limitations imposed by the above inequality by way of an example. For this purpose we consider a simply supported steel beam of rectangular cross-sections. Thus

$$\sigma_o/E \approx 2\times10^{-3} \qquad (A.8)$$

The limits on the nondimensional impulse parameter $\beta = I^2/mhP_o$ corresponding to the above limits on τ will now be evaluated. Simple algebraic manipulation on the inequality (A.7) yields

$$0.002\,(\frac{L}{h})^2 < \beta < 0.04\,\bar{P}^2\,(\frac{L}{h})^2 \qquad (A.9)$$

where $\bar{P} = P_m/P_o$.

For specific values of L/h (half-span to depth ratio), the above limits on β can be evaluated. It should be noted that, as rotary inertia and deformation due to shear have been neglected, the above criterion is applicable only to slender beams. This implies that the results are reasonably accurate, provided that L/h > 5. For L/h = 10, say, the criterion for the validity of the rigid-plastic assumption is approximately given by

$$0.2 < \beta < 4\bar{P}^2 \qquad (A.10)$$

It is clear from Figures 4.1, 4.3 and 4.4 that this criterion is satisfied by the majority of the isodamage curves shown.

APPENDIX B

Closed Form Summation of Some Fourier Series

$$\sin\theta + \frac{1}{3}\sin 2\theta + \frac{1}{5}\sin 5\theta + \ldots\ldots = \frac{\pi}{4}\ ;\ 0 < \theta < \pi \qquad \text{(B.1)}$$

$$\cos\theta + \frac{1}{3^2}\cos 3\theta + \frac{1}{5^2}\cos 5\theta + \ldots\ldots = \frac{\pi}{4}\left(\frac{\pi}{2} - \theta\right);\ 0 \leq \theta \leq \pi \qquad \text{(B.2)}$$

$$\sin\theta - \frac{1}{3^2}\sin 3\theta + \frac{1}{5^2}\sin 5\theta - \ldots\ldots = \frac{\pi}{4}\theta\ ;\ -\pi/2 \leq \theta \leq \pi/2$$

$$= \frac{\pi}{4}(\pi - \theta)\ ;\ \pi/2 \leq \theta \leq 3\pi/2 \qquad \text{(B.3)}$$

$$\sin\theta + \frac{1}{3^3}\sin 3\theta + \frac{1}{5^3}\sin 5\theta + \ldots\ldots = \frac{\pi}{8}\theta\,(\pi-\theta)\ ;\ 0 \leq \theta \leq \pi \qquad \text{(B.4)}$$

$$\cos\theta - \frac{1}{3^3}\cos 3\theta + \frac{1}{5^3}\cos 5\theta - \ldots\ldots = \frac{\pi}{8}\left(\frac{\pi^2}{4} - \theta^2\right)\ ;$$

$$-\pi/2 \leq \theta \leq \pi/2$$

$$= \frac{\pi}{8}\left[(\pi - \theta)^2 - \frac{\pi^2}{4}\right]\ ;$$

$$\pi/2 \leq \theta \leq 3\pi/2 \qquad \text{(B.5)}$$

On writing $\theta = 0$ in (C.5) we find

$$1 - \frac{1}{3^3} + \frac{1}{5^3} - \frac{1}{7^3} + \ldots\ldots = \frac{\pi^3}{32} \qquad \text{(B.6)}$$